Spatial and Non-spatial Memory Subnetworks in the Medial Temporal Lobe: Focus on the Dentate Gyrus

Thesis

for the degree of

doctor rerum naturalium (Dr. rer. nat.)

approved by the Faculty of Natural Sciences of Otto von Guericke University Magdeburg

by Rukhshona Kayumova, M.Sc.

born on 03. January 1994 in Dushanbe, Tajikistan

Examiner: Prof. Dr. Magdalena Sauvage

Prof. Dr. Jill Leutgeb

submitted on: 07.11.2023 defended on: 05.08.2024

Abstract

Remembering past unique experiences - episodic memory - is an important aspect of our daily lives. Recent anatomical and functional evidence supports a new model for episodic memory, which posits that spatial and non-spatial aspects of memories might be processed by distinct subnetworks segregated along the proximodistal axis of the hippocampus. This model of segregated information processing might be relevant when one of the dimensions of a given memory, i.e. spatial or non-spatial, is overly important compared to the other and the integration of the least important information is dispensable. According to this model, the spatial subnetwork consists of the enclosed blade of the dentate gyrus (DG), the distal part of CA3, and the proximal part of CA1. The non-spatial subnetwork, on the other hand, comprises the exposed blade of the DG, proximal CA3 and distal CA1. However, to date, functional support for the existence of these subnetworks is available only for the CA1 and CA3 and whether spatial and non-spatial information are processed differently by the enclosed and exposed blades of the DG, remains unknown.

In the present work, I show by combining behavioural, optogenetic, and molecular imaging approaches that the exposed blade of the DG is critical for non-spatial memory processing and is part of the non-spatial hippocampal subnetwork. In contrast, the enclosed blade of the DG preferentially supports spatial memory retrieval and interacts with both, spatial and non-spatial hippocampal subnetworks. Additionally, I present anatomical tracing data suggesting that the origin of cortical projections to the individual DG blades from the lateral and medial entorhinal cortices, which are differentially tuned to spatial/non-spatial processing, might give rise to the spatial/non-spatial double dissociation of the DG blades. Altogether, these data strongly support the claim that the DG blades are parts of distinct hippocampal subnetworks embedded in larger-scale medial temporal lobe subnetworks with selective functional ties to spatial and non-spatial information processing. These insights improve our knowledge about the neural circuits supporting episodic memories and will be helpful for future research aimed at preventing and rescuing memory deficits.

Table of Contents

Table of Figures

I.

General Introduction

Multiple neural systems for episodic memory processing

In the animal world remembering unique past experiences (episodic memories) – is essential for future planning and survival. The medial temporal lobe (MTL) is one of the most important brain areas for episodic memory across a variety species, including humans (Allen and Fortin, 2013). The research of neural correlates of episodic memories, which linked it to the MTL, began in the 1950s with the famous case of patient H.M. (1926-2008), who underwent a bilateral MTL resection to treat his severe focal epilepsy. Following the surgery, H.M. developed memory loss and a severe lifelong inability to create new memories for unique events (Scoville and Milner, 1957). This case delivered the first irrefutable proof that the MTL is critically involved in episodic memory processes.

The MTL is exceptionally well conserved across mammal species (Insausti, 1993) and is an umbrella term for several distinct brain regions that are nowadays known to play different roles and to contribute to different aspects of episodic memory (e.g. Beer et al., 2013; Hitti and Siegelbaum, 2014; O'Mara, 2005; Save and Sargolini, 2017). It includes the hippocampal complex (with its CA1, CA2, CA3 and the dentate gyrus), the subicular complex and the adjacent entorhinal, perirhinal and parahippocampal (in rodents: postrhinal) cortices (Squire and Zola-Morgan, 1991).

A simplistic model of episodic memory and MTL connectivity describes two main information processing pathways that originate from the 'two-stream hypothesis' for visual processing first described by Mishkin et al. (1983). The 'what' pathway is a continuation of the ventral visual stream. It courses through the perirhinal and the lateral entorhinal cortices (LEC) and is relevant for preferential processing of non-spatial information, for example objects (Deshmukh et al., 2012; Deshmukh and Knierim, 2011; Tsao et al., 2013; Brown and Aggleton, 2001). The 'where' pathway, on the other hand, is a continuation of the dorsal visual stream. It is composed of the postrhinal and the medial entorhinal cortices (MEC) and is presumably involved in processing spatial information (Fyhn et al., 2008; Tennant et al., 2018; Hargreaves et al., 2005; LaChance et al., 2019).

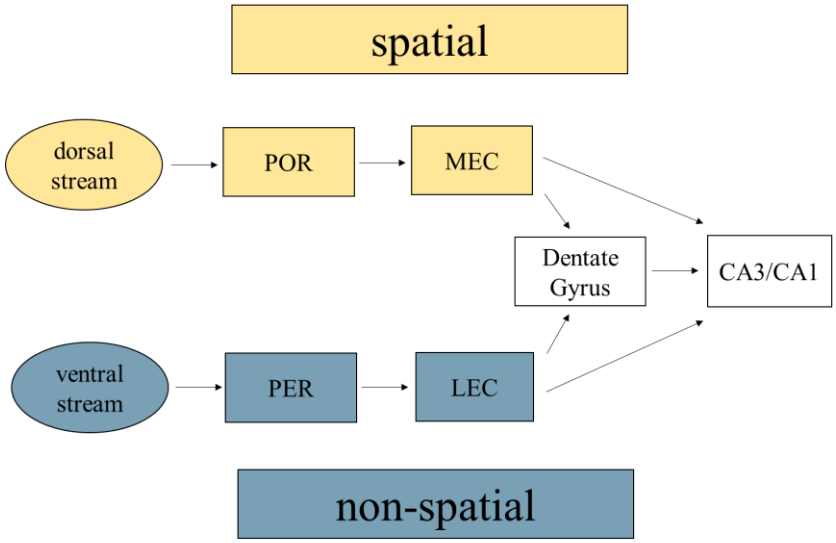

Figure 1: Schematic model of functionally segregated cortical areas involved in preferential processing of spatial or non-spatial information. Segregated information is believed to be integrated in the hippocampal dentate gyrus, CA1 and CA3, which allows formation and retrieval of episodic memories. POR: postrhinal cortex; PER: perirhinal cortex; MEC: medial entorhinal cortex; LEC: lateral entorhinal cortex.

The original formulation of segregated information flow has since been adapted into a model for episodic memory, in which spatial and non-spatial signals are processed in a segregated manner in the cortical parts of the MTL until they reach the hippocampus - the dentate gyrus (DG), CA1, and CA3, - where they are thought to be systematically integrated (**Figure 1**). The convergence of spatial and non-spatial information in the hippocampus is believed to support the formation and retrieval of episodic memories. It is important to mention that this model has been revised several times (e.g. Nilssen et al., 2019; Knierim et al., 2013; Save and Sargolini,

2017). For example, it was shown that the postrhinal cortex in fact projects mostly to the LEC and not the MEC (Doan et al., 2019); also, the LEC is not exclusively involved in non-spatial information processing, but processes both spatial and non-spatial signals and is important for object-place associations (Tsao et al., 2013; Deshmukh and Knierim, 2011; Beer et al., 2013; Kuruvilla et al., 2020).

Another revision comes from a body of evidence suggesting that spatial and non-spatial information is not systematically integrated in the hippocampus, but instead, at least under certain circumstances, kept segregated. This might specifically be the case when only one information domain is relevant and the integration of the less or non-relevant information is dispensable. For example, the recall of where one has left their house key last does not necessarily require memories of the shape, colour or other non-spatial features of the key. In this scenario, it might be beneficial for the brain to preserve its resources and only retrieve the important information. The idea of spatial and non-spatial segregation in the hippocampus is a stark contrast but not contradictory to the integration view, which received support by many studies (e.g. Ergorul and Eichenbaum, 2004; Gilbert and Kesner, 2002; Gilbert and Kesner, 2003; Day et al., 2003; Goodrich-Hunsaker et al., 2009). However, the studies supporting the integration model usually used lesioning or pharmacological approaches to explore the influence of hippocampal integrity on the conjoint information processing, which *per se* does not deliver direct proof for the convergence of the two information pathways (but see Komorowski, Manns and Eichenbaum, 2009). Therefore, it is plausible to think that different mnemonic dimensions may be processed in a segregated manner in the hippocampus and that the integration of information may emerge as a product of concomitant activity of distinct subnetworks, each preferentially supporting spatial or non-spatial processing.

The first evidence for the hippocampal segregation model came from anatomical studies, which established that the LEC and MEC project to different proximodistal levels of the hippocampal CA1 area (Tamamaki and Nojyo, 1995; Steward, 1976). Proximal CA1 (close to CA2) receives preferential projections from the MEC and distal CA1 (close to subiculum) is predominantly targeted by the LEC. Thus, if spatial and non-spatial information is meant to be systematically integrated in the hippocampus, it is counterintuitive that the end points of the cortical ‘what’ and ‘where’ streams (i.e. the LEC and MEC) project to different levels in the CA1. Cortical projections aside, intrahippocampal wiring also supports the segregated information flow. Proximal and distal CA1 receive proportionally different inputs from distinct proximodistal levels of the CA3: proximal CA3 (close to DG) targets preferentially distal CA1, while distal CA3 (close to CA2) innervates more proximal CA1 (Ishizuka et al., 1990). Finally, the

projections from the DG to CA3 are also not homogeneous: distinct parts of the DG project differently to distal and proximal CA3 subregions (for more details see later; Claiborne et al., 1986) (**Figure 2**).

Despite this anatomical knowledge being available for a while, very little attention has been paid to the gradients of entorhinal-hippocampal and intrahippocampal wirings. Only recently has functional evidence started to emerge indicating that, at the level of the CA1 and CA3, spatial and non-spatial information is processed preferentially within distinct proximodistal subnetworks (Ku et al., 2023 – co-authored manuscript under revision in *Neuron*; Flasbeck et al., 2018; Nakamura et al., 2013; Beer and Vavra et al., 2018; Henriksen et al., 2011; Nakazawa et al., 2016; Burke et al., 2011). Consequently, a pattern of functionally and anatomically segregated pathways for spatial and non-spatial processing seems to exist not only in the cortical MTL areas, but also in the hippocampal CA1 and CA3 regions.

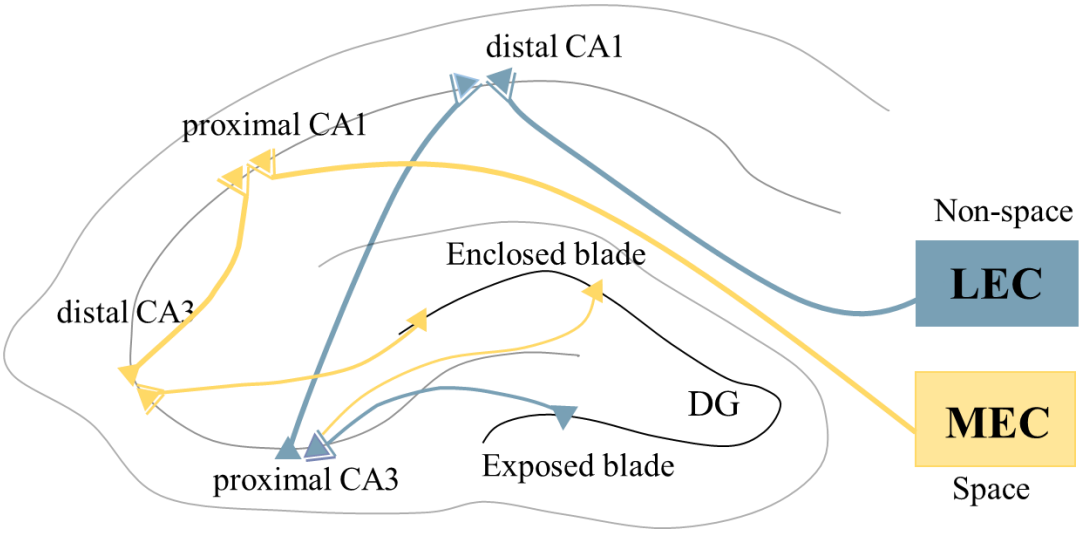

Figure 2: Preferential anatomical connectivity of entorhinal cortex with CA1 and intrahippocampal wiring between CA1, CA3 and DG blades. Anatomical connectivity suggests the existence of hippocampal subnetworks, preferentially involved in spatial or non-spatial information processing. The LEC and MEC project to distinct proximodistal levels in the CA1. Distal CA3 is preferentially wired with proximal CA1, while proximal CA3 – with distal CA1. Distal CA3 receives inputs mostly from the enclosed blade of the DG, while proximal CA3 – from the enclosed and exposed DG blades. Modified from Beer and Vavra et al., 2018.

Anatomical evidence indicates that the DG is also part of the spatial and non-spatial subnetworks, yet, virtually no functional evidence exists to support it. To date, it is believed that the anatomical organisation of the DG supports functional integration in this region (Witter,

2007; also see ‘binding hypothesis’ below). It seems unreasonable, though, that segregated cortical inputs would be integrated upon arrival in the DG but then relayed to functionally distinct hippocampal subnetworks. To clarify this, it must be investigated whether spatial and non-spatial information, similarly to the upstream and downstream areas, is functionally segregated at the level of the DG. Answering this question is the central objective of the present work. But before exploring the experimental goals and questions, let us consider in more detail which parts of the DG might support spatial and non-spatial processing in a segregated manner.

The dentate gyrus

The dentate gyrus (DG) is an area within the hippocampal complex, which in its transverse organisation (plane perpendicular to the longitudinal DG axis) resembles the letter ‘V’ or ‘U’ and can be divided into two parts: the enclosed and the exposed blade. In the present work I use the ‘enclosed/exposed’ nomenclature as was suggested by Witter (2007), since these terms are describing the two subregions independently from the viewing point (e.g. frontal vs horizontal) and are not intermixed with other terms (e.g. supra- vs infrapyramidal mossy fibre bundles – axonal DG projections to the CA3). The enclosed blade (also referred to as inner, suprapyramidal, upper or lateral blade) receives its name from the fact that it is surrounded or ‘enclosed’ by the CA3 and CA1 hippocampal areas. This blade lays opposite to its counterpart – the exposed blade (also known as outer, infrapyramidal, lower or medial blade).

Both DG blades receive most of their input from the LEC and MEC and mainly innervate the hippocampal CA3 area, albeit in a disproportionate manner. Distal CA3 predominantly receives projections from the enclosed blade, while proximal CA3 is targeted by both DG blades (Claiborne et al., 1986). Yet, the connectivity of the proximal CA3 might be stronger with the exposed blade of the DG, since this blade in addition to the main DG-CA3 innervation, i.e. via suprapyramidal mossy fibre bundle, targets the proximal CA3 via infrapyramidal mossy fibre bundle, which courses below the CA3 pyramidal cell layer (Claiborne et al., 1986) **(Figure 3)**.

This anatomical gradient in DG to CA3 innervation suggests that the enclosed and exposed blades of the DG might have differing roles in spatial and non-spatial processing, considering preferentially distinct functional profiles of the distal and proximal CA3 (Ku et al., 2023; Flasbeck et al., 2018; Nakamura et al., 2013; Beer and Vavra et al., 2018). This observation, however, has been overshadowed by reports that the LEC and MEC (in rodents) project to both blades and are likely innervating the same granule cells, but at different dendritic levels (Hjorth-Simonsen and Jeune, 1972; Steward, 1976; Tamamaki, 1997; Wyss, 1981) (**Figure 3**). The LEC

contacts the most distal dendrites of the granule cells (the main excitatory cell type in the DG), in contrast to the MEC, which innervates more middle segments of their dendritic trees. Thus, the consensus is that spatial and non-spatial information carried by the MEC and LEC is integrated in the DG at the level of a single granule cell in both blades of the DG (***'binding hypothesis'***, for reviews see: Lee and Jung, 2017; Kesner, 2018).

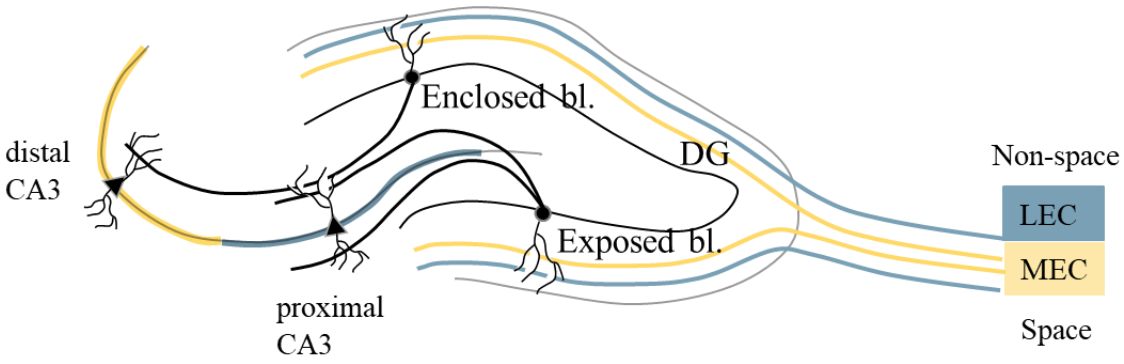

Figure 3: Schematic representation of the information flow to and from the DG. The LEC projects to the distal dendritic portions of the granule cells, the MEC projects closer to the soma. Such anatomical organisation is believed to support integration of spatial and non-spatial information in the DG ('binding hypothesis'). The spatially tuned distal CA3 receives projection mainly from the enclosed blade of the DG; the non-spatially tuned proximal CA3 receives innervation from both DG blades superficially to the pyramidal cell layer and from the exposed blade – deep to the pyramidal cell layer. bl.: blade

Despite the proposed 'binding' role of the DG in spatial and non-spatial processing, several reports indicate that the innervation pattern by the LEC and MEC might be not homogeneous between the enclosed and exposed blades (Wyss, 1981; Tamamaki, 1997; Witter, 2007; for details see Chapter III). This implies that, while different information types could converge in the DG, the two blades may still be preferentially tuned to differing inputs. Moreover, the two blades might have fundamentally different organisation, for example in their local circuits, which might be another reason behind the hypothesised functional segregation of spatial and non-spatial information processing in the DG. In line with this argumentation, a variety of studies have reported differences between the DG blades regarding their organisation and functional relevance in certain processes. I will summarise these differences in the following section.

The dentate gyrus is a heterogeneous structure

Cellular and morphologic differences

The enclosed and exposed blades of the DG exhibit different transcriptomic profiles. A recent study by Wang et al. (2022) identified 161 transcripts enriched in the enclosed blade, which differ from the 88 transcripts enhanced in the exposed blade. These differences likely represent different cell types within the blades; for example, the enclosed blade contains a specific subset of Penk-expressing granule cells (*semilunar granule cells*: Williams et al., 2007; Erwin et al., 2020). Neurogenesis – the birth of new neurons in the adult brain - occurs at initially higher rates in the exposed blade, but those cells are less likely to survive, which leads to comparable levels of the newborn cells between the blades (Snyder et al., 2012). The enclosed blade is under stronger inhibitory control, as illustrated by the number of inhibitory cells present in this region (Scharfman 2002; Woodson et al., 1989; Seress and Pokorny, 1981; Meyer et al., 2020). The blades also differ in their dendritic morphology, with the enclosed blade having a greater dendritic length, a higher number of the dendritic segments, a higher density of spines and a higher number of mushroom spines (Claiborne et al., 1990; Desmond and Levy, 1985). The dendritic field spread of this blade is more transverse, while that of the exposed blade is rather longitudinal (Desmond and Levy, 1982). The development of the blades follows different ontogenetic profiles (Pérez-Delgado et al., 1992; Gould et al., 1991; Schlessinger et al., 1975), with the majority of the cells in the enclosed blade being born during the embryonic stages and those in the exposed blade born postnatally (Altman and Bayer, 1990; Ha et al., 2020). Also, the perforant path and the commissural/associational (C/A) innervation systems develop at different time points and in opposing order, with C/A fibres arriving after the perforant path in the enclosed blade, but entering the exposed blade before the perforant path (Fricke and Cowan, 1977; Tamamaki 1999). Moreover, the innervation by C/A projections is not homogeneous across blades, with the ratio of the commissural to associational fibres being 1:3 in the enclosed blade, but 1:1 in the exposed blade (Gottlieb and Cowan, 1972). Further, the enclosed and the exposed blades differ in the distribution and functional roles of several receptors, particularly metabotropic glutamate receptors (Shigemoto et al., 1997; Huang et al., 1999; Rush et al., 2001; Rush et al., 2002; Wang et al., 2016; Lawston et al., 2000).

Vulnerability to different conditions

The exposed blade is more vulnerable to ageing processes (Sugaya et al., 1996; Simonyi et al., 2000). This is in line with the evidence from human and rodent studies reporting hyperactivity

in the CA3/DG network as a hallmark of ageing and pathologic cognitive decline (Reagh et al., 2018; Yassa et al., 2011; Fontana et al., 2017). Detrimental hyperactivity is also a well-known feature of the DG accompanying the epilepsy development (Dengler and Coulter, 2016; Lynch and Sutula, 2000). As with ageing, the exposed blade of the DG seems to be more affected in epilepsy (Scharfman, 2002; Druga et al., 2010; Kim et al., 2004; Covolan and Mello, 2000). The enclosed blade, on the other hand, seems to be more vulnerable to alcohol consumption (Cadete-Leite et al., 1997), hypoxia (Kreisman et al., 2000; Hara et al., 1990) and ischemia (Pforte et al., 2005).

Functional differences outside of cognition

Differential roles of the blades have been established in sleep and stress. The enclosed blade is activated during the awake state and the REM-sleep, while the exposed blade is preferentially activated during sleep (Yamazaki et al., 2021). Consequently, sleep deprivation affects the activity and causes spine loss in the exposed, but not the enclosed blade (Wang et al., 2023; Raven et al., 2019). There are mixed reports regarding the stress-induced responses of the blades. Some studies indicate a selective role of the enclosed blade in stress (Chandramohan et al., 2006). However, others report that stress affects the exposed blade of the DG, while leaving the enclosed blade unaffected (Hoffman et al., 2014). Also, some studies report that stress affects both DG blades but in an opposing manner (Fevurly and Spencer, 2004; Alves et al., 2017).

Cognitive differences

The evidence from a few studies that report differences in the DG blades' involvement in cognitive tasks indicates that the enclosed blade of the DG might play a specific role in spatial exploratory/navigation or spatial mnemonic tasks (Ramírez-Amaya et al., 2005, Chawla et al., 2005, Soulé et al., 2008; Satvat et al., 2011; Snyder et al., 2011). These studies use molecular imaging techniques, for example, immunohistochemistry or *in situ* hybridization for visualisation of immediate early genes (IEG) – markers of neuronal activation. However, among the commonly used IEGs, only *Arc* reliably reflects task demands (Guzowski et al., 2001) and is tightly connected to memory processes (Sauvage et al., 2013). Yet, its temporal kinetics in the DG (but not CA1 or CA3) do not allow for a direct linking of the detected neuronal activity to an isolated episode (e.g. memory retrieval), since *Arc* RNA transcription in the DG is prolonged and detectable up to eight hours following an event (Ramirez-Amaya et al., 2013). Thus, the results of the above-mentioned studies should be treated cautiously. Furthermore, two studies potentially support the role of the exposed blade in non-spatial

memories (Hoang et al., 2018; Chaillan et al., 1997). The study by Hoang et al. (2018) used IEGs *Homer* and *Arc* as markers for neural activity and hence, a similar caution should be applied to this study. The study by Chaillan et al. (1997) correlated the extent of the DG lesions to the rats' behavioural performance in an olfactory mnemonic task. The lesions were usually covering both blades of the DG and therefore, a contribution of the enclosed blade lesions to the observed behavioural deficits cannot be excluded

Overall, the data indicate that the enclosed blade might be specifically important for spatial processing, while non-spatial processing could be supported by the exposed blade. Still, the evidence for this remains correlational and scarce. Moreover, no studies investigated the roles of either of the blades in both spatial and non-spatial memories. Anatomical evidence as illustrated by the projections from the DG to CA3, however, points out that the two blades of the DG likely support spatial and non-spatial memories to a different extent. This hypothesis is further supported by the evidence summarised in the last paragraphs, which indicates that the enclosed and exposed blades of the DG are different from each other in multiple aspects, including structurally and functionally. Thus, the main goal of the present work is to investigate whether spatial and non-spatial memories are processed in a segregated manner in the DG, with its blades being the potential sites of segregated information processing.

Outline of the thesis

The overall aim is to explore the routes through which spatial and non-spatial information are processed, with particular focus paid to the DG and its blades. The following questions will be investigated: 1) What is the role of the enclosed blade of the DG in spatial and non-spatial memories? 2) How does its counterpart, the exposed blade, contribute to spatial and non-spatial memories? 3) Are the enclosed and exposed blades further elements of the spatial and non-spatial hippocampal subnetworks? 4) Are the functional roles of the blades supported by a pattern of cortical projections to the DG?

In Chapter II, the role of the enclosed and exposed blades of the DG in terms of spatial and non-spatial memory is described. I investigated the effects of preferential optogenetic inactivation of the enclosed or exposed blade on memory performance in murine object-location and object-recognition tasks.

In Chapter III, the focus shifts to the hippocampal spatial and non-spatial subnetworks. In particular, I investigated whether the DG blades are parts of the downstream CA1-CA3 spatial and non-spatial subnetworks. For this purpose, I performed high resolution molecular imaging

based on the detection of the immediate early gene *Arc* to investigate the activity of the CA1-CA3 subregions during retrieval of spatial and non-spatial memories upon optogenetic silencing of the enclosed or the exposed blade of the DG.

In Chapter IV, I investigated whether the functional segregation of the DG blades, reported in Chapter II, is supported by a pattern of anatomical innervation arising from the cortical areas. Specifically, the tested hypothesis was whether the enclosed and exposed blades of the DG receive proportionally different inputs from the MEC and LEC, which are differently tuned to spatial and non-spatial processing. To this aim, I performed retrograde fluorescent tracing of the perforant path origins in optically cleared mouse brains.

Finally, the results of the experiments and their implications are discussed in Chapter V. The findings reveal a missing piece of the puzzle regarding the segregated information flow in the MTL networks and show that, in addition to the MTL cortical areas and the hippocampal CA1 and CA3 regions, spatial and non-spatial information also remains functionally segregated (at least under specific circumstances) at the level of the DG.

II.

Spatial and Non-spatial Memory Processing in the Enclosed and Exposed Blades of the Dentate Gyrus

Introduction

The dentate gyrus (DG) is a part of the hippocampus, believed to play a key role in discriminating highly similar inputs via a process known as pattern separation (Leutgeb et al., 2007; Jung and McNaughton, 1993; McHugh et al., 2007; Clelland et al., 2009; Gilbert et al., 2001). Studies supporting this idea are typically performed in spatial behavioural settings and thus, it is well-established that the DG supports spatial information processing. Successful discrimination of mnemonic events, however, requires not only the processing of spatial but also of non-spatial information. To date, it is thought that the latter processing mainly occurs in brain regions other than the DG, for example, the perirhinal and the lateral entorhinal (LEC) cortices, olfactory bulb, and amygdala (Bartko et al., 2007; Petrulis et al., 2005; Gschwend et al., 2015; Gilbert and Kesner, 2002; but see Miranda et al., 2021; Bakker et al., 2008; Yassa et al., 2010). However, it is well-known that non-spatial information reaches the DG via a strong

projection originating in the LEC (Witter, 2007; Deshmukh et al., 2012; Deshmukh and Knierim, 2011; Tsao et al., 2013). Spatial information, on the other hand, is believed to be relayed to the DG by efferents of the medial entorhinal cortex (MEC) (Witter, 2007; Fyhn et al., 2008; Tennant et al., 2018; Hargreaves et al., 2005). Consequently, it is plausible to assume that the DG is involved in processing both spatial and non-spatial information.

Both entorhinal subdivisions project to the same granule cells in the DG, but at distinct proximodistal levels of the dendritic tree (Hjorth-Simonsen and Jeune, 1972, Steward, 1976), possibly suggesting a conjoint processing of the spatial and non-spatial information within the DG. Few studies indicate, however, that the pattern of the LEC/MEC to DG projection differs between the enclosed and exposed blades (Wyss, 1981; Tamamaki, 1997). Moreover, it has been shown that the distal part of CA3, which is preferentially involved in spatial processing (Beer and Vavra et al., 2018; Flasbeck et al., 2018), predominantly receives projections from the enclosed blade of the DG. The exposed blade, in contrast, seems to innervate more the proximal CA3 (Claiborne et al., 1986), which is mainly supporting non-spatial processing (Ku et al., 2023; Nakamura et al., 2011). Consequently, one might hypothesise that the enclosed blade of the DG is preferentially spatially tuned, while the exposed blade is predominantly the site of non-spatial processing.

Supporting this hypothesis, a few immediate early gene (IEG) studies revealed a selective recruitment of the enclosed blade upon spatial exposure. For example, novel environment exploration leads to an increased *Arc* expression in the enclosed, but not the exposed blade of the DG (Ramírez-Amaya et al., 2005, Chawla et al., 2005). Exploration of the spatial configuration of objects similarly increases *Arc* expression in the enclosed blade of the DG (Soulé et al., 2008). Expression of other IEGs (*c-Fos* and *Zif268*) is also found preferentially in the enclosed as opposed to the exposed blade when rats engage in spatial memory or navigation tasks (Snyder et al., 2011, Satvat et al., 2011). In contrast, the activity of the exposed blade seems to be correlating with performance in non-spatial tasks (Hoang et al., 2018; Chaillan et al., 1997). Overall, however, the cumulative evidence remains sparse and correlative.

To address the hypothesis, I investigated the causal relevance of the enclosed and exposed blades of the DG for spatial and non-spatial memories. I implemented optogenetic silencing of cell firing preferentially in the enclosed or exposed blades *in vivo* in mice engaging in spatial and object recognition tasks, specifically designed to maximise the DG's recruitment (Van Hagen et al., 2015; Oulé et al., 2021).

Methods

Animals: Ten- to fifteen-week-old male C57BL/6N mice bred at the Leibniz Institute for Neurobiology, Magdeburg were used (n=103). Mice were group-housed prior to the experiments. Following surgery, subjects were single-housed and kept under a reversed 12-hour light/dark cycle (7.00 A.M. light off; 7.00 P.M. light on). All animals received ad libitum access to food and water at all times. All procedures were approved by an ethics committee of the State of Saxony-Anhalt under the licence 42502-2-1555 LIN and carried out in accordance with the European Communities Council Directive of September 22nd, 2010 (2010/63/EU).

Spatial and non-spatial memory performance assessment

To investigate the effects of the enclosed or exposed blade inhibition upon spatial and non-spatial memory performance, mice were tested in one-trial learning paradigms similar to the classical object-location and object-recognition tasks. These tasks use the natural preference of rodents to explore novel stimuli (locations/objects) as opposed to familiar ones (Ennaceur and Delacour, 1988). The tasks were modified from their original versions to maximise the recruitment of the DG, which is assumed to be involved in discriminating highly similar stimuli by performing pattern separation (Van Hagen et al., 2015; Oulé et al., 2021). Thus, the spatial

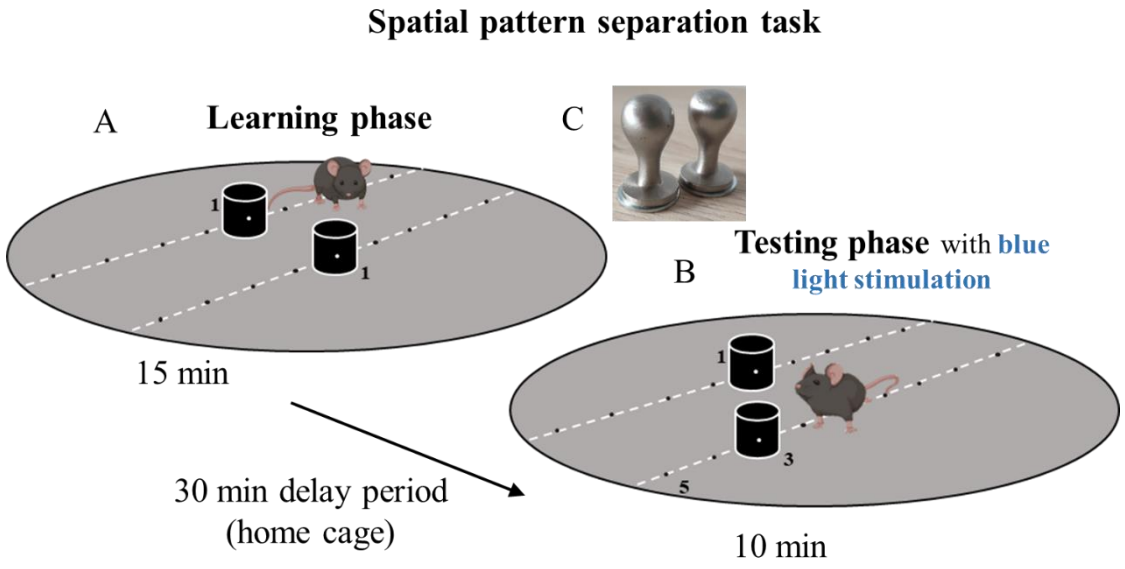

Figure 4: Schematic illustration of the spatial pattern separation (SPS) task. A: positioning of objects during the learning phase. B: positioning of objects during the testing phase C: Photograph of the objects used in the SPS task. Inhibition of cell firing in the enclosed or the exposed blade of the DG occurred during the testing phase of the task.

and the non-spatial task versions test the ability of animals to detect *small* changes in the spatial layout of objects or objects' features.

Spatial (SPS) and object pattern separation (OPS) tasks

The tasks were performed as described previously (Oulé et al., 2021). In the SPS task, animals were familiarised with two identical objects (**Figure 4C**) placed at central positions (positions 1) in a round arena (40 cm in diameter; 50 cm high) for 15 minutes (learning phase) (**Figure 4A**). Afterwards, mice were returned to their home cage for a 30-minute-long delay period and then reintroduced to the same arena for 10 minutes (testing phase). In the testing phase, one of the objects remained at position 1, while a second object was moved along its vertical axis away from the centre to position 3 (**Figure 4B*)***. Of note, the displacement in the SPS task (position 1 vs 3) is more difficult to detect than in standard versions of object-location tasks (position 1 vs 5) and hence, it is more likely that the DG is recruited under such conditions (Van Hagen et al., 2015). The displaced object and the possible new locations were counterbalanced between the animals. After each phase, the testing arena and the objects were cleaned with a 10% ethanol solution.

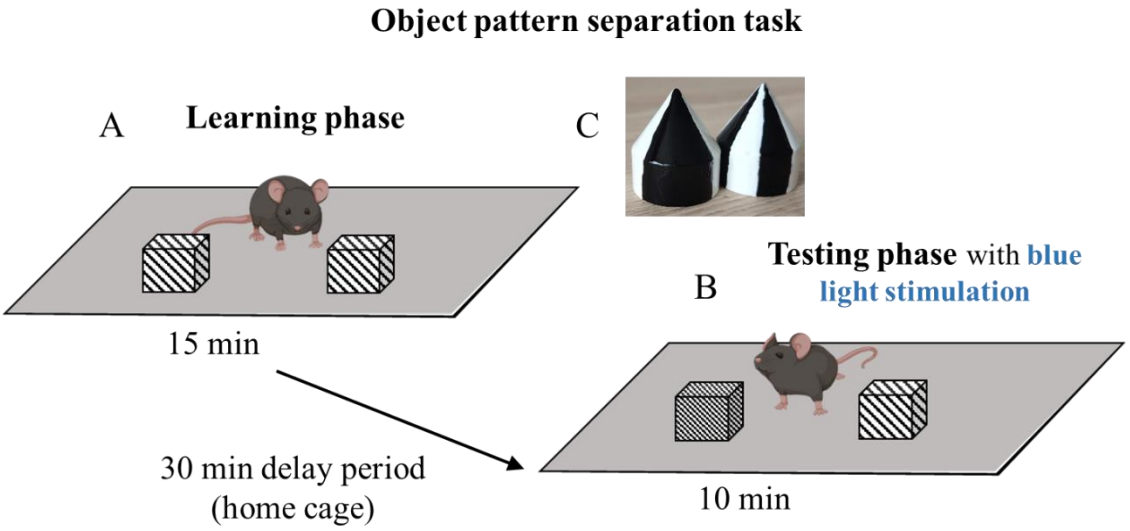

Figure 5: Schematic illustration of the object pattern separation (OPS) task. A: learning phase. B: testing phase C: Photograph of the objects used in the OPS task. Inhibition of cell firing in the enclosed or the exposed blade of the DG occurred during the testing phase of the task.

A similar procedure to the SPS was used during the OPS task. In the learning phase (**Figure 5A**), animals were familiarised with two identical objects (**Figure 5C**) placed in the adjacent

corners of a square arena (30x30x40 cm). After the delay period, mice were reintroduced to the arena, in which one of the objects was exchanged for a new one with highly similar features (**Figure 4F**). To avoid any biassed results due to side preferences, the positions of the objects during the learning and the test phases were counterbalanced across animals.

Handling and habituation

Mice were handled following the recovery from viral injections and optic fibre implantation for five days. Subsequently they were habituated to the testing procedure for nine days over the period of eleven days. On days 1-2, animals were habituated to an empty open field arena. On days 3-5 and 8-11, animals were habituated to the presence of two different objects in an arena twice per day (5-minute-long trials with 30-minute-long intertrial interval). On day 12, mice were tested in spatial or object pattern separation tasks.

All behavioural procedures were carried out in a dimly lit room with low-amplitude white noise. Behaviour was recorded with a camera (Sony Handycam, FDR-AX53) positioned above the testing arena.

Behavioural analysis

Behavioural performance was evaluated as time spent exploring objects and scored manually off-line by two independent experimenters blind to the experimental conditions and then averaged. The scores of both experimenters were highly correlated ($r=0.85$, $p<0.001$). Exploration behaviour was defined as interaction (looking, sniffing, licking) with an object in close proximity (less than a head-length distance to objects). Climbing, sitting on or touching the objects while looking at a different point in the arena were not considered exploration behaviour. Memory performance was quantified as a discrimination ratio calculated for the testing phase using following formula:

$$\frac{(\text{Exploration time displaced/novel object}) - (\text{Exploration time stationary/familiar object})}{\text{Total exploration time}}$$

A discrimination ratio higher than zero (no preference for either of the objects is reflected by numbers close to zero) indicates a successful memory performance (Ennaceur and Delacour, 1988). Mice that did not reach exploration times of at least 10 seconds for each object during the learning phase were excluded from the analysis (Ennaceur and Delacour, 1988; Beer et al., 2013).

Enclosed and exposed blades' inactivation during memory retrieval

To transiently inactivate cell firing in one of the DG blades, an inhibitory opsin ArchT was expressed in the excitatory cells of the enclosed or the exposed blade leading to neuronal silencing upon blue light stimulation.

Experimental animals received stereotactic intracranial injections of AAV5-CamKII-ArchT-GFP (titer: ≥ 7×10^{12} vg/mL; Addgene, USA) three weeks before the memory test to allow for maximal ArchT expression. Injections were placed in the enclosed (60 nl per hemisphere; coordinates in reference to bregma: AP -2.0; ML ±1.45; DV -1.65 mm) or the exposed blade of the DG (40 nl; AP -2.0; ML ±1.3; DV -2.35 mm). Animals with no clear preferential AAV spread in the enclosed or the exposed blade of the DG identified by histological assessment were excluded from further analyses. Optical fibres were implanted during the same surgery above the enclosed (1.8-mm-long) or the exposed (2.3-mm-long) blade (Plexon Inc., USA). Continuous blue light (465 nm) was delivered through optic cables connected to an LED driver system (Plexon Inc., USA) for the whole duration of the testing phase. Optic cables were attached to the fibre implants on the animals shortly before the start of the test phase. In control animals, light stimulation did not occur.

Evidence for granule cell firing inhibition via ArchT stimulation

To verify that ArchT effectively silenced granule cells, spontaneous activity of the granule cells in the enclosed blade of the DG was recorded during periods (10 trials) of light-on (60 s) and light-off (60 s) stimulations in an anaesthetised mouse (n=1) three weeks after the AAV injection surgery. The mouse was anaesthetised with a ketamine-xylazine mixture, placed in a stereotactic frame and an optrode was lowered to the granule cell layer of the enclosed blade.

Optrodes were built by glueing a glass-coated tungsten electrode (Alpha-Omega, Israel, 0.5MΩ, shank diameter 125uM, total diameter 250uM) to a 200-µm-thick optical fibre (Plexon Inc., USA) with a maximal tip-to-tip distance of 300 µm. Broadband neural activity was continuously recorded, with intermittent periods of light application (Neuralynx Digital Lynx SX, USA; band-pass filter 0.5Hz~8 kHz, 32 kHz sampling rate). The optogenetic stimulation and electrophysiology recordings were synchronised through a DAQ system with customised LabView scripts (National Instrument, USA). After recording, mice were perfused with 4% paraformaldehyde for histological analysis of the optrode location and AAV spread. For opto-electrical recordings data analysis was performed with customised MATLAB codes

(Mathworks, 2018). Broadband recordings were high-pass filtered at 300 Hz. Multiunit activity was detected by thresholding at four standard deviations above baseline.

Stereotactic Surgeries

Mice were anaesthetised using ketamine 10 mg/kg and xylazine 20 mg/kg i.p., their eyes covered with moisturising balm, and placed into a stereotactic frame (Kopf Instruments, USA) with a mouse adaptor (Stoelting, Germany). After injecting Carprofen (0.2 ml of 1mg/ml) s.c. in the neck area, the skin on the head was shaved and treated with betadine. 0.5% Bupivacaine (0.05 ml) was injected in the head skin and the skull was exposed. Stereotactic coordinates were calculated from bregma. Craniotomies were performed using a drill with a 0.6-mm-wide drill bit (Proxxon, Germany). Injections were performed using a glass fibre pipette attached to a Nanoject II (Drummond Scientific, USA). The needle was left in place for 10 minutes after the injection to prevent the backflow of the virus and then slowly withdrawn. For implantation of the optic fibres, the surface of the skull was thoroughly dried, scratched with a scalpel blade and the implants were fixed to the skull using dental cement. After surgery, mice were injected with saline (0.5 ml s.c.) to protect from dehydration and treated with Carprofen chewing tablets as painkillers for three consecutive days.

Histology

Following behavioural experiments, brains were removed, flash frozen in isopentane and stored at -80°C until sectioning. 20-µm-thick sections were cut in coronal plane on a cryostat (Leica CM 3050 S; Leica Biosystems, Germany) and mounted on polylysine-coated slides. Virus spread and optic fibre placement was assessed on digital images captured with a Keyence Fluorescence Microscope (BZ-9000E; Japan) using a 2× objective lens.

Statistical analysis

Statistical analyses were performed using SPSS software (version 27, IBM, SPSS Inc.).

All data sets were tested for deviations from normal distribution using the Shapiro-Wilk test for appropriate use of parametric data analysis. All data followed the normal distributions, with the exception of the cell firing data collected to assess the efficiency of optogenetic inactivation. These data were logarithmically transformed to approximate the normal distribution (note: in the results section the non-transformed data were graphically presented). To evaluate the effects of the enclosed and exposed blade inhibition on spatial and non-spatial memory performance, one-sample t-tests were performed to establish whether group performances are different from the chance level. Furthermore, a three-way ANOVA was calculated to compare the

performances between different groups. The following variables were set as between-subject factors: ‘blade’ (enclosed or exposed), ‘inhibition’ (ArchT/light-on or ArchT/light-off) and ‘task’ (spatial or object). Specific pairwise comparisons were carried out in post-hoc analyses with two-sample t-tests with Bonferroni corrections.

Results

Cell firing inhibition of the enclosed or the exposed blade of the DG

To achieve optogenetic inhibition of cell firing predominantly in the enclosed or the exposed blade, the appropriate conditions of viral injections needed to be established first. The results suggested that it was feasible to restrict the viral spread preferentially to the enclosed blade of the dorsal DG by injecting a small volume (60 nl) of AAV-CamkII-ArchT-GFP and targeting the molecular layer of the enclosed blade. To reliably restrict the viral spread to the exposed blade of the DG, further reducing the injection volume and targeting the molecular layer of the exposed blade proved helpful. For behavioural assessments, final volumes of 60 nl and 40 nl of AAV-CamKII-ArchT-GFP were injected bilaterally into the enclosed or the exposed blades, respectively (**Figure 6**).

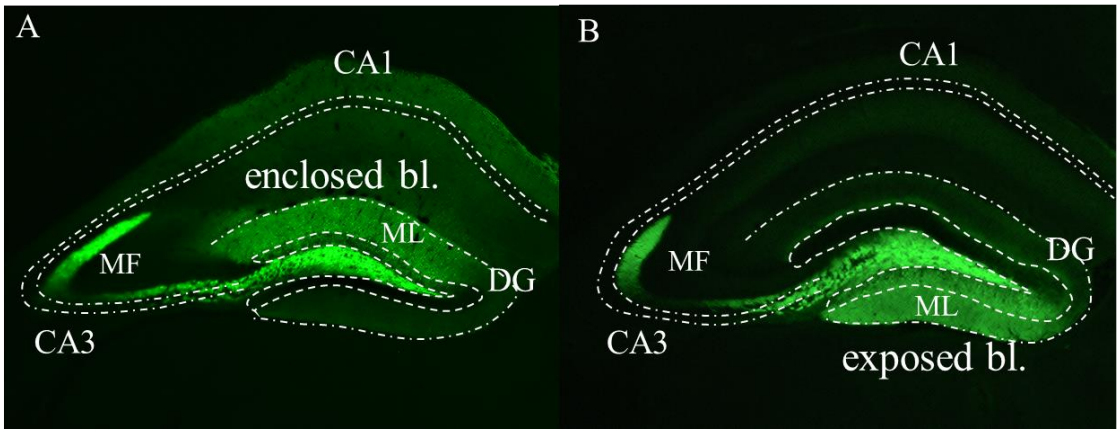

Figure 6: Exemplary expression of AAV-CamKII-ArchT-GFP injected in the enclosed (A) or the exposed (B) blade. White dashed lines delineate the borders of the granule and pyramidal cell layers as well as the molecular layer in the DG. bl: blade; ML: molecular layer; MF: mossy fibres (DG axons).

Controlling the inhibition of DG granule cells' spontaneous activity by ArchT stimulation

To transiently inactivate the granule cells, an adenoviral vector expressing ArchT (archaerhodopsin from Halorubrum strain TP009) was injected into the targeted blade. ArchT is an outward proton pump, which upon light stimulation allows for optogenetic inhibition of the infected neurons (Han et al., 2011). To verify that ArchT effectively induced granule cell silencing, spontaneous activity of the granule cells in the enclosed blade of the DG was recorded during periods (10 trials) of light-on (60 s) and light-off (60 s) stimulations in an anaesthetised mouse (**Figure 7**).

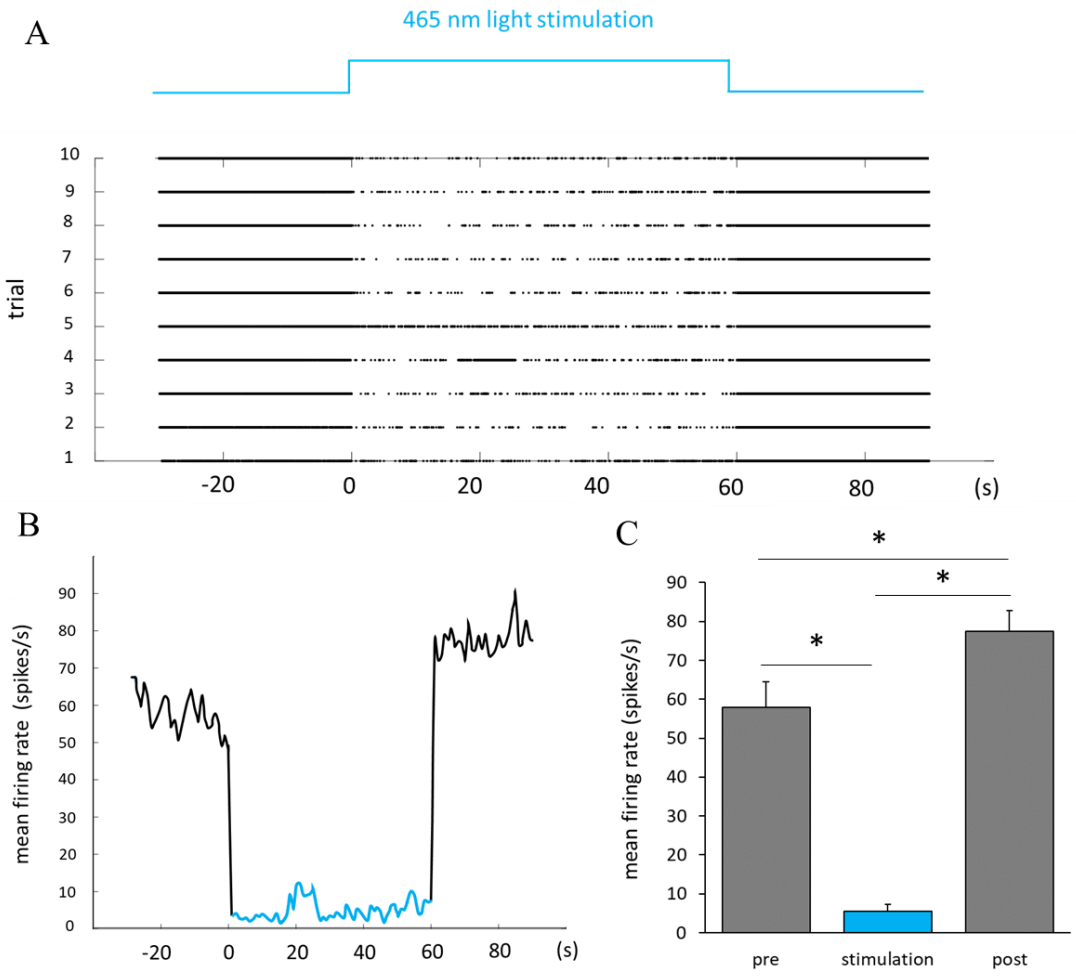

Figure 7: Inhibition of granule cell firing upon blue light stimulation. A: raster plot of firing activity in 10 trials (120s per trial: 30 s pre-stimulation, 60 s 465 nm light stimulation, 30 s post-stimulation). B: Mean firing rate of the granule cells across 10 trials. C: Mean firing rate averaged for pre-stimulation, stimulation and post-stimulation periods. Blue light stimulation of the ArchT effectively reduced spontaneous cell firing activity in the enclosed blade of the DG *: $p < 0.001$.

Results show that the firing rate of granule cells was drastically reduced during stimulation with blue light (465 nm) and fully recovered during the post-stimulation period (one-way ANOVA

with repeated measurement, stimulation effect: $F_{(1.088,\ 9.789)}$=125.24, p< 0.001; of note, the degrees of freedom were adjusted (Greenhouse-Geisser correction) due to non-sphericity of the data; post-hoc comparisons: pre vs stimulation: p<0.001, 95% C.I. [0.79, 1.43]; stimulation vs post: p<0.001, 95% C.I. [-1.54, -0.96]; pre vs post: p=0.001, 95% C.I. [-0.222, -0.065]; Bonferroni corrected) (**Figure 7**).

Preferential inactivation of the enclosed or exposed blade of the DG causes domain-selective behavioural deficits

To directly address the contribution of the DG blades to spatial and non-spatial information processing, the behavioural performance of mice engaging in spatial or non-spatial pattern separation tasks was evaluated during transient inhibition of the enclosed or the exposed blade. These tasks exploit the innate preference of rodents to explore novel objects (non-spatial) or novel locations (spatial), which reflects their recognition ability (memory) for objects and locations (Ennaceur and Delacour, 1988). These tasks were adapted from the standard versions of the object-recognition and object-location tasks to increase the engagement of the DG, which is expected to be involved in discriminating highly similar inputs by performing pattern separation. Thus, the tasks used stimuli (objects/locations) with a higher degree of similarity than the classical versions of object-location and object-recognition tasks.

The results revealed that control groups (ArchT/light-off) showed a discrimination index significantly above zero for both spatial and object tasks (one-sample t-tests, two-tailed, light-off: enclosed blade/spatial task: $t_{(8)}$=4.30; p=0.003; enclosed blade/non-spatial task: $t_{(13)}$=5.85, p<0.001; exposed blade/spatial task: $t_{(7)}$=8.11, p<0.001; exposed blade/non-spatial task: $t_{(11)}$=6.50, p<0.001). Thus, ArchT expression in the enclosed or the exposed blades of the DG without light stimulation at retrieval did not *per se* impair the animals' capability to detect small changes in objects' locations or features.

Animals that did receive light stimulation during the testing phase of the tasks (inhibition groups) showed different performance patterns. The enclosed blade inhibition group had a discrimination index that did not significantly differ from zero in the spatial task (one-sample t-test, two-tailed: $t_{(7)}$=-0.49, p=0.641), but had a discrimination index significantly higher than zero in the non-spatial task (one-sample t-test, two-tailed: $t_{(14)}$=6.24, p<0.001). This indicates that inhibition of the enclosed blade causes selective deficits in spatial but not non-spatial discriminations. Conversely, the exposed blade inhibition group had a discrimination index that did not significantly differ from zero in the non-spatial task (one-sample t-test, two-tailed: $t_{(10)}$=1.24, p=0.244), while the discrimination index was significantly higher than zero for this

group in the spatial task (one-sample t-test, two-tailed: $t_{(7)}=3.67$, $p=0.008$). This shows that inhibition of the exposed blade, in contrast to the inhibition of the enclosed blade, affects non-spatial memory only.

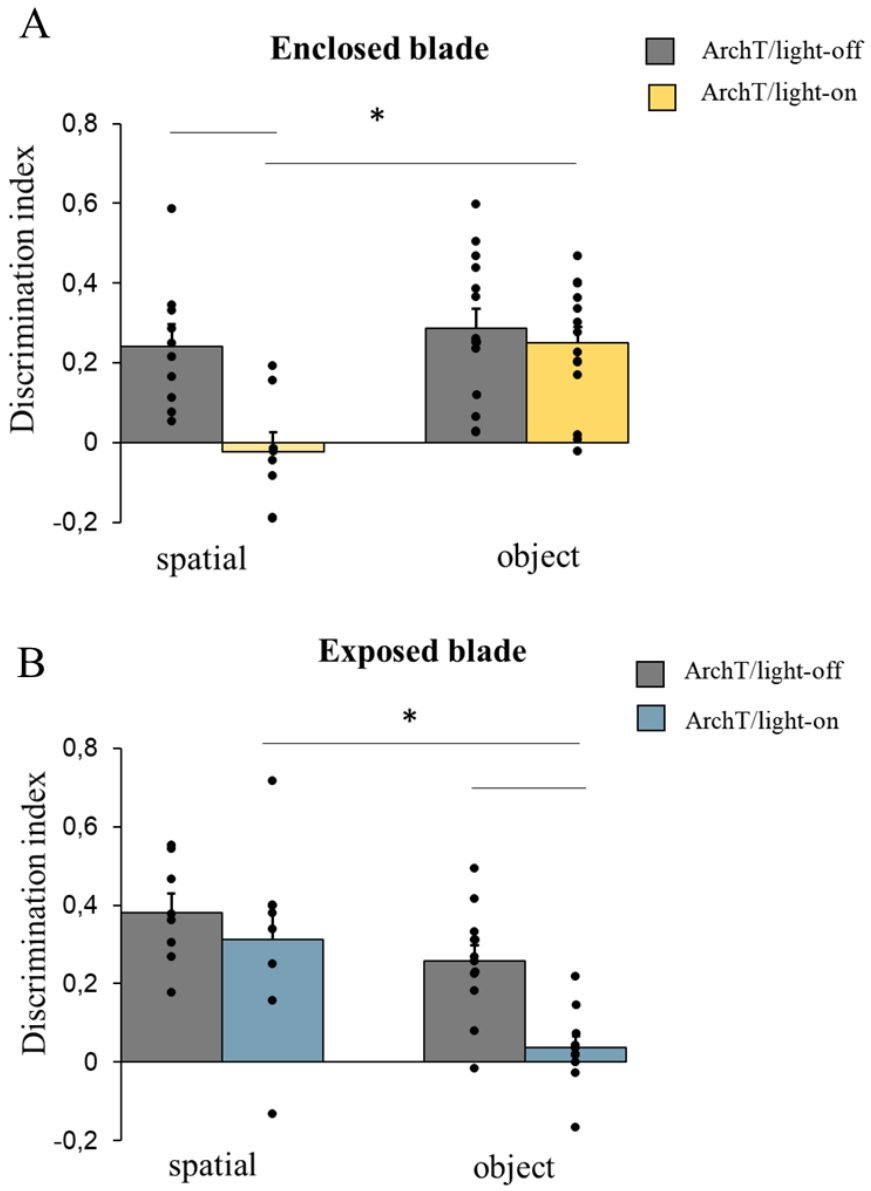

Figure 8: Behavioural performance of mice with enclosed (A) and exposed (B) blade inhibition in non-spatial (object) and spatial memory tasks. Enclosed blade inhibition selectively affected memory performance in the spatial version of the tasks. Exposed blade inhibition affected only memory performance in the non-spatial version of the tasks. *: $p<0.050$. Error bars: Mean + SE.

A direct comparison of the effects of enclosed and exposed blades' inhibition on memory performance revealed a significant main effect of inhibition (three-way ANOVA with blade

(enclosed/exposed), inhibition (light/no-light), task (spatial/object) as between-subject factors: main effect of 'inhibition': $F_{(1,77)}=17.07$, $p<0.001$; no significant effects of 'task'or 'blade'p-values >0.050). The average discrimination index of all control groups was significantly higher than the average discrimination index of all inhibition groups. Importantly, a significant interaction effect of 'inhibition × blade × task' was found ($F_{(1,77)}=7.17$, $p=0.009$). This indicated that differential effects of 'blade', 'inhibition' and 'task' existed between specific pairwise group comparisons (**Figure 8**).

Post-hoc pairwise comparisons revealed that mice with enclosed blade inhibition performed significantly worse in the spatial task in comparison to (1) their controls, (2) mice with exposed blade inhibition and (3) in comparison to the animals in the object task but with similar inhibition (i.e. enclosed blade) (spatial task/enclosed blade (light-off vs. light-on): $t_{(15)}=3.50$, $p=0.018$; spatial task/light-on (enclosed vs. exposed): $t_{(14)}=-3.42$, $p=0.024$; enclosed blade/light-on (spatial vs object): $t_{(21)}=-4.16$, $p=0.006$). However, no performance differences in the spatial task were detected between mice with exposed blade inhibition and their controls (spatial task/exposed blade (light-off vs. light-on): $t_{(14)}=0.70$, $p>0.050$). This suggests that the enclosed, but not the exposed blade of the DG, contributes to spatial memory retrieval. Conversely, in the non-spatial task, mice with exposed blade inhibition showed a reduced discrimination index when compared to (1) their controls, (2) to mice with enclosed blade inhibition or (3) to mice with a similar exposed blade inhibition but in the spatial task (object task/exposed blade (light-off vs. light-on): $t_{(21)}=4.43$, $p=0.006$; object task/light-on (exposed vs. enclosed): $t_{(24)}=-4.02$, $p=0.006$; exposed blade/light-on (spatial vs. non-spatial): $t_{(17)}=3.47$, $p=0.018$). Yet, the performance of the enclosed blade inhibition group and their controls was similar in the non-spatial task (object task/enclosed blade (light-off vs. light-on): $t_{(27)}=0.57$, $p=0.999$). This indicates that the exposed, but not the enclosed blade, contributes to non-spatial memory retrieval.

Occasionally, a slight GFP expression was observed in the CA1 area of the animals with enclosed blade injections. To investigate the extent to which the abovementioned spatial behavioural deficit observed in the enclosed blade inhibition group stems from CA1 inactivation, a subset of mice (n=9) received optical fibre implantation above the CA1 area with the same injection as other animals (i.e. injection in the enclosed blade of the DG). Both inhibition and control groups showed discrimination indices significantly above zero with no significant differences between the groups (spatial task, one-sample t-tests, comparisons to zero, two-tailed: light-off: $t_{(2)}=7.96$, $p=0.015$; light-on: $t_{(5)}=3.63$, $p=0.015$; two-sample t-test, two-tailed, light-off vs. light-on: $t_{(7)}=0.571$, $p=0.586$) (**Figure 9A**). Moreover, increasing the

ArchT expression in CA1 (fibre placement and ArchT injection in CA1; 1000 nl per hemisphere instead of previous 60 nl in the DG, n=8) also did not affect the performance of animals in the spatial task (one-sample t-tests, comparisons to zero, two-tailed: light-off: $t_{(2)}$=5.67, p=0.030; light-on: $t_{(4)}$=3.95, p=0.017; two-sample t-test, two-tailed, light-off vs. light-on: $t_{(6)}$=0.67, p=0.529) (**Figure 9B**). This suggests that CA1 unlikely contributes to a critical extent to the effects reported on spatial memory upon enclosed blade inhibition.

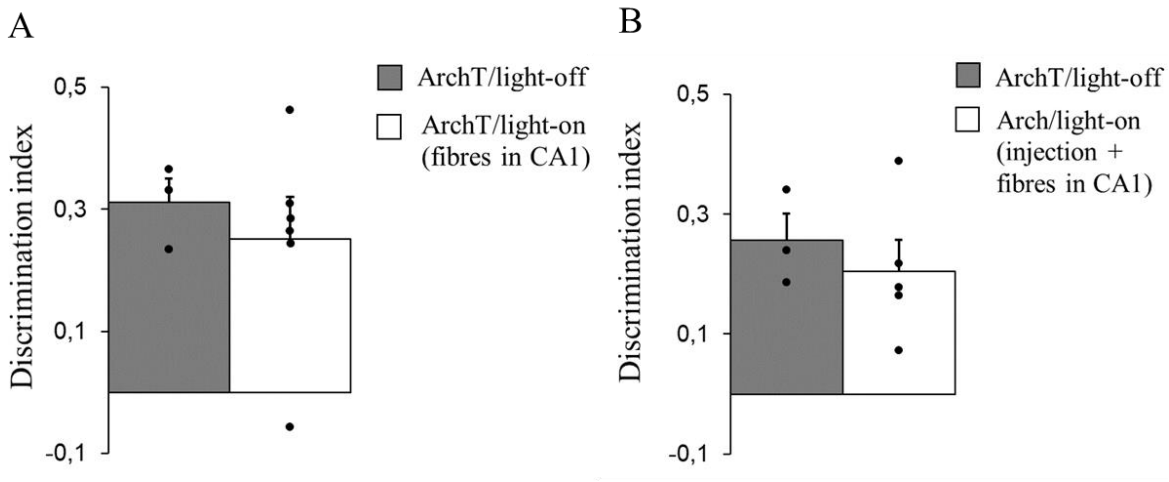

Figure 9: Behavioural performance of CA1 control mice in the spatial memory task. A: ArchT injected in the enclosed blade, but the optic fibres placed above the CA1 area. B: both, ArchT and optic fibres, in CA1. All groups showed an intact spatial memory performance. No significant differences were observed between the control and the inhibition groups. Error bars: Mean + SE

Together, these results show that the enclosed blade of the DG, potentially independently from the CA1, is critical for the retrieval of spatial information, while the exposed blade processes the object-related information.

Discussion

The present study provides new evidence regarding the role of the DG in memory-related processes. It shows that the DG is a functionally heterogeneous structure, processing spatial and non-spatial information in anatomically segregated subregions, namely the enclosed and exposed blades of the DG. By preferentially perturbing one blade or the other it was established that the enclosed blade is carrying out spatial mnemonic discriminations and is not required for the retrieval of the non-spatial ones. In contrast, the exposed blade is involved in non-spatial discriminations and does not play a role in tasks with more spatial demands.

Integration of the results

In accordance with the present results, several studies indicate a role of the enclosed blade in behaviours related to spatial processing (Ramírez-Amaya et al., 2005; Chawla et al., 2005; Satvat et al., 2011; Snyder et al., 2011). However, most of these studies investigated the DG blades' activity in spatial processes but not directly in spatial mnemonic processes. For example, Ramírez-Amaya et al. (2005) and Chawla et al. (2005) showed that *Arc* expression is selectively increased in the enclosed blade during novel environment exploration. Similar patterns of activation were also reported by Satvat et al. (2011), where animals participated in a navigation task. Only one study implicated the relevance of the enclosed blade in spatial memories (Snyder et al., 2011). More importantly, all the aforementioned studies used molecular imaging of immediate early genes (*Arc*, *c-Fos* or *Zif268*) as markers for neuronal activity. First, such methodological approach should be treated cautiously, since it has been demonstrated that only *Arc* is reliably reflecting task demands (Guzowski et al., 2001). Second, in the hippocampus, nuclear *Arc* RNA peaks within six to eight minutes following a behavioural stimulation (Vazdarjanova et al., 2002), allowing for precise linking of the detected expression levels to neural activation due this stimulation. In the DG, on the other hand, *Arc* RNA transcription is prolonged and is detectable up to eight hours (Ramirez-Amaya et al., 2013), rendering its presence in the DG a less direct indicator of neuronal activity due to a specific event. Moreover, regardless of the above methodological constraints, the molecular imaging approach is correlative. From this perspective, the present study is the first to show in a causal manner that the enclosed blade of the DG is necessary for spatial mnemonic processes.

The present study is also the first to show that the enclosed blade is not important for non-spatial processes. This result departs from the observations of two recent studies reporting that the enclosed blade is also involved in non-spatial processing, as it contains odour- and object-responsive cells (Tuncdemir et al., 2022; Goodsmith et al., 2022). Even though the two studies did not specifically investigate the activity of the enclosed blade, it is likely that the majority of data came from this region because the exposed blade (due to its 'buried' location within the hippocampus) is more difficult to image with techniques such as calcium imaging (Tuncdemir et al., 2022) or *in vivo* electrophysiology with microdrives (Goodsmith et al., 2022). Importantly, the two studies reported that the activity of the identified odour- and object-responsive cells was influenced by space or spatial manipulations, e.g. was location-dependent. Therefore, it might be that the non-spatial signals in the enclosed blade are useful for spatial processing, for example, landmark-based environment exploration. This speculation is in accordance with results shown in Soulé et al. (2008) who report that the enclosed blade of the

DG shows higher activity levels following animals' exploration of spatially arranged objects. On the other hand, in a study, where a familiar object was exchanged for a new one in an already familiar arrangement of objects, higher *Arc* and *Homer* activity levels were found in the exposed blade of the DG (Hoang et al., 2018). This supports the second part of the present study's results, which indicate that the exposed blade is sensitive to the changes in objects' features. Of note, Hoang et al. (2018) discuss their findings in a framework of 'spatial learning'. However, their behavioural manipulation resembles standard non-spatial protocols (i.e. novel object recognition paradigms), since the objects but not the locations were changed between the exploration sessions. Therefore, my interpretation of the results by Hoang et al. is that higher *Arc* and *Homer* activity of the exposed blade was due to the non-spatial nature of the implemented behavioural task. Interestingly, increased activity levels in this study were observed not only in the exposed blade of the DG, but also in the proximal part of CA3. This further reinforces the notion that the implemented task in Hoang et al. is non-spatial, since it is known that the proximal CA3 is preferentially involved in non-spatial mnemonic processes (Ku et al., 2023, Nakamura et al., 2011; Beer and Vavra et al., 2018).

Importantly, the present study's conclusion that spatial memories are processed preferentially in the enclosed and non-spatial memories – in the exposed blade, is established based on the investigations in the dorsal pole (longitudinal axis) of the DG. Optogenetic perturbation of the DG blades did not occur throughout their full longitudinal extent and the focus was laid on the dorsal pole of the DG due to its prominent role in cognitive processes, i.e. learning and memory (Kesner, 2013; Ramirez et al., 2013; Kheirbek et al., 2013). Thus, different spatial/non-spatial functional gradients of the blades (or no gradients at all) might exist at the more ventral levels of the DG, which are presumably more tightly connected to emotional processing (Weeden et al., 2015; Anacker et al., 2018; Fanselow and Dong, 2010). However, several reports point out that a similar functional dissociation of the blades in terms of spatial and non-spatial memories might exist at the more ventral DG levels. First, the ventral hippocampus (including the DG) also plays a role in spatial learning (Snyder et al., 2009) or non-spatial discriminations (Atucha et al., 2017; Weeden et al., 2014; Kirk et al., 2017). Second, spatial and non-spatial proximodistal functional gradients in the CA1 and CA3 exist at multiple longitudinal levels (Nakamura et al., 2013), which indicates that a similar preservation of functional dissociation might exist for the enclosed and exposed blades in the ventral DG. At this point it is important to mention that different volumes of adenoviral vectors were injected per hemisphere into the enclosed (60 nl) or the exposed (40 nl) blade. However, it is unlikely that the difference in the injection volumes affected the output of the present study. A lower volume for the exposed blade

was chosen to restrict the main viral spread to its target in order to more reliably isolate the contribution of either of the blades to spatial and non-spatial memories. Despite a potentially lower ArchT transduction in the exposed blade, inhibition of this region caused a profound performance deficit in mice participating in the non-spatial task. This signifies that the lower injection volume sufficed to achieve a substantial silencing of the exposed blade. Importantly, the non-spatial behavioural deficit of this group cannot be explained by other factors, for example, light stimulation *per se*, since shining light did not produce a deficit in this group during the spatial memory task. This indicates that the non-spatial memory deficit of the mice with exposed blade inhibition was specifically caused by ArchT stimulation and hence, the inclusion of further control animals, i.e. GFP- or saline-controls with light stimulation, might be redundant and was deemed unnecessary. The sufficiency of a single control condition (ArchT/light-off) has been also demonstrated in previous works by our group (Lux et al., 2017; Atucha et al., 2023).

A possible reconciliation of the segregated and 'binding' processing in the DG

How can the functionally different profiles of the enclosed and exposed blades be integrated with the view that the DG is involved in 'binding' of spatial and non-spatial information arriving from the LEC and MEC ('binding hypothesis', for reviews see: Lee and Jung, 2017; Kesner, 2018)? At first, the results of the present study seem to be contraire to the 'binding' theory. However, a possible reconciliation of the two views is that the cortical spatial and non-spatial inputs are 'bound' in the DG blades, but they are processed in a fundamentally different manner between the two DG blades. In particular, it could be that in the enclosed blade of the DG non-spatial LEC and spatial MEC inputs are processed in a manner that is necessary for spatial memories. For example, non-spatial features of a certain spatial context (e.g. colour, landmarks) might help distinguish it from other spatial contexts. Similarly, spatial signals might help to form and to retrieve non-spatial representations. For example, different objects could be distinguished based on the spatial arrangements/relations of distinct elements present within the objects (e.g. length, width, and orientation of objects' elements). In other words, one could speculate that spatial and non-spatial signals in the DG blades are used for different purposes. Alternatively, it might be that the converged signals within the enclosed and the exposed blade of the DG are from the start either preferentially spatial or non-spatial. In fact, this explanation seems more plausible, as there are reports that, for example, the LEC also processes spatial representations (Tsao et al., 2013; Deshmukh and Knierim, 2011; Beer et al., 2013; Kuruvilla et al., 2020). Thus, functionally spatial LEC signals might be sent to the enclosed blade, while the non-spatial LEC inputs may be relayed to the exposed blade of the DG. A similar

argumentation is also applicable to the MEC inputs to the DG blades (for further discussion see Chapter V). Together, the discovered functional double dissociation of the DG blades for spatial and non-spatial memories is not necessarily contradicting the long-standing belief that the DG is involved in binding of the cortical inputs to the hippocampus. A better understanding of the mechanisms supporting both segregation and binding views will require further investigations.

A possible contribution of the DG to memory processing in the MTL

The results of the present study are often discussed in terms of spatial or non-spatial 'processing'. It is important to remember that such term is very broad and includes a variety of 'processes', for example, formation, consolidation or recall of memories. The present study specifically focused on mnemonic discriminations, since the DG is believed to be involved in distinguishing highly similar stimuli via a process called 'pattern separation'. Hence, it is more accurate to state that the present study provided causal proof that the enclosed blade of the DG is required for spatial mnemonic discriminations, while the exposed blade of the DG is involved in non-spatial mnemonic discriminations.

The first part of the above statement is broadly supported by the evidence collected from a variety of studies focusing on pattern separation function in the DG (e.g. Leutgeb, 2007; Neunuebel and Knierim, 2014; Clelland et al., 2009). These studies were not specifically focusing on the roles of the enclosed or exposed blades of the DG, but they illustrated that the DG is generally important for discriminating overlapping spatial stimuli. Importantly, the present study is the first to show that the DG is relevant and necessary for the retrieval of non-spatial mnemonic discriminations, which has not been clearly shown to date (Dees and Kesner, 2013; Miranda et al., 2021). Specifically, it is considered that object discriminations are carried out, for example, by the perirhinal cortex (Olarte-Sánchez et al., 2015; Mumby et al., 2002; Miranda et al., 2017). Also, the CA1 seems to be involved in such processes (Cinalli et al., 2020; Stackman et al., 2016). Of note, the LEC does not seem to be specifically required for object discriminations, since lesioning this area does not lead to an impaired ability to discriminate objects (Kesner et al., 2001; Wilson et al., 2013).

How does the well-established role of the perirhinal cortex and that of CA1 in object discriminations relate or differ from the proposed role of the exposed blade in object discriminations? Cumulative evidence indicates that the perirhinal cortex is involved in familiarity-based recognition memory, i.e. discriminations are carried out based on a vague sense of stimulus familiarity (Atucha et al., 2017; Bowles et al., 2007, 2010; for review see: Brown & Aggleton, 2001; Eichenbaum et al., 2007). Parallel to it, the hippocampus is

considered especially important for recollection-based recognition memory, i.e. detailed recall of stimuli (Diana, Yonelinas and Ranganath, 2007; Wixted and Squire, 2010; Fortin, Wright and Eichenbaum, 2004; Eichenbaum et al., 2012; Sauvage, 2010). Given these evidences, it might be that the perirhinal cortex and the exposed blade of the DG both contribute to non-spatial discriminations, but the former is supporting familiarity-based and the latter supports the recollection-based recognition. When compared to the hippocampal CA1 area, both blades of the DG seem to be particularly involved in discriminating highly similar stimuli, while the CA1 is rather tuned to discriminations of more dissimilar stimuli (Beer and Vavra et al., 2018; Clark et al., 2000; Cohen et al., 2013). This was also demonstrated by the observation from the present study that silencing CA1 did not impair the animals' performance in the spatial version of the task. In line with this evidence, Oulé et al. (2021) demonstrated that affecting the DG function results in an impairment to distinguish similar stimuli, while discriminating dissimilar stimuli remains unaffected by such manipulations. Considering the above, it is tempting to speculate that the enclosed and exposed blades of the DG in comparison to the rest of the MTL areas are specifically required for detailed (recollection-based) spatial and non-spatial discriminations of highly similar stimuli.

In summary, the present study is the first to report a functional double dissociation of the DG blades in mnemonic discriminations. This expands our knowledge regarding the networks preferentially supporting spatial and non-spatial information processing in the MTL areas and provides new venues for investigating the neural mechanisms supporting either types of memories. In this regard, in the next chapter I present findings describing the communication of the enclosed and exposed blades of the DG with the downstream spatial and non-spatial hippocampal subregions at memory retrieval.

III.

Interaction of the Enclosed and Exposed Blades of the Dentate Gyrus with CA1-CA3 Spatial and Non-spatial Subnetworks

Introduction

In a simplistic model of hippocampal connectivity, the dentate gyrus (DG) is a part of a circuit known as 'the trisynaptic loop', which also involves the entorhinal cortex (EC) and the hippocampal areas CA1 and CA3 (Andersen et al., 1971; Amaral and Witter, 1989). Several anatomical and functional studies indicate that this circuit model might include two parallel paths, each preferentially supporting spatial or non-spatial processing (Ishizuka et al., 1990; Nakamura et al., 2013; Flasbeck et al., 2018; Beer and Vavra et al., 2018; Ku et al., 2023; Henriksen et al., 2011; Nakazawa et al., 2016). These two paths are segregated along the proximodistal axis of the CA1 and CA3. The evidence described in Chapter II suggests that the enclosed and exposed blades of the DG might be further parts of these subnetworks due to their selective contribution to either spatial or non-spatial memory processing. Areas belonging to the spatial hippocampal subnetwork (distal CA3-proximal CA1) preferentially receive

projections from the enclosed blade of the DG (Claiborne et al., 1986), which is important for retrieving spatial memories. In contrast, it is known that the proximal CA3, which together with the distal CA1 constitutes the non-spatial subnetwork, receives projections from both DG blades (Claiborne et al., 1986). However, proximal CA3 might be modulated more by the exposed blade as it exhibits stronger responses after stimulations of this region compared to the stimulations of the enclosed blade (Scharfman et al., 2002). In contrast to the enclosed blade, the exposed one is predominantly involved in the retrieval of non-spatial memories.

Although the enclosed blade shares its role in processing spatial information with the distal CA3-proximal CA1 subnetwork and the exposed blade processes non-spatial stimuli similarly to the proximal CA3-distal CA1 subnetwork, the individual subregions' contributions to spatial and non-spatial memories were established independently from each other. Until now, there has been no evidence that the enclosed blade is functionally linked to the spatial hippocampal subnetwork and that the exposed blade communicates with the non-spatial one. Importantly though, such interregional communication might be more relevant for mnemonic processes than the isolated activity of the DG blades. For example, the relevance of subregions' interactions during memory retrieval was recently demonstrated for the CA1 and CA3 areas by Ku et al. (2023; co-authored manuscript), who showed that synchronisation of the proximal CA3 and distal CA1 activities' is important for successful behavioural performance in a non-spatial memory task.

Interestingly, evidence from different studies indicates that communication between the enclosed blade and the rest of the hippocampus might differ from that of the exposed blade. For example, the mossy fibres from both DG blades mostly target the apical dendrites of CA3 pyramidal cells. However, a portion of axons originating exclusively in the exposed blade (i.e. infrapyramidal mossy fibre bundle) projects onto the basal dendrites of the proximal CA3 cells (Claiborne et al., 1986). Targeting apical or basal CA3 dendrites might in turn influence the 'responsiveness' of proximal vs distal CA3 cells to the enclosed or exposed blade signals. Further, granule cells are known to activate not only CA3 pyramidal cells, but also CA3 interneurons (Acsady et al., 1998; Henze et al., 2002), which in turn inhibit the pyramidal cells (Yamamoto, 1972; Brown and Johnston, 1983; Barrionuevo et al., 1986; Buzsáki, 1984). Importantly, distal CA3 contains a higher number of interneurons (Sun et al., 2017). This might indicate that the communication between the enclosed blade and distal CA3 (due to their prominent anatomical connection) might involve an inhibitory feedforward circuitry to a greater extent than the communication between the exposed blade and proximal CA3.

In summary, it is well-established that the DG blades communicate with the downstream CA3 and (indirectly) CA1 areas. Here, I investigated whether spatial (distal CA3-proximal CA1) and non-spatial (proximal CA3-distal CA1) hippocampal subnetworks are affected to different extents by inhibiting the enclosed and exposed blades of the DG. If the enclosed blade supports spatial memories by preferentially communicating with the distal CA3 and proximal CA1, one expects that perturbation of this blade should affect the recruitment of the spatial subnetwork. On the other hand, affecting the activity of the exposed blade should change the involvement of the non-spatial subnetwork during retrieval of non-spatial memories. To test these hypotheses, I quantified the recruitment of proximodistal spatial and non-spatial hippocampal subregions during the retrieval of spatial and non-spatial memories upon optogenetic silencing of the enclosed or the exposed blade. This was done by detecting the expression of *Arc* RNA, which tightly reflects synaptic plasticity and memory processes (Sauvage et al., 2013).

Methods

Note: For information regarding animals' housing conditions, behavioural procedures and stereotactic surgeries see Chapter II, Methods, pp. 13-17.

Mice used for molecular *Arc* imaging (n=23) underwent a similar behavioural procedure (i.e. spatial or object pattern separation tasks) as the animals used for the behavioural performance assessments (Chapter II, Methods, pp. 13-15), except the testing phase of the tasks was shortened to six minutes to accommodate the maximal detection of *Arc* RNA (Beer et al., 2013). An additional group of age-matched animals (home-caged imaging controls, n=10) that did not undergo surgical procedures were placed in the experimental room together with the test animals. Imaging controls were habituated to the room conditions for the same amount of time as the test groups to ensure that the pattern of *Arc* RNA expression is more tied to the demands of the task and not to other conditions such as handling, light, and noise levels, etc. (Guzowski et al., 1999; Vazdarjanova et al., 2006; Nakamura et al., 2013; Beer et al., 2013; Flasbeck et al., 2018; Sauvage et al., 2019)

Imaging activity in hippocampal CA1 and CA3 areas

To evaluate the effects of the enclosed or exposed blade's inhibition on the activity levels of the hippocampal CA1 and CA3 areas, fluorescent *in situ* hybridization of *Arc* RNA was used. This method allows for the investigation of neural activity levels with high cellular resolution even in adjacent brain areas such as the CA1 and CA3. In contrast to other activity markers, e.g. *c-Fos* and *Zif268, Arc* more reliably reflects retrieval-induced activity and has been widely

employed to map memory-like activity in the hippocampus (Sauvage et al., 2013; Sauvage et al., 2019).

Fluorescent *in situ* hybridization

Using a previously described protocol (Beer and Vavra et al., 2018), intranuclear *Arc* signals were detected and analysed. In summary, experimental mice (and home-caged imaging controls) were sacrificed immediately after the completion of the behavioural tasks and their brains were removed, flash frozen in isopentane and stored at -80°C until sectioning. 8-µm-thick sections were cut in coronal plane on a cryostat (Leica CM 3050 S; Leica Biosystems, Germany), mounted on polylysine-coated slides and stored at -80°C until further treatment. *Arc* RNA probes were generated using the digoxigenin-labelled UTP kit (Roche Diagnostics) and purified using Probe quant G-50 Micro columns (GE Healthcare). Brain sections were fixed with cold 4% PFA followed by rinsing with 0.1 M PBS. Slides were then treated with acetic anhydride/triethanolamine/hydrochloric acid mixture (0.25% acetic anhydride in 0.1 M triethanolamine/HCl), rinsed with 0.1 M PBS and soaked with pre-hybridization solution for 30 minutes at room temperature. The pre-hybridization solution contained 50% formamide, 25% 20×SSC, 5% 50×Denhardt's solution, 2.5% yeast tRNA (10mg/ml), and 5% denatured salmon sperm DNA (10mg/ml) in DEPC-treated water. Afterwards, the hybridization was performed with digoxigenin-labelled *Arc* probe (0.13 ng/µl RNA probe per slide in pre-hybridization solution) in a humidified chamber at +65˚C for 17 hours. To control signal specificity, 'negative' controls were used, which were hybridized using the hybridization solution without the RNA probe. After hybridization, the unbound probe was removed in SSC buffer solutions at +65˚C, the slides were incubated with 3% BSA in TBST buffer for 30 minutes and a secondary antibody against digoxigenin (anti-DIG) conjugated with HRP (Roche Diagnostics) was applied for 3 hours at room temperature (anti-DIG dilution: 1:2000 in BSA/TBST). Anti-DIG was detected using a cyanin-5 substrate kit (Cy5, TSA-Plus system, Perkin Elmer). Nuclei were counterstained with 4',6'-diamidino-2-phenylindole (DAPI; Vector Laboratories).

Several slides with mounted sections were treated at once. Each hybridization batch consisted of slides from three experimental conditions (light-on, light-off, and home-caged imaging controls).

Image acquisition and analysis

Slides contained four non-consecutive brain sections (approximate AP: -2.0 mm from bregma). Six images (three from each hemisphere) per four regions of interest (**Figure 10**) were captured with a Keyence Fluorescence microscope (BZ-X710; Japan). A 40× objective lens was used for acquisition of a z-stack (0.7-µm–thick images). Exposure times and light intensity were kept similar for all slides.

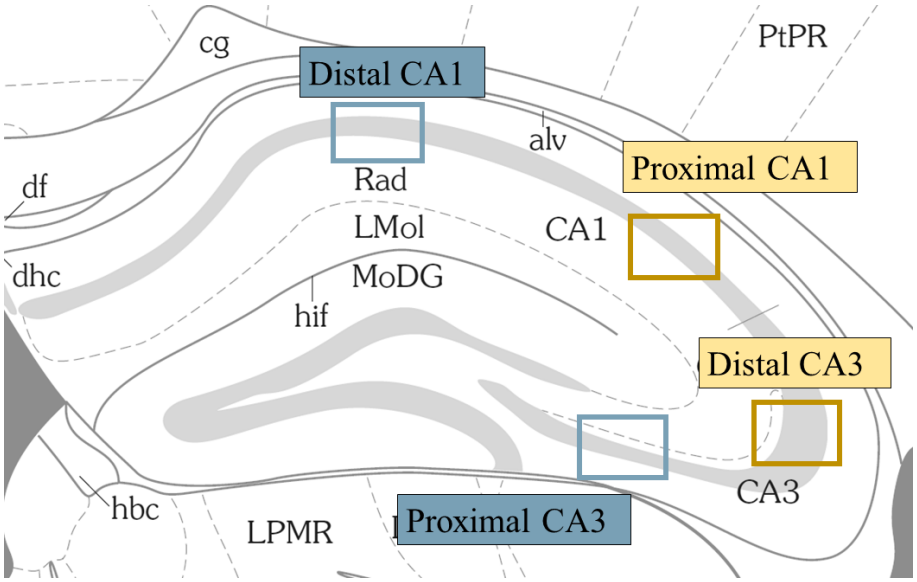

Figure 10: Regions of interest for *Arc* imaging. Location of z-stacks captured with 40× objective lens for distinct subregions: distal CA1 and proximal CA3 (non-spatial subnetwork), proximal CA1 and distal CA3 (spatial subnetwork).

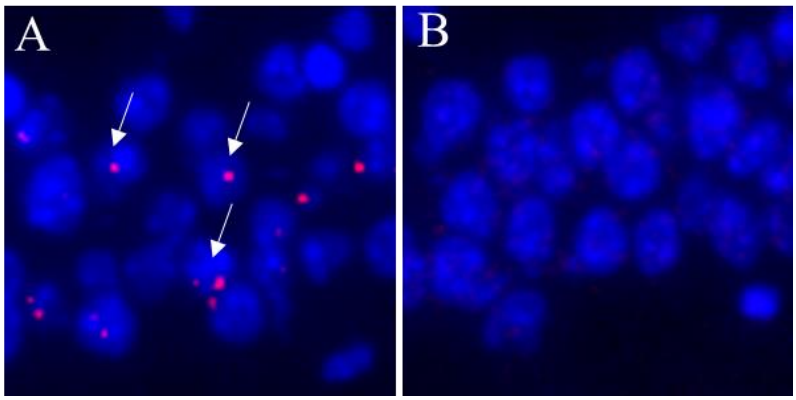

Figure 11: Nuclear *Arc* RNA expression. A: Exemplary image taken in distal CA1. *Arc* signal is labelled with Cy5 (red). White arrows indicate *Arc*-positive neurons. Unlabelled neurons are visible as DAPI labelled nuclei (blue) without the characteristic intranuclear fluorescence signals in red. B: Exemplary image of distal CA1 on a slide processed without the *Arc* probe (negative control). No distinct intranuclear *Arc* signal is detectable.

For stereological considerations, neurons were counted on 8-µm–thick sections that contained one layer of cells, and only cells containing whole nuclei were included in the analysis (West, 1999). The quantification of Arc expression was performed in the central 60% of the stack because this method minimises the likelihood of taking partial nuclei into consideration and decreases the occurrence of false negatives. Counting was performed on putative pyramidal cells that can be distinguished from the interneurons or non-neuronal cells based on their shape and DAPI intensity. *Arc*-positive neurons were defined as cells with DAPI-labeled nuclei with one or two characteristic intranuclear areas of fluorescence (Cy5) (**Figure 11**). Nuclei that did not contain intranuclear foci were counted as *Arc*-negative neurons (Guzowski et al., 1999). The percentage of *Arc*-positive neurons was calculated as follows and averaged between the six captured images per region of interest:

$$\frac{Arc(\text{positive})}{Arc(\text{positive}) + Arc(\text{negative})} * 100$$

To estimate the *Arc* signal induced due to memory retrieval, data were normalised and task-induced *Arc* levels were calculated by subtracting *Arc* levels observed in the imaging (home-caged) control group.

Statistical analysis

Statistical analyses were performed using SPSS software (version 27, IBM, SPSS Inc.).

All data sets were tested for deviations from normal distribution using the Shapiro-Wilk test for appropriate use of parametric data analysis. Whether a region of interest was recruited during memory retrieval in different groups was assessed with one-sample t-tests (comparisons to zero) using task-induced (normalised) data. To test the effects of the enclosed and exposed blade inhibition on the activity levels of the downstream hippocampal spatial and non-spatial subnetworks, two-way ANOVAs with repeated measures were performed using data normalised to the imaging control group and the non-normalised data. ‘Inhibition’ (ArchT/light-on or ArchT/light-off) was set as a between-subject factor, while ‘subregion’ (distal CA1, proximal CA1, distal CA3, and proximal CA3) varied within subjects. Post-hoc pairwise comparisons were carried out with two-sample t-tests with Bonferroni corrections.

Results

The activity levels of the proximal and distal CA1 and CA3 were measured by quantifying and comparing the proportions of neurons activated during the retrieval of spatial or non-spatial memories between the inhibition (enclosed/exposed) and the control groups. The expression of *Arc* RNA was used as a marker of coincidental cell activation (Guzowski et al., 2001). Of note, the quantification of the *Arc*-positive cells in the enclosed and exposed blades of the DG was not performed because of prolonged *Arc* RNA transcription in the DG (up to eight hours in contrast to six to eight minutes in the CA1 and CA3), which renders *Arc* RNA expression inadequate to reflect the contribution of the DG solely to the retrieval phase of the behavioural task (Ramirez-Amaya et al., 2013). To minimise the contribution of factors other than the cognitive demands of the task (e.g. noise, lighting conditions, handling etc.), activity levels measured in the experimental mice were normalised by subtracting *Arc*-positive cells assessed in home-caged imaging control animals that did not undergo the testing procedure but were brought to the experimental room together with the experimental mice.

Before analysing group-related differences, it was first determined whether inhibition of the enclosed and exposed blade produced similar behavioural deficits as those observed in Chapter II. Indeed, inhibiting the enclosed blade impaired spatial memory retrieval, while inhibiting the exposed blade impaired object memories (see Supplementary data, p. 117, Figure S1). Of note, hippocampal recruitment was studied only in the tasks, in which a behavioural effect of the DG blades' inactivation was observed: the 'enclosed blade mice' were tested in the spatial task, the 'exposed blade mice' – in the object task. Next, whether hippocampal CA1 and CA3 subregions were significantly recruited during retrieval of spatial and non-spatial memories was investigated. Results show that all hippocampal subregions had *Arc* RNA expression levels significantly above zero in both inhibition and control groups (one-sample t-tests, comparisons to zero: all p-values <0.050). This shows that retrieval of spatial and object memories led to an engagement of the hippocampal subregions in the control animals and that the inhibition of either of the DG blades did not completely abolish this activity.

Exposed blade inhibition specifically decreases the activity in the non-spatial hippocampal subnetwork

Two-way ANOVAs (between-subject factor: 'inhibition' (light-on/light-off), within-subject factor: 'subregion' (distal CA1/proximal CA1/distal CA3/proximal CA3)) were performed to compare the recruitment of hippocampal subregions between the control and inhibition groups.

These comparisons were performed separately in animals with the enclosed and exposed blade injections because the enclosed and exposed blade groups were tested in different tasks. Of note, comparable patterns of activity as described in the remaining parts of the results' section were observed when performing analyses with non-normalised (raw) data (see Supplementary data, pp. 102-103, Figures S2, S3).

First, the *a priori* hypothesis that the exposed blade inhibition leads to differential recruitment of the non-spatial hippocampal subregions compared to the spatial ones during the retrieval of an object memory was tested. Significant effects of 'subregion' and 'subregion × inhibition' were found on hippocampal recruitment levels (main effect 'subregion': $F_{(3,27)}= 6.79$, $p=0.001$; interaction effect: $F_{(3,27)}= 5.14$, $p=0.006$; no significant main effect of 'inhibition' was detected: $p>0.050$).

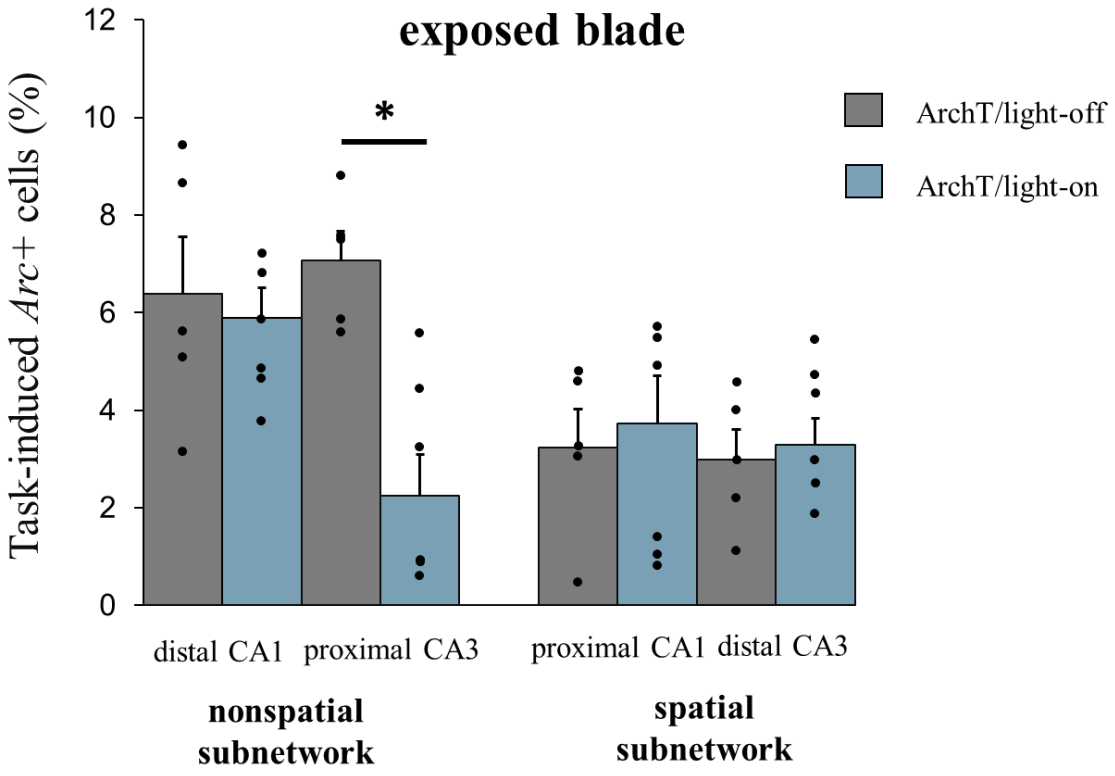

Figure 12: Effects of the exposed blade inhibition on the recruitment of hippocampal spatial and non-spatial subregions during object memory retrieval. Task-induced percentage of *Arc*-positive cells in distal CA1, proximal CA1, distal CA3, and proximal CA3 compared between the inhibition (light-on) and control (light-off) groups. Inhibiting the exposed blade during non-spatial memory retrieval significantly decreases the recruitment of the proximal CA3. *: $p<0.050$

Further post-hoc pairwise comparisons revealed that only the activity levels of the proximal CA3 were significantly decreased by exposed blade inhibition and no effects were detected for other hippocampal subregions (two-sample t-tests, two-tailed: proximal CA3 (light-off vs light-on): $t_{(9)}$=4.07, p=0.012; distal CA3 (light-off vs light-on): $t_{(9)}$=-0.79, p>0.050; proximal CA1 (light-off vs light-on): $t_{(9)}$=0.01, p>0.050; distal CA1 (light-off vs light-on): $t_{(9)}$=0.71, p>0.050; Bonferroni corrected) (**Figure 12**).

To reinforce the observation that the exposed blade selectively affected the recruitment of the non-spatial CA3 subregion but not that of the CA1, proximal CA3 recruitment levels were compared to the activity of the distal CA1 in control and inhibition groups. Results reveal that while no activity differences were observed in the control animals, a trend effect was found when comparing the recruitment of proximal CA3 with distal CA1 in the inhibition group (two-sample paired t-test, one-tailed: light-off, distal CA1 vs. proximal CA3: $t_{(4)}$=-0.49, p=0.648; light-on, distal CA1 vs. proximal CA3: $t_{(4)}$=2.40, p=0.062; Bonferroni corrected). Additionally, the selective effect of the exposed blade manipulation on the non-spatial CA3 subregion as opposed to the CA1 subregion of the same network is strengthened by the findings in control animals that non-spatial subregions (distal CA1 and proximal CA3) had higher activity levels than their respective spatial counterparts (proximal CA1 and distal CA3) (two-sample paired t-test, one-tailed: light-off, distal CA1 vs. proximal CA1: $t_{(4)}$=3.50, p=0.048; distal CA3 vs proximal CA3: $t_{(4)}$=-10.97, p=0.004). However, in the inhibition group this difference was preserved only between the CA1 subregions (light-on, distal CA1 vs proximal CA1: $t_{(5)}$=4.26, p=0.016; distal CA3 vs proximal CA3: $t_{(5)}$=1.35, p=0.468; Bonferroni corrected). This shows that exposed blade inhibition reduced the recruitment of the proximal CA3 to a level comparable to its spatial counterpart (distal CA3). Together, the results indicate that inhibiting the exposed blade specifically decreases the recruitment of the non-spatial subnetwork by exerting its effects primarily on the proximal CA3.

Enclosed blade inhibition enhances the activity in both hippocampal subnetworks

Next, whether the enclosed blade inhibition differentially affects the recruitment of spatial hippocampal subregions in comparison to the non-spatial ones was tested. A significant interaction effect of ‘subregion × inhibition’ was found (interaction effect: $F_{(3,30)}$= 4.10, p=0.015; no significant main effects of ‘inhibition’ or ‘subregion’ were detected, p-values >0.050). This indicates that inhibiting the enclosed blade led to specific differences between hippocampal subregions’ recruitment levels.

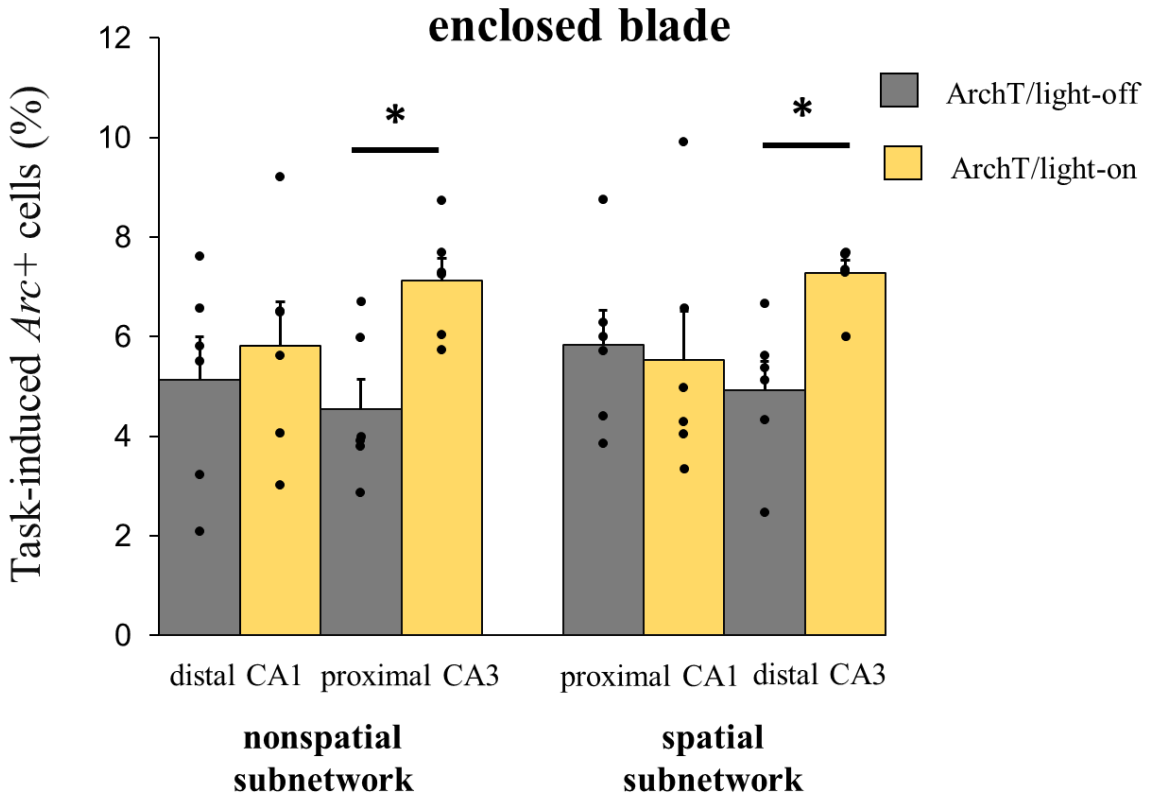

Figure 13: Effects of the enclosed blade inhibition on the recruitment of hippocampal spatial and non-spatial subregions during spatial memory retrieval. Task-induced percentage of *Arc*-positive cells in distal CA1, proximal CA1, distal CA3, and proximal CA3 compared between the inhibition (light-on) and control (light-off) groups. Inhibiting the enclosed blade during spatial memory retrieval increases the recruitment of the proximal and distal CA3. *: $p<0.050$.

After performing further post-hoc pairwise comparisons, it was revealed that enclosed blade inhibition caused an increase in *Arc* expression in the distal CA3 (part of the spatial subnetwork) and proximal CA3 (part of the non-spatial subnetwork), but not in the proximal CA1 or distal CA1 (two-sample t-tests, two-tailed: distal CA3 (light-off vs light-on): $t_{(10)}=-3.67$, $p=0.016$; proximal CA3 (light-off vs light-on): $t_{(10)}=-3.44$, $p=0.024$; proximal CA1 (light-off vs light-on): $t_{(10)}=0.258$, $p>0.050$; distal CA1 (light-off vs light-on): $t_{(10)}=-0.553$, $p=0.050$; Bonferroni corrected). However, the selective effect of enclosed blade inhibition on the CA3 subregions could not be further demonstrated by comparisons of activity levels in distal CA1 vs proximal CA3 and in proximal CA1 vs distal CA3 in the control or inhibition groups (p-values >0.050). Moreover, in control animals the spatial hippocampal subregions were not significantly more recruited than the non-spatial subregions (p-values >0.050). Together, these results indicate that spatial memory retrieval recruited both hippocampal subnetworks to a similar extent in control

animals and that enclosed blade inhibition increased the recruitment of both spatial and non-spatial subnetworks, especially the engagement of their CA3 elements (**Figure 13**).

In summary, inactivation of the enclosed or the exposed blade of the DG during the retrieval of spatial and non-spatial memories had differential effects on the recruitment of the downstream hippocampal subregions, especially CA3. The exposed blade inhibition affected the recruitment of the non-spatial hippocampal subnetwork by decreasing the activity levels in the proximal CA3. The enclosed blade inhibition, on the other hand, affected the recruitment of both spatial and non-spatial subnetworks by primarily increasing the activity levels in the proximal and distal CA3.

Discussion

The present study shows that optogenetic perturbation of the enclosed or exposed blades of the DG not only leads to selective behavioural deficits in spatial or non-spatial mnemonic discriminations, but also alters the activity of the downstream regions. Molecular *Arc* imaging was used to reveal whether the enclosed blade is functionally linked to the spatial hippocampal subnetwork (distal CA3-proximal CA1) during spatial memory retrieval and whether the exposed blade is linked to the non-spatial hippocampal subnetwork (proximal CA3-distal CA1) during non-spatial memory retrieval. The results showed that exposed blade inhibition indeed affected the activity of the non-spatial subnetwork, while silencing the enclosed blade altered the recruitment of both spatial and non-spatial subnetworks. Specifically, exposed blade inhibition decreased the activity of the proximal CA3, while inactivating the enclosed blade increased the recruitment of the proximal and distal CA3. CA1 subregions, on the other hand, were not affected by silencing either of the DG blades.

Integration of the results

These patterns of effects are in line with the anatomical gradients of DG-CA3 projections. Specifically, it was previously described that the distal CA3 is mostly targeted by the granule cells of the enclosed blade, while the proximal CA3 receives projections originating from both the enclosed and exposed blades (Claiborne et al., 1986). Interestingly, in the absence of enclosed blade inhibition (i.e. in the control group), both spatial and non-spatial hippocampal subnetworks were recruited to a similar extent during spatial memory retrieval. This could indicate that during the retrieval phase of the spatial memory task both mnemonic dimensions were represented at the level of the CA1 and CA3, even though only spatial information is relevant for successfully ‘solving’ the task. Since the spatial memory task used in the present

work is designed in a way that spatial information is indicated by the locations of objects, it is likely that object information is also retrieved during this task's testing phase. Thus, it could be that object-location associations are processed by the enclosed blade of the DG, which then relays object-related information to the proximal CA3 and location-related information to the distal CA3. Hence, inhibition of the enclosed blade affected the activity of both CA3 subregions. Alternatively, because inhibiting the enclosed blade caused a memory deficit only in the spatial task (but not the object task), this region might be irrelevant for any object-related information (including object-location associations) and its effect on the non-spatial (proximal CA3) subnetwork might not be as determinant as that on the spatial (distal CA3) subnetwork. The fact that the distal CA3 sends extensive autoassociative projections to the entire proximodistal extent of the CA3, while the proximal CA3 wires preferentially with itself only (Witter, 2007) may indicate that proximal CA3 activity during spatial memory retrieval may be a byproduct of the distal CA3 activation. In other words, it might be that the effect of the enclosed blade inhibition on the proximal CA3 is not due to a direct interaction between these regions, but because of the transmission of the effects from the distal to the proximal CA3 via recurrent collaterals. Altogether, it can be concluded that the enclosed blade of the DG might be a part of the spatial hippocampal subnetwork (at least not exclusively). The observation that the exposed blade of the DG affected the recruitment of the proximal CA3 only, indicates that this region is likely a part of the non-spatial hippocampal subnetwork.

The results of this study also suggest that the DG does not influence CA1 activity, at least under the experimental conditions (i.e. spatial and object pattern separation tasks) used in this study. The lack of effects of the DG blades' inactivation on the proximal and distal CA1 activity may be partially explained by the lack of direct projections from the DG to the CA1. An indirect connection through the CA3 was likely not sufficient to transmit activity changes from the DG to the CA1, since studies demonstrate that even activity changes in the CA3 do not necessarily lead to altered activity of the CA1 (Atucha et al., 2023; Kesner et al., 2005; Brun et al., 2002; for review see: Manns and Eichenbaum, 2005). Also, the present results might imply that, in certain behavioural tasks, the CA1 and DG could function as independent systems supporting mnemonic processes. This idea is reinforced by other reports (Gilbert et al., 2001; Dimsdale-Zucker et al., 2018; Liu et al., 2014) and is illustrated by the result that an intact CA1 is not necessary for successful memory retrieval in the spatial pattern separation task (see Chapter II, Figure 9).

Different mechanisms underlie spatial and non-spatial memory retrieval

Interestingly, it was observed that the effects of the enclosed and exposed blade inactivation on CA3 activity levels differed in their directionality, suggesting that distinct mechanisms are at play for the discriminating between objects and locations. The inhibition of the exposed blade caused a *decrease* in proximal CA3 engagement. A possible mechanism for this observation could be that silencing the granule cells in the exposed blade reduced their excitatory drive on the pyramidal cells of the proximal CA3. This explanation is in line with the traditional view that signal propagation through the trisynaptic pathway, and specifically from the DG to the CA3, is excitatory. For example, in the earliest investigations of DG-CA3 connectivity, stimulations of the DG caused an excitatory response in the CA3 (Gloor et al., 1963; Andersen et al., 1969). Also, McNaughton and Morris (1987) proposed that the DG-CA3 connections act as 'detonator synapses', which illustrates the strong potential of single granule cells to effectively activate their targets. Most importantly, however, it was shown that electrical stimulations of the exposed blade of the DG induce spiking activity in pyramidal cells of the proximal CA3, which interestingly was stronger than a similar spiking activity induced by stimulations of the enclosed blade (Scharfman et al., 2002). Thus, the decreased activity of the proximal CA3 following exposed blade inhibition in the present study is likely the result of the removal of the excitatory drive in this circuit.

In contrast, enclosed blade inhibition led to an *increase* in the activity of the proximal and distal CA3. Parallel to the excitation of the CA3 by the DG, several studies report inhibitory postsynaptic potentials recorded in the CA3 pyramidal cells upon DG stimulation (Yamamoto 1972; Brown and Johnston, 1983; Barrionuevo et al., 1986). Among the possible explanations for this effect is that granule cells contact not only the pyramidal cells, but also CA3 interneurons, which in turn inhibit the pyramidal cells (Henze et al., 2002; Acsady et al., 1998). This suggests that during spatial memory retrieval, feedforward inhibition (DG granule cell→ CA3 inhibitory cell → CA3 pyramidal cell) may dominate over the direct excitation in the enclosed blade-CA3 network. Thus, inhibiting cell firing in the enclosed blade might have a disinhibitory effect on the CA3 pyramidal cells via reduced excitation of the inhibitory neurons (for further discussion see Chapter V).

The present study provided the first-time evidence that the communication between the enclosed and exposed blades of the DG with the downstream hippocampal regions occurs in a different manner, with potentially distinct mechanisms supporting the processing of spatial and non-spatial memory retrieval. To my knowledge, no previous studies investigated the effects of

inhibiting the individual DG blades on the activity of other hippocampal regions. Moreover, studies focusing on the effects of DG inactivation usually assessed only the behavioural consequences of such manipulations and not how it influenced the activity of downstream regions (for review see: Kesner, 2018). Only a few studies looked at general effects of full or partial DG inactivation on downstream hippocampal activity. For example, McNaughton et al. (1989) delivered some of the first evidence that DG lesions, despite the traditional view of the trisynaptic pathway organisation, have little effect on the CA3-CA1 firing activity. In fact, DG inactivation in that study led to a change in the temporal organisation of pyramidal cell firing. Furthermore, Sasaki and Piatti et al. (2018) showed that lesioning DG does not lead to an overall reduction in CA3 activity, but rather to decreased memory-related (occurrence of sharp wave ripples) CA3 activity. Also, in mice lacking the NR1 subunit of NMDA receptors in the DG, a reduction of rate remapping (changes in firing rate) was observed in CA3 population activity when animals were exploring two different contexts (McHugh et al., 2007). Another study reported an increase in memory-related CA3 activity in a mouse model with defective communication between the DG and the CA3 (Ruediger and Vittori et al., 2011). Lastly, ablation of neurogenesis or inhibition of adult-born granule cells impairs population coding and population sparsity in the CA3 region (Niibori et al., 2012; McHugh et al., 2022). Cumulatively these studies indicate that partial or full DG inactivation primarily leads to qualitatively different activity (i.e. temporal firing organisation, rate remapping, different vs same cell populations activation) in the hippocampal CA3 region (McNaughton et al., 1989; McHugh et al., 2007; Niibori et al., 2012). Only when the DG-CA3 circuit is involved in memory-related processes are quantitative changes (increase and decrease) in CA3 activity patterns observed (Sasaki and Piatti et al., 2018; Ruediger and Vittori et al., 2011, McHugh et al., 2022). This is in line with the results of the present study, which found quantitatively different involvement of the proximal and distal CA3 subregions following inhibition of the enclosed and exposed blades of the DG during spatial and non-spatial memory retrieval.

In summary, different mnemonic information is not only processed through different DG-CA3 routes, but also involves different changes in the activities of spatial and non-spatial hippocampal subregions following inhibition of the enclosed and exposed DG blades. Inhibition of the enclosed blade increases the recruitment of the proximal and distal CA3, which are parts of the non-spatial and spatial hippocampal subnetworks, respectively. Silencing the exposed blade, on the other hand, decreases the engagement of the proximal CA3 only (non-spatial subnetwork). Increased CA3 engagement is observed during impaired spatial memory retrieval, while reduced CA3 recruitment accompanies deficits in non-spatial memory retrieval.

IV.

Anatomical Connectivity of the Enclosed and Exposed Blades of the Dentate Gyrus with the Entorhinal Cortex

Introduction

In Chapter II it was established that the enclosed and exposed blades of the dentate gyrus (DG) have domain-specific roles in mnemonic discriminations. Specifically, the enclosed blade preferentially supports spatial memory retrieval, while the exposed blade is necessary for non-spatial processing. Subsequently, a question arises regarding the origin of this difference. Since the DG receives heavy projections from both the lateral and medial parts of the entorhinal cortex (MEC and LEC), which are preferentially tied to spatial and non-spatial information processing (Fernández-Ruiz et al., 2021; Hunsaker et al., 2013; Fyhn et al., 2008; Tennant et al., 2018; Hargreaves et al., 2005; Deshmukh et al., 2012), one possibility is that the DG blades receive different proportions of the LEC and MEC innervation.

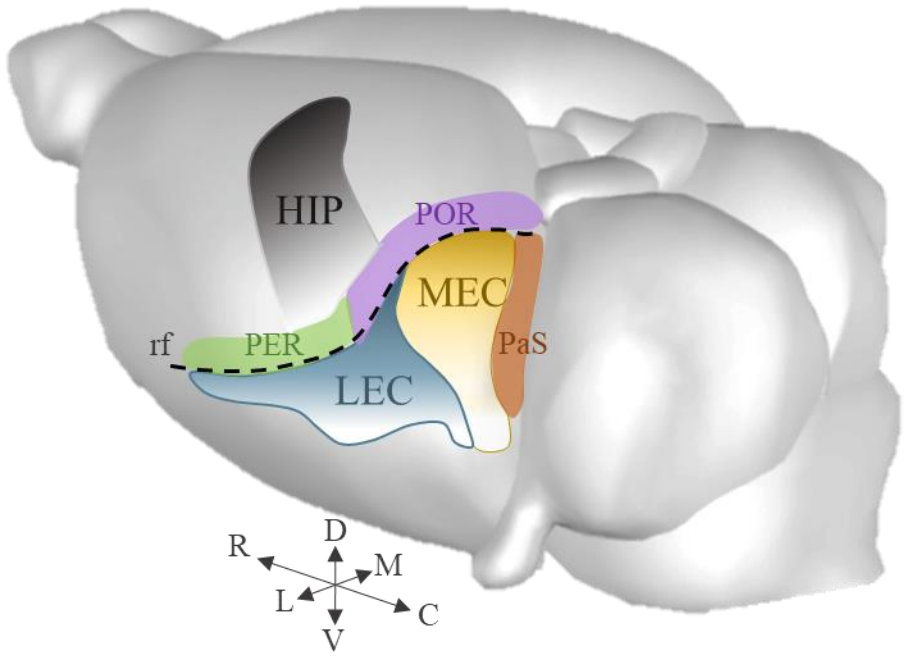

Figure 14: Schematic representation of the location of the lateral (LEC) and medial (MEC) entorhinal subdivisions in rodent brain. HIP: hippocampus; PER: perirhinal cortex; POR: postrhinal cortex, PaS: parasubiculum; rf: rhinal fissure. Orientation of the brain is indicated by the arrows. D: dorsal; V: ventral; L: lateral; M: medial; R: rostral; C: caudal

In rodents, the LEC occupies rostrolateral portions of the entorhinal cortex (EC) and is bordering olfactory as well as amygdaloid cortices rostrally, and perirhinal cortex dorsally. The MEC is located in caudal and medial portions of the EC and is bordering parasubiculum medially and postrhinal cortex dorsally (**Figure 14**). Both subdivisions of the EC differ from each other in many aspects (Witter et al., 2017). For example, the MEC and LEC have distinct genetic profiles (Blankvoort et al., 2018) and differently exhibit neuronal markers (Gall et al., 1981, Kobro-Flatmoen and Witter, 2019), e.g. parvalbumin is strongly present in the MEC but less in the LEC. The two regions are preferentially connected to different brain areas, with the LEC receiving strong inputs, for example, from the perirhinal and the piriform cortices and the MEC – from the presubiculum and the retrosplenial cortex (Canto et al., 2008; Kerr et al., 2007; Nilssen et al., 2019). Most importantly, the MEC and LEC preferentially process different types of stimuli. The LEC is inclined to process non-spatial signals, e.g. objects or odours (Deshmukh et al., 2012; Tsao et al., 2013). The MEC, on the other hand, is preferentially tuned to spatial processing (Fyhn et al., 2008; Tennant et al., 2018; Hargreaves et al., 2005). Such functional segregation at the level of the EC might be the source of the functional segregation of the enclosed and exposed blades of the DG.

Much is known about the topography of the EC to the DG projections. The projection from the MEC and LEC to the DG is comprised of two pathways – the medial (MPP) and lateral (LPP) perforant paths – originating mainly from the superficial layer II cells (Steward and Scoville, 1976; van Groen et al., 2003). A minor component of these pathways also originates in the deep layers (V-VI) of the EC (Deller et al., 1996; van Groen et al., 2003). Layer III EC cells, on the other hand, mainly project to the CA1 (Steward and Scoville, 1976). Both the LEC and MEC project mostly unilaterally to the ipsilateral DG (Van Groen et al., 2003; Steward and Scoville, 1976). After crossing the hippocampal fissure, entorhinal axons contribute to a widespread longitudinal innervation of the DG (Amaral and Witter, 1989), which is topographically organised. In brief, the most dorsal portions of the MEC and LEC (next to the rhinal fissure) project to the dorsal levels of the DG, while the most ventral portions of the MEC and LEC target the DG at its ventral levels (Dolorfo and Amaral, 1998; Ruth et al., 1988, 1982).

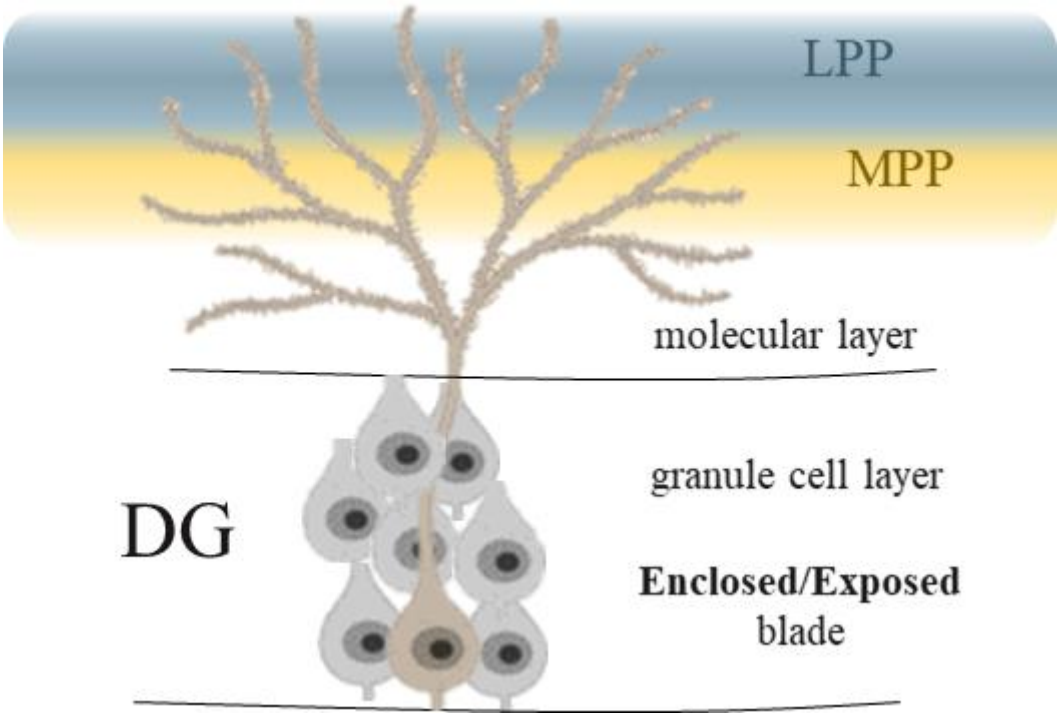

Figure 15: Schematic representation of the lateral (LPP) and medial perforant path (MPP) projections to a single DG granule cell. The LPP targets the outer molecular layer, while the MPP projects more to the middle dendritic segments. The scheme is applicable to both the enclosed and exposed blades of the DG.

In the transverse plane, MPP and LPP fibres were reported to innervate both the enclosed and exposed blades of the DG (for review see: Witter, 2007). The current consensus is that the MPP and LPP axons project onto a single granule cell, independently of its transverse location, i.e.

in the enclosed or exposed blade. This conclusion originated from the observation that (in rodents) the entorhinal fibres build synapses with the dendrites of granule cells at distinct proximodistal levels in respect to the cell soma in the molecular layer of the DG (Hjorth-Simonsen and Jeune, 1972, Steward, 1976) (**Figure 15**). LPP fibres project to the outer portions of the molecular layer in the DG, while MPP fibres occupy the middle parts of the molecular layer. These studies indicate that the MEC and LEC homogeneously innervate the DG covering both, the enclosed and exposed blades.

However, evidence indicates that while a single layer II EC cell can innervate both blades, some cells may have a target preference (Tamamaki and Nojyo, 1993). Importantly, to date, there is a lack of studies that attempt to elucidate which cells within the MEC and LEC have a preference for either of the DG blades. Moreover, a few studies that have investigated the innervation of the DG blades by the MEC and LEC report differences that contradict the functional profiles of the EC subdivisions and the DG blades. According to Wyss (1981) and Tamamaki (1997), the LPP tends to target the enclosed blade of the DG, while the MPP projects predominantly to the exposed or to both blades equally. Based on the functional gradients, however, one would expect that the MEC preferentially projects to the enclosed blade and the LEC – to the exposed one. The two studies, however, conducted anterograde tracing of the EC to DG efferents and thus, were using the thickness of the LPP and MPP laminas (Tamamaki, 1997) or the grain density of tracing particles present in the molecular layer of the blades (Wyss, 1981) as a measurement of MPP and LPP target preference. Consequently, the results of these studies are more likely to indicate the spread of the MPP and LPP axons, but not the amount of the innervation from the LEC or MEC cells *per se*.

Altogether the aim of the current study is to address whether the MEC is preferentially targeting the enclosed blade and the LEC - the exposed one, which could explain the spatial/non-spatial double dissociation of the enclosed and exposed blades of the DG for memory processing. To this aim, retrograde tracing of the origins of the entorhinal efferents was performed simultaneously for the enclosed and exposed blades within optically cleared mouse brains, thus allowing for the detection of small differences in innervation patterns that are otherwise difficult to observe with single tracing approaches.

Methods

Note: For information regarding animals' housing conditions and stereotactic surgeries see Chapter II, Methods, pp. 13-17.

Tracing projections from the MEC and LEC to the DG blades

To establish the origin of entorhinal projection cells to the enclosed or the exposed blade of the DG, retrograde tracing of these cells was performed in optically cleared brains. C57BL/6N mice (n=11) received injections of tracers CTB-555 and CTB-647 (cholera toxin subunit-b conjugated with Alexa Fluor 555 or 647; Fisher Scientific, Germany) unilaterally in the enclosed (5-10 nl, AP -2.0; ML ±1.5; DV -1.7 mm) and the exposed (5-10 nl, AP -2.0; ML ±1.3; DV -2.4 mm) blade of the DG, with each tracer targeting different blades (**Figure 16**). For control purposes, one further animal received a double injection aimed at the CA1 and CA3 areas. The tracers supplied in the powder form were reconstituted to 1, 0.1 or 0.01 % w/v in 0.1 M PBS with 0.1 % NaN3 prior to surgeries. N=4 animals were excluded from further analysis due to an absence of labelling in most of the projection regions, which was most likely caused by a low titration of the injected tracers (5 nl; 0.1% and 0.01% w/v). The combinations of tracer, target blade and target hemisphere were counterbalanced across animals.

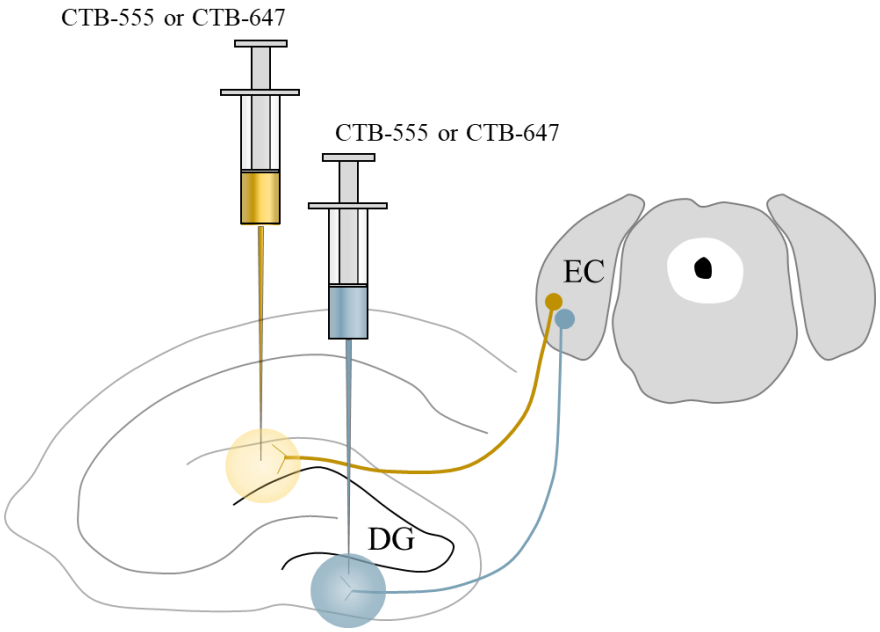

Figure 16: Scheme of retrograde double injections in the DG. Each blade was targeted by CTB-555 or CTB-647. Transported tracers were observed as fluorescent signals in the LEC and MEC.

Optical clearing

After a seven-day survival period following tracer injections, animals were deeply anaesthetised using a ketamine-xylazine mixture and perfused intracardially. A previously described protocol with slight modifications was used to clear the brains (Ertürk et al., 2012). Briefly, brains were removed, post-fixed in 4% PFA for three hours at room temperature and stepwise dehydrated with a series of tetrahydrofuran solutions (50%, 70%, 80%, 90%, 96%, 2× 100%) with each step performed overnight. Consecutively, brains were treated with dichloromethane for three hours, optically cleared and stored in ethyl cinnamate at room temperature until further processing.

3D-image acquisition

For visualisation, cleared brains were imaged using an UltraMicroscope Blaze (Miltenyi Biotec, Germany) equipped with a SuperK Fianium FIU-15 white light laser (NKT Photonics, Denmark). Tile z-stacks (3×3; 2-µm-thick) through two-sided triple-sheet excitation optics were captured with a LVMI-Fluor 4× objective (Miltenyi Biotec, Germany). Images illuminated from the left and right sides were automatically fused with a built-in blend algorithm. For excitation (exc.) and detection (emission, em.), the following filterpairs were used: exc. 480/20nm - em. 515/30nm (autofluorescence channel), exc. 555/20nm - em. 595/40nm (Alexa Fluor 555) and exc. 640/30 - em. 680/30nm (Alexa Fluor 647). The dynamic focusing function was used to achieve uniform z-resolution across the x-axis of the brains. Image z-stacks with a format of 2048×2048 were stitched and visualised with the Imaris software package (version 9.8, Bitplane, Zürich, Switzerland).

Demarcation of the LEC and MEC

To distinguish caudal LEC from rostral MEC (areas close to the border between the two regions), expressions of two proteins were investigated. It is known that layer II of the MEC and LEC expresses calbindin and reelin. However, in the LEC, reelin is expressed superficially in relation to the calbindin. On the other hand, in the mouse MEC, calbindin expression overlaps with reelin or is even superficial to it (Kobro-Flatmoen and Witter, 2019) (**Figure 17**). Therefore, by visualising the expression of the two proteins an approximate border between the LEC and MEC can be identified.

For this purpose, immunohistochemical stainings against calbindin and reelin were performed on a mouse brain (n=1). After perfusion, the brain was extracted and horizontal and coronal

sections (the two hemispheres were cut in different planes; 30 µm-thick slices; Leica CM 3050 S) were collected free-floating in 0.1 M PBS.

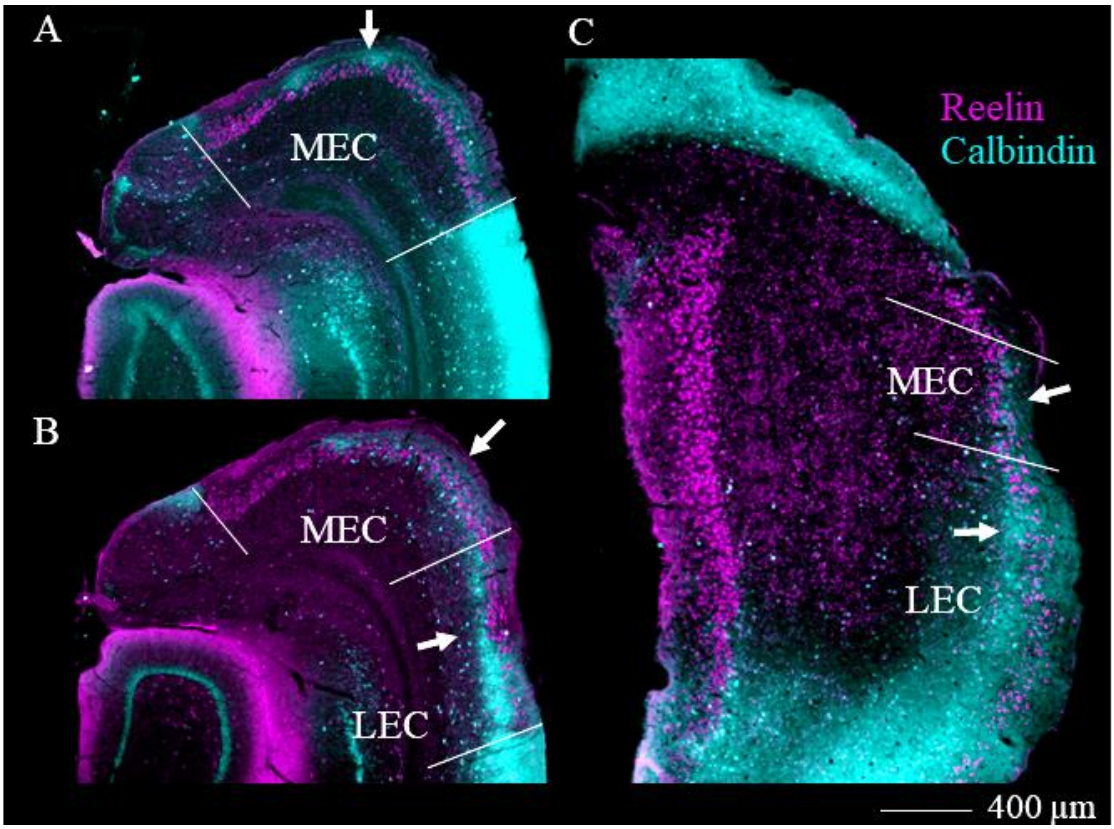

Figure 17: Immunohistochemical staining for reelin (purple) and calbindin (turquoise) in the LEC and MEC. A, B: horizontal sections, C: coronal section. The borders of the entorhinal subdivisions are marked with white lines. White arrows indicate the location of the calbindin expression in relation to reelin. In the MEC, calbindin is superficial to reelin. In the LEC, calbindin lays deep in relation to reelin. Scale bar 400 µm.

Immunohistochemical analysis

Sections were washed in 0.1 M PBS and preincubated in a blocking solution (0.1 M PBS, 0.3 % Triton X-100, 3 % BSA) for 30 minutes at room temperature. Primary antibodies for calbindin (rabbit IgGs, 1:400; Sigma, Germany) and reelin (mouse IgGs, 1:500; Sigma, Germany) were added to the buffer (blocking solution) and slices were incubated in it overnight at room temperature. Next, the sections were rinsed in 0.1 M PBS and incubated with secondary antibodies Alexa Fluor-647 (goat anti-rabbit IgGs, 1:200; Jackson Immunoresearch, UK) for two hours at room temperature. After washing the slices in 0.1 M PBS, they were then incubated in secondary antibodies Alexa Fluor-488 (goat anti-mouse IgGs, 1:200; Jackson

Immunoresearch, UK) for two hours at room temperature. Lastly, the sections were rinsed with 0.1 M PBS and coverslipped with a mounting medium.

On the following day, the results of the immunohistochemical staining were assessed on digital images captured with a Keyence Fluorescence Microscope (BZ-9000E, Japan) using a 4× objective lens.

Results

Injection sites and fluorescent labelling

Table 1: Summary of analysed cases with double retrograde injections

(note: bilateral labelling is marked with *)

Case	CTB-555	CTB-647	Hemisphere
TC15	**Exposed, 5 nl, 1% w/v** LEC II	**Enclosed, 5 nl, 1% w/v** LEC II LEC III * MEC II MEC III *	**right**
TC16	**Exposed, 10 nl, 0.1% w/v** Hilus * LEC II MEC II	**Enclosed, 10 nl, 0.1% w/v** Hilus * LEC II MEC II MEC III*	**right**
TC17	**Enclosed, 10 nl, 0.1% w/v** LEC II LEC III * MEC II MEC III *	**Exposed, 10 nl, 0.1% w/v** LEC II MEC II	**right**
TC18	**Dist. CA3/CA2, 5-10 nl, 0.1% w/v** LEC II MEC II	**Failed (injection in ventricle)**	**left**

TC19	**Exposed, 5 nl, 0.1% w/v**	**Enclosed, 5 nl, 0.1% w/v**	**left**
	LEC II	Hilus *	
	MEC II		
TC24	**Enclosed, 10 nl, 1% w/v**	**Exposed, 10 nl, 1% w/v**	**right**
	Hilus *	Hilus *	
	LEC II	LEC II	
	MEC II	MEC II	
	MEC III *		
TC25	**Prox. CA3, 10 nl, 1% w/v**	**Enclosed, 10 nl, 1% w/v**	**left**
	Hilus *	LEC II	
	CA3 *	MEC II	
	LEC II	MEC *	
	MEC II		
TC26	**CA1/CA2, 5 nl, 1% w/v**	**CA3/CA2, 5 nl, 1% w/v**	**right**
	CA3/CA2 *	LEC II	
	Subicular complex *	MEC II	
	LEC II	MEC III *	
	LEC III *		
	MEC II		
	MEC III *		

Table 1 summarises the injection sites and areas with fluorescent signals across all analysed brains (n=8). All injections were performed at comparable AP levels (~ -2.0 mm from bregma). The volume of injections (5-10 nl per injection site), the tracer concentration (0.1-1% w/v) and the target hemisphere (left vs right) varied between different brains. The longitudinal spread of the tracers was restricted to the dorsal half of the DG (**Figures 18, 19**). Both, in the MEC and LEC, retrogradely labelled fluorescent cells were found mostly in the dorsal and intermediate levels, i.e. close to the rhinal fissure (**Figure 20**).

Overall, all brains with entorhinal labelling revealed the strongest and the most consistent labelling pattern in the superficial layer II of the LEC. In most cases fluorescent signals could be observed in the superficial layer II of the MEC. Often, layer III of the MEC as well as the hilus contained bilaterally labelled cells. More rarely, fluorescent cells were observed in layer III of the LEC. Altogether, n=5 brains (TC 15, 16, 17, 24, 25) had injections centred in the

molecular layer of the enclosed blade and were considered when analysing the EC to the enclosed blade projections. Further, n=5 brains (TC 15, 16, 17, 19, 24) had injections centred in the molecular layer of the exposed blade and were considered when analysing the EC to the exposed blade projections.

Assessments of injection sites (**Figures 18, 19**) revealed that several brains could be used as controls for entorhinal labelling after injections outside of the DG (TC 18, 19, 25, 26). An injection into the proximal CA1 region (and CA2) resulted in strong bilateral MEC layer III and unilateral MEC/LEC layer II labelling (TC 26). As mentioned above, layer III MEC labelling was also often observed in other brains, but only after enclosed blade injections. The cases with the strongest MEC layer III labelling coincided with the weakest MEC layer II labelling. This, together with the observation that no MEC layer III labelling was found after exposed blade injections led to a conclusion that layer III labelling represents CA1 projecting cells, which is in line with previous reports (Steward and Scoville, 1976; van Groen et al., 2003). Further, injections into the proximal CA3 (TC 25) and distal CA3/CA2 (TC 18, 26) resulted in unilateral EC layer II labelling. This indicates that the EC projections to the CA3 and CA2 are similar to the EC-DG projections, as was also reported before (Steward and Scoville, 1976; Tamamaki and Nojyo, 1993; Cui et al., 2013; Hitti and Siegelbaum, 2014; Kohara et al., 2014). Additionally, in case TC 19 it was concluded that the tracer was taken up mostly by the commissural and associational pathway, since there was fluorescent labelling in the bilateral hilus only and none in the EC (Swanson et al., 1978). Finally, no entorhinal labelling was detected in a brain with an injection below the hippocampal fissure (TC 18), which illustrates that the EC labelling detected in other cases is hippocampus-specific and not due to, for example, cells' autofluorescence.

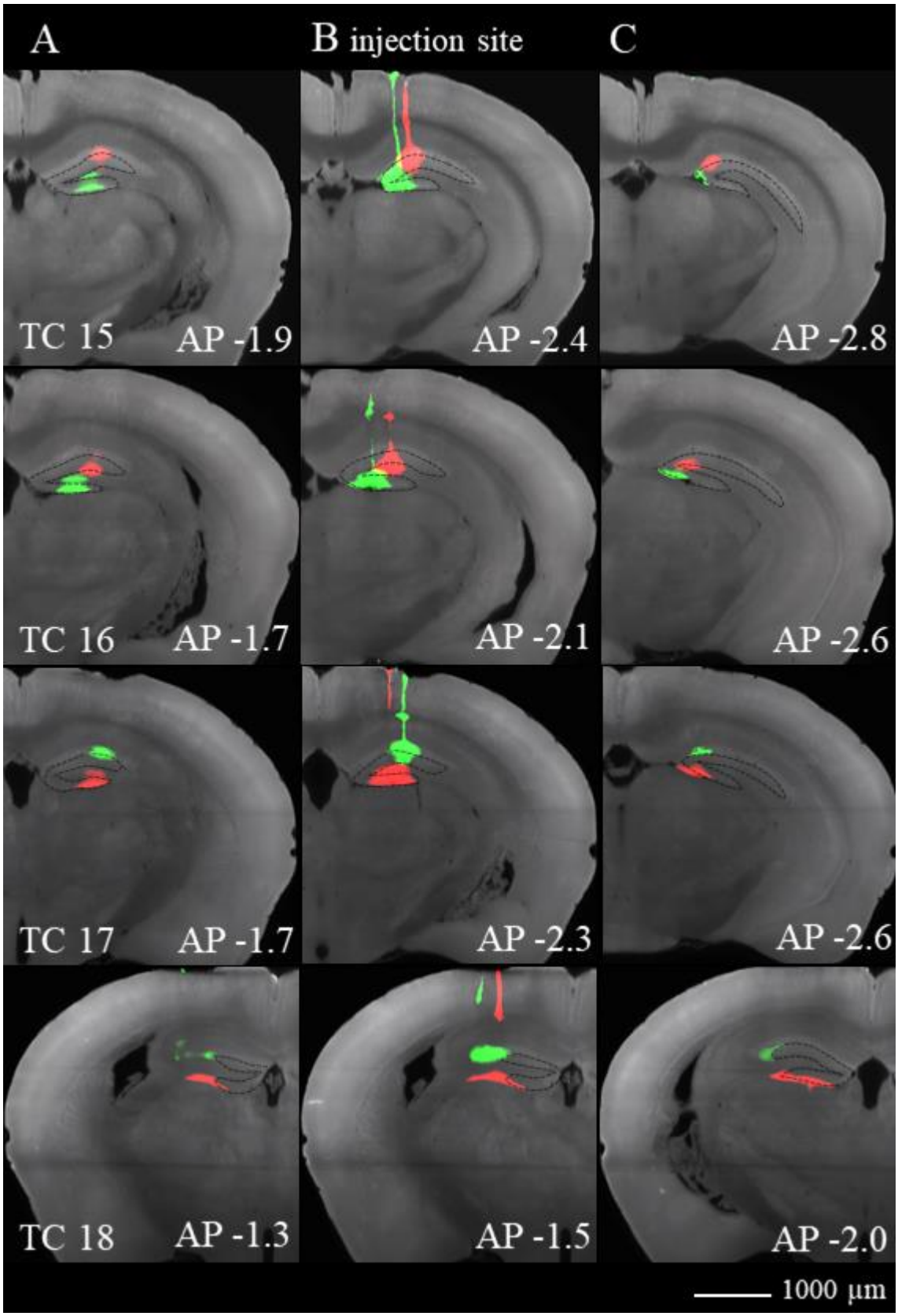

Figure 18: Overview of injection spreads in brains TC 15-18. A: rostral (anterior) extent of the tracers' spread; B: injection site; C: caudal (posterior) extent of the tracers' spread in coronal view (50-µm-thick). In green - CTB-555, in red - CTB-647, in grey – autofluorescence channel. The outlines of the DG molecular layer are indicated by the black dashed lines. Scale bar 1000 µm.

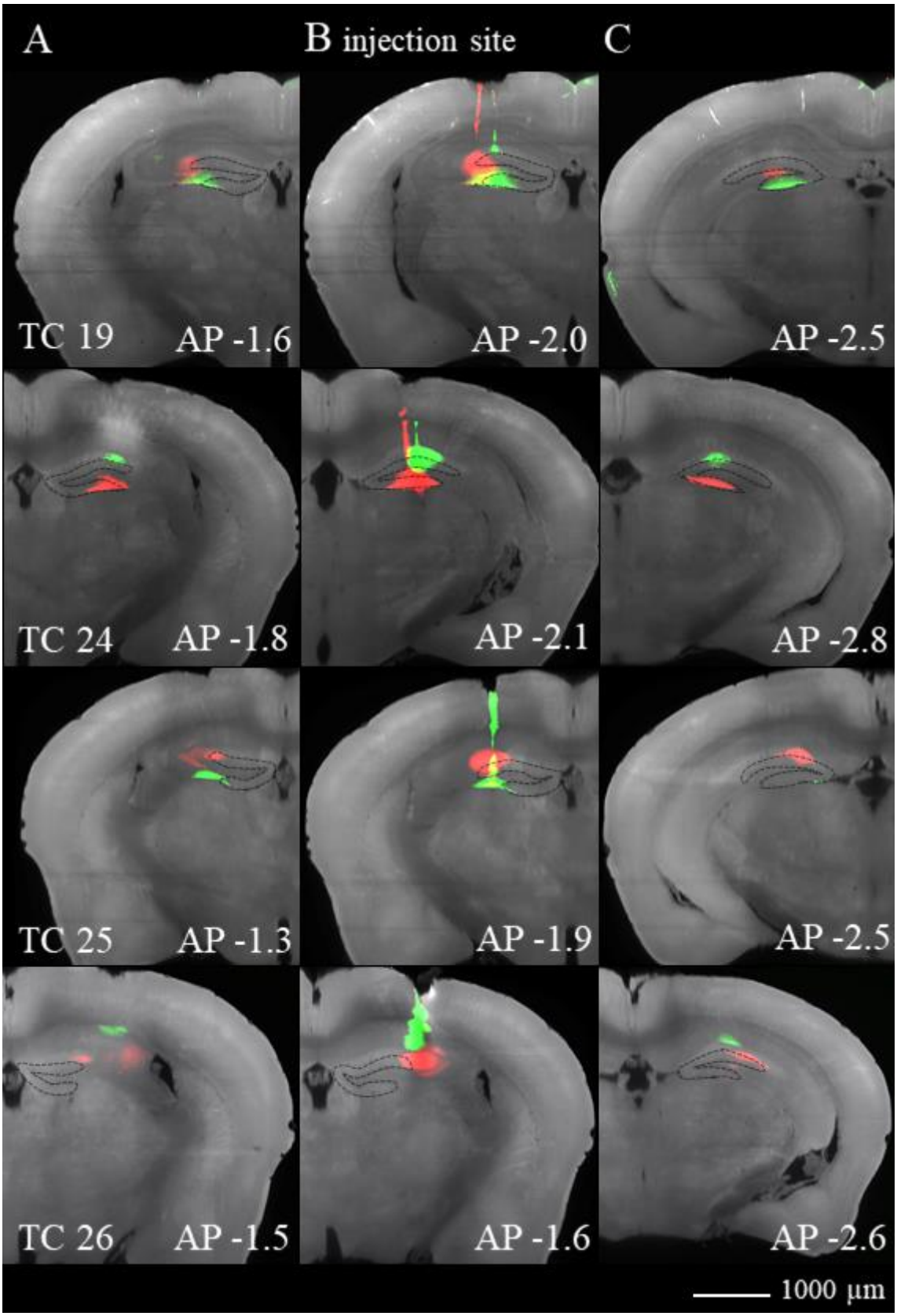

Figure 19: Overview of injection spreads in brains TC 19, 24-26. A: rostral (anterior) extent of the tracers' spread; B: injection site; C: caudal (posterior) extent of the tracers' spread in coronal view (50-µm-thick). In green - CTB-555, in red - CTB-647, in grey – autofluorescence channel. The outlines of the DG molecular layer are indicated by the black dashed lines. Scale bar 1000

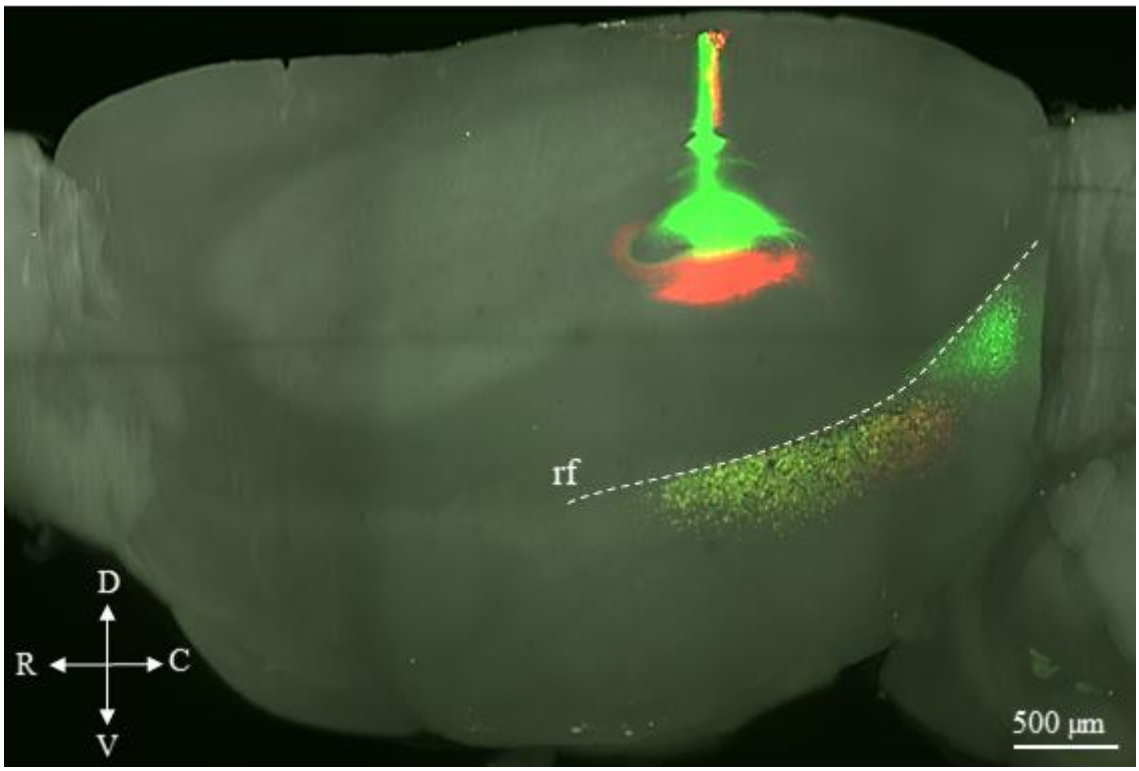

Figure 20: Full volume, sagittal view of fluorescent retrograde labelling in case TC 17. The labelling in the LEC and MEC is indicated by white arrows. Following injections into the dorsal pole of the DG, locations of retrogradely labelled cells were restricted to the dorsal levels of the LEC and MEC. In green - CTB-555, in red - CTB-647, in yellow – overlap of the two tracers. rf: rhinal fissure, D: dorsal, V: ventral, C: caudal, R: rostral. Scale bar 500 µm.

Rostral LEC targets both the enclosed and exposed blade of the DG

In the LEC, regardless of the injection origins (enclosed/exposed blade), labelling was consistently observed in layer II of the most dorsal parts (regions closest to the rhinal fissure) throughout most of the LEC's rostrocaudal extent. This is shown in an exemplary manner in one selected case (TC 24) in **Figure 21**. Interestingly, the most rostral LEC levels (see **Figure 21** horizontal and sagittal views) contained cells traced from both the enclosed and exposed blades. At these levels, it was clear that the vast majority of cells expressed both tracers and resulted in 'yellow' labelling (coronal view).

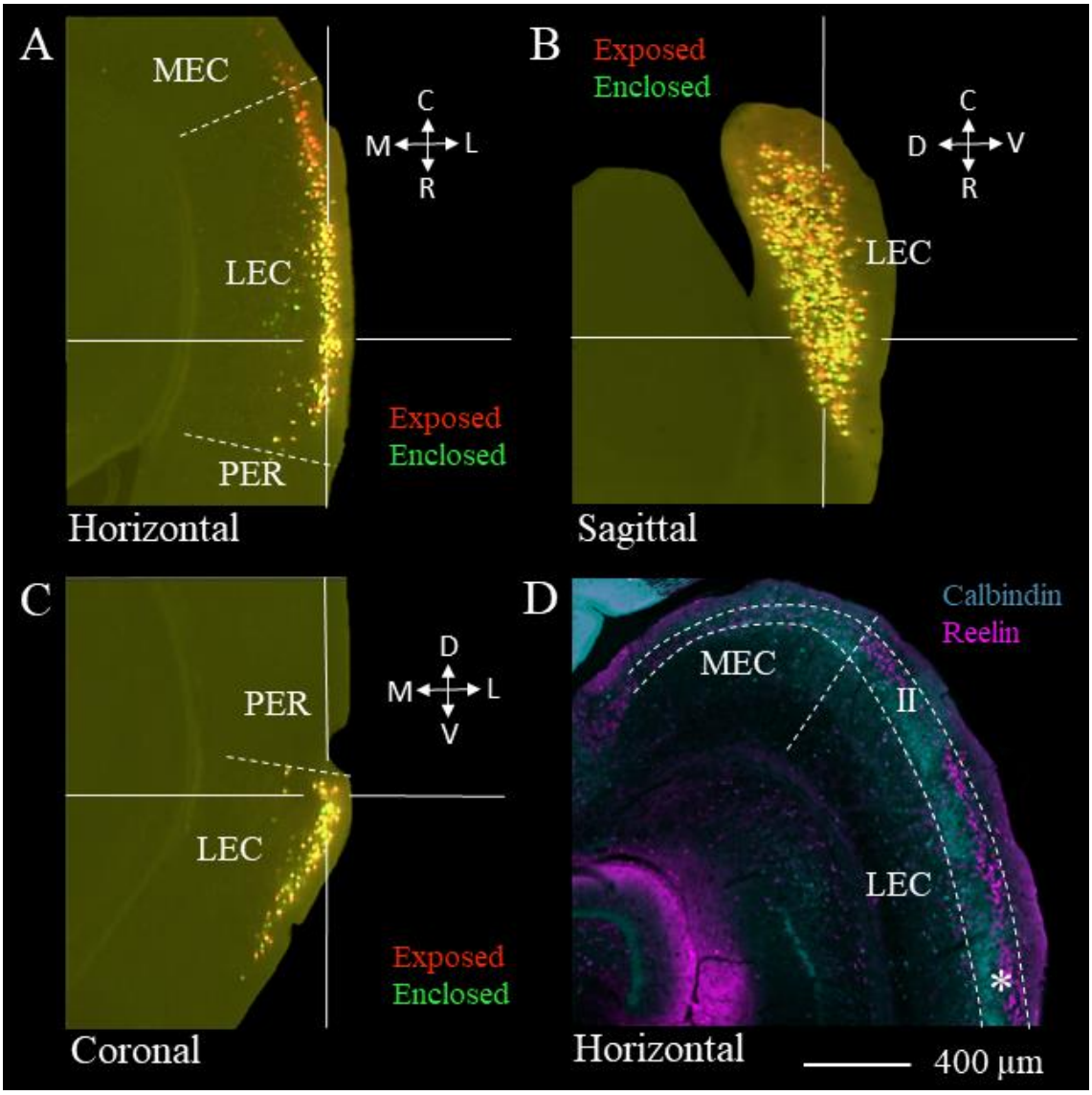

Figure 21: Rostral LEC labelling in case TC 24.

Cells located in the rostral LEC do not have a preference for either of the DG blades.

A: Labelling pattern in horizontal plane; B: sagittal plane; C: coronal plane. The sectioning planes are indicated by horizontal and vertical straight white lines. The intersection across the lines is in the rostral LEC and the same point across A-C snapshots. Following the enclosed blade injection labelling is visible in green, after the exposed blade – in red. Cells with both tracers are visible in yellow. D: calbindin and reelin expression in a horizontal slice from a similar horizontal level as in A. The star (*) indicates an estimated position of the intersection point. Note the superficial labelling of reelin (purple) in comparison to calbindin (turquoise), which is typical for the LEC in mice. PER: perirhinal cortex; C: caudal, V: ventral, R: rostral, D: dorsal, M: medial, L: lateral. To snapshoot the images, digital zoom-in was applied to an original dataset captured with a 4× objective lens. Scale bar 400 µm.

In the caudal LEC dorsally located cells preferentially target the enclosed blade, while slightly more ventrally located cells project to the exposed blade

Inspection of the caudal LEC levels revealed a dorsoventral separation of the cells projecting to the enclosed or the exposed blade of the DG (**Figure 22**). Cells projecting to the enclosed blade (visible in green in coronal view) are in the most dorsal parts of the caudal LEC (closest to the rhinal fissure), while cells that target the exposed blade spread from the rhinal fissure to further ventral locations (visible in red in coronal view). In addition, an intermediate population located between the dorsal and ventral populations projected to both the enclosed and exposed blades (visible in yellow in coronal view).

The rostral and caudal LEC pattern of labelling was observed in three out of four cases (TC 16, 17, 24) with successful double injections into the enclosed and exposed blades. In the fourth case (TC 15), injection into the enclosed blade resulted in labelling only in the rostral LEC with no labelling present in the caudal LEC (for possible explanation see Discussion). Thus, in the latter case, the caudal LEC appeared to be labelled only with a tracer injected into the exposed blade. The rostral LEC, however, appeared to be labelled with both tracers, supporting the claim that these LEC cells project to both DG blades. In a control brain TC 25 (injections into the enclosed blade and proximal CA3) no dorsoventral gradient at the level of the caudal LEC was detected. Throughout the entirety of the rostrocaudal extent of the LEC, the cells marked with tracers injected into the enclosed blade and proximal CA3 appeared to be mostly colocalised.

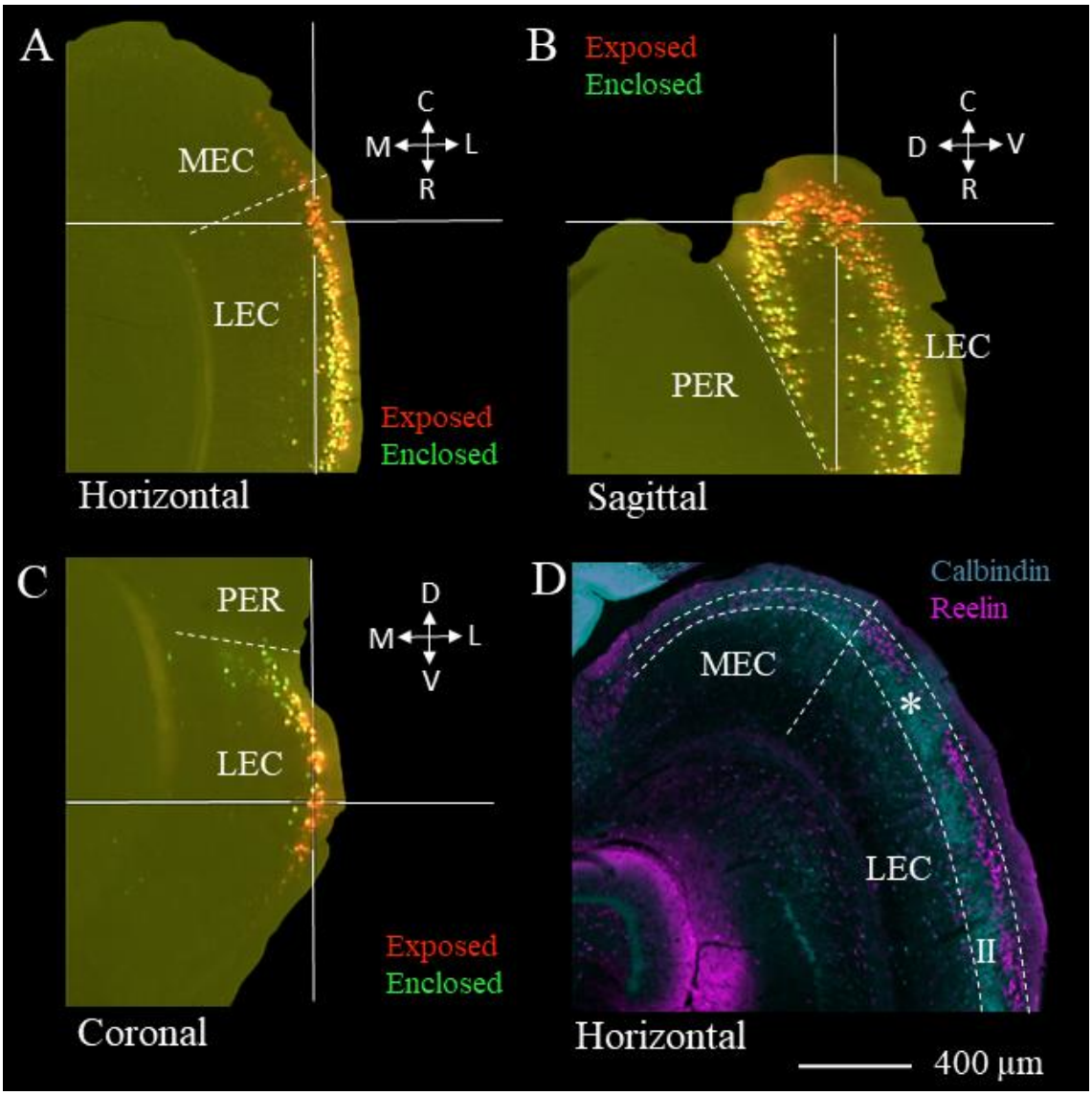

Figure 22: Caudal LEC labelling in case TC 24.

Dorsally located cells in the caudal LEC preferentially project to the enclosed blade of the DG, while cells located slightly more ventral have a preference for the exposed blade.

A: Labelling pattern in horizontal plane; B: sagittal plane; C: coronal plane. The sectioning planes are indicated by horizontal and vertical straight white lines. The intersection across the lines is in the caudal LEC and the same point across A-C snapshots. Following the enclosed blade injection labelling is visible in green, after the exposed blade – in red. Cells with both tracers are visible in yellow. D: calbindin and reelin expression in a horizontal slice from a similar horizontal level as in A. The star (*) indicates an estimated position of the intersection point. Note the superficial labelling of reelin (purple) in comparison to calbindin (turquoise), which is typical for the LEC in mice. PER: perirhinal cortex; C: caudal, V: ventral, R: rostral, D: dorsal, M: medial, L: lateral. To snapshoot the images, digital zoom-in was applied to an original dataset captured with a 4× objective lens. Scale bar 400 µm.

Dorsal cells of the rostral MEC preferentially project to the enclosed blade, while ventral cells target mainly the exposed blade of the DG

The dorsoventral gradient of cells projecting to the enclosed or the exposed blade of the DG observed in the caudal part of the LEC extended into the MEC, i.e. its rostral parts (case TC 24, **Figure 23**). In contrast to the caudal LEC though, the rostral MEC cells showed an even stronger preference for one blade than the other, since very few cells expressed both fluorescent markers (visible in yellow). This indicated that the two populations of cells projecting to either of the DG blades were mostly non-overlapping. Dorsally located cells predominantly projected to the enclosed blade (visible in green in coronal and sagittal views), while cells at the adjacent ventral levels preferentially targeted the exposed blade (visible in red in coronal and sagittal views).

This pattern of labelling was observed in three out of four cases with successful double injections into the enclosed and the exposed blade (TC 16, 17, 24; in the fourth case TC 15 no layer II cells were detected in the rostral parts of the MEC). As was the case for the LEC labelling patterns, no dorsoventral MEC gradient was observed in the control brain TC 25 (injections into the enclosed blade and proximal CA3), which signifies that the two populations (dorsal vs ventral) only emerge when comparing the enclosed vs exposed blade projections.

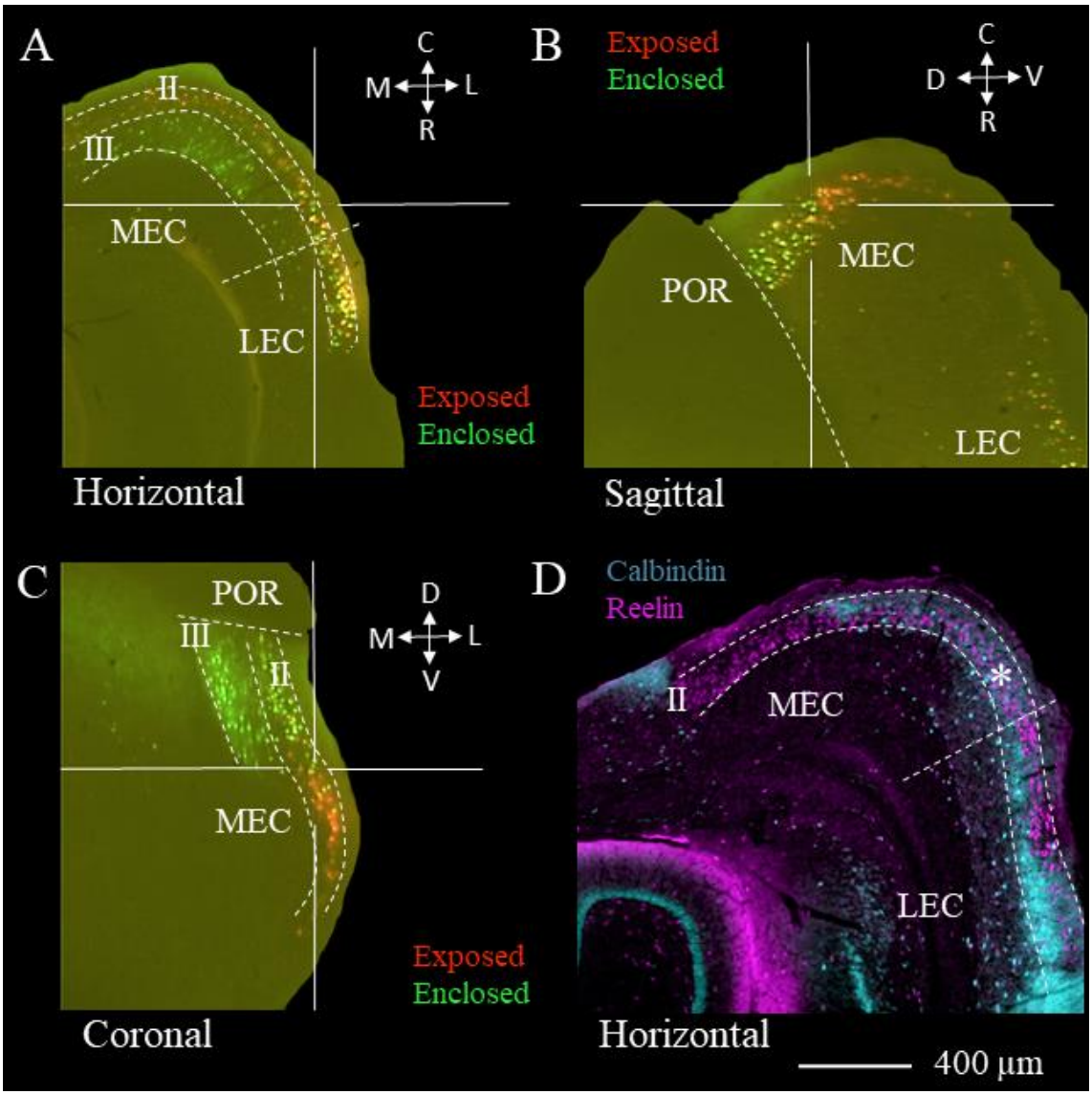

Figure 23: Rostral MEC labelling in case TC24.

Dorsally located cells in the rostral MEC preferentially project to the enclosed blade of the DG, while cells located slightly more ventral have a preference for the exposed blade.

A: Labelling pattern in horizontal plane; B: sagittal plane; C: coronal plane. The sectioning planes are indicated by horizontal and vertical straight white lines. The intersection across the lines is the same point across A-C snapshots. Following the enclosed blade injection labelling is visible in green, after the exposed blade – in red. Cells with both tracers are visible in yellow. D: calbindin and reelin expression in a horizontal slice from a similar horizontal level as in A. The star (*) indicates an estimated position of the intersection point. Note the superficial labelling of calbindin (turquoise) in comparison to reelin (purple), which is typical for the MEC in mice. POR: postrhinal cortex; C: caudal, V: ventral, R: rostral, D: dorsal, M: medial, L: lateral. To snapshoot the images, digital zoom-in was applied to an original dataset captured with a 4× objective lens. Scale bar 400 µm.

In the caudal MEC, the enclosed blade preferentially receives innervation from dorsally located cells, which are different from the 'exposed blade'-projecting cells located at dorsal and ventral levels

At the most caudal levels of MEC, the strongest labelling was observed in the dorsal levels and originated from the enclosed blade injections. Photographs of the caudal MEC are depicted in **Figure 24** (case TC 24). At progressively more ventral levels, the labelling with the exposed blade tracer increased. However, weak labelling with a tracer from the exposed blade was also present at the dorsal levels. Closer inspection of the caudal MEC revealed that, while the labelling linked to the exposed blade injection was weaker in comparison to that of the enclosed blade, it was present at both the dorsal and ventral levels. Interestingly, it was apparent that virtually no double labelled cells were present in the caudal MEC. The overlap of the two tracers ('yellow' cells), as observed, for example, in the rostral LEC, was rarely detected in the caudal MEC in case TC 24 (see coronal view in **Figure 24**: 'red' cells are intermixed at the dorsal level with 'green' cells, but almost no 'yellow' cells can be detected; additionally very few 'green' cells are present at the ventral parts).

Following enclosed blade injections, dorsal labelling of the caudal MEC was observed in two out of four brains (TC 16, 24; other two cases TC 15, 17 were devoid of caudal MEC labelling). In relation to the exposed blade, labelled cells in the caudal MEC were observed only in case TC 24 (brains TC 15, 16, 17, 19 were devoid of caudal MEC labelling after exposed blade injections). Thus, TC 24 is the only case with *double* caudal MEC labelling, while TC 16 is the case with caudal MEC labelling related only to the enclosed blade injection. Considering that TC 24 had the highest volume and concentration of the injected tracers (each 10 nl, 1% w/v), it might be that in other cases a low load of tracer uptake by MPP axons caused the lack of caudal MEC labelling. Thus, despite caudal MEC labelling after exposed blade injections being present in only one of the cases, it is unlikely that the caudal MEC projects only to the enclosed but not to the exposed blade. Moreover, pilot cases (see Supplementary data, pp. 104-105, Figure S4) support that the caudal MEC projects to both DG blades, and hence, the caudal MEC labelling related to the exposed blade as detected in TC 24 is not an 'anomalous' observation. Technical considerations aside, the most interesting observation in TC 24 was that cells labelled by different tracers hardly overlapped, which suggests that two different populations in the caudal MEC project to the enclosed and exposed blades.

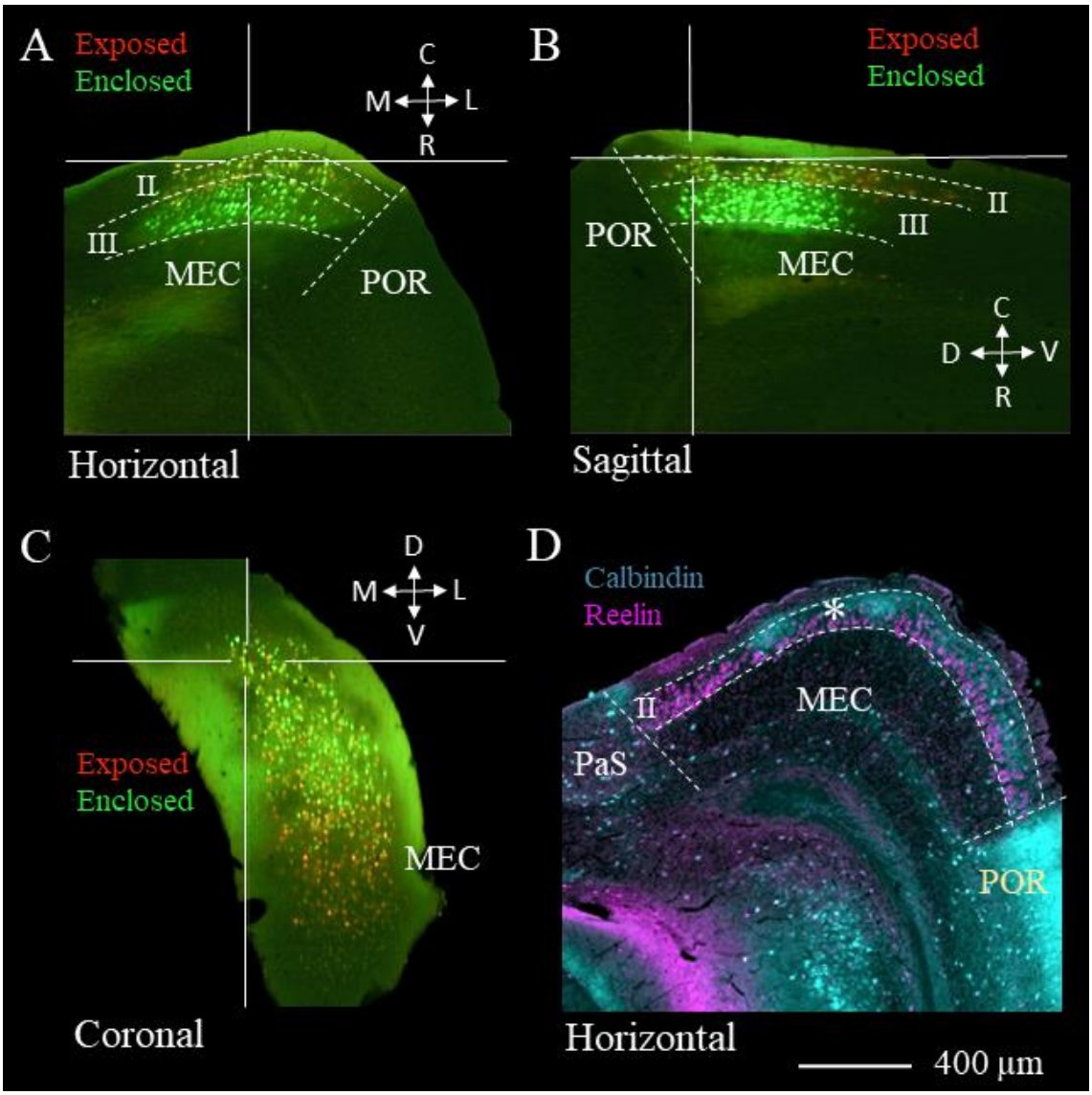

Figure 24: Caudal MEC labelling in case TC24.

Different cells in the caudal MEC project to the enclosed and the exposed blade of the DG.

A: Labelling pattern in horizontal plane; B: sagittal plane; C: coronal plane. The sectioning planes are indicated by horizontal and vertical straight white lines. The intersection across the lines is in the caudal MEC and the same point across A-C snapshots. Enclosed blade labelling is visible in green, exposed blade – in red. D: calbindin and reelin expression in a horizontal slice from a similar horizontal level as in A. The star (*) indicates an estimated position of the intersection point. Note the superficial labelling of calbindin (turquoise) in comparison to reelin (purple). POR: postrhinal cortex; PaS: parasubiculum. C: caudal, V: ventral, R: rostral, D: dorsal, M: medial, L: lateral. To snapshoot the images, digital zoom-in was applied to an original dataset captured with a 4× objective lens. Scale bar 400 µm.

Discussion

The enclosed and exposed blades of the DG are differentially involved in spatial and non-spatial memories, but it remains unresolved where this functional gradient comes from. Here, I investigated whether the enclosed blade of the DG preferentially receives inputs from the spatially tuned MEC, while the non-spatially modulated LEC is mainly targeting the exposed blade. To do so, I implemented dual retrograde tracing of entorhinal cells projecting to the enclosed or the exposed DG blades in mice.

Recapitulation of the results

The gathered tracing data suggest that the two blades of the DG do not receive similar innervation from the MEC and LEC. However, the observed projection pattern does not rigorously follow the original hypothesis. In fact, both DG blades receive strong projections originating from the entire rostrocaudal extent of the LEC and MEC. At more rostral levels of the LEC, the same cells project to both DG blades. At more caudal LEC levels, a dorsoventral gradient becomes increasingly more apparent. Dorsally located cells in the caudal LEC predominantly project to the enclosed blade; slightly more ventral cells target the exposed one and an intermediate dorsoventral population projects to both blades. Further caudal, when crossing the border to the MEC, the dorsoventral populations become increasingly more segregated (i.e. cells are essentially projecting either to the enclosed or to the exposed blade; the intermediate dorsoventral population becomes virtually non-existent). The topographical organisation, however, remains similar. Dorsally located cells preferentially project to the enclosed blade, ventrally located cells – to the exposed blade. Moreover, one out of four analysed cases suggests that the same dorsoventral segregation might persist until the most caudal part of the MEC. Of note, in the caudal MEC, a few dorsally located cells seem to innervate not only the enclosed but also the exposed blade, but these cells do not overlap with the enclosed blade projecting cells. Meanwhile ventrally located caudal MEC cells seem to exclusively target the exposed blade. However, these observations will require further proof, since no caudal MEC labelling (see later for potential explanations) was detected in the remaining three animals with double blade injections.

It should be noted that the present results describe the pattern of dorsal DG afferents, since the tracer spread affected mostly the dorsal half of the DG. Thus, at ventral hippocampal levels the innervation of the enclosed and exposed blades by the LEC or MEC might be different. To date, it is well-established that the ventral DG receives mainly inputs from the most ventrally located

EC cells (i.e. furthest away from the rhinal fissure) (Dolorfo and Amaral, 1998; Ruth et al., 1988, 1982). It was previously reported that the pattern of the entorhinal axonal distribution to the enclosed vs exposed blades does not differ between the dorsal and ventral DG levels (Wyss, 1981). Thus, it might be that the dorsoventral gradient detected in the current study could also be found at the most ventral EC levels that project to the ventral DG. However, this inference remains purely speculative and further investigations are necessary to conclude whether similar patterns as those observed in this study could be applied to the ventral DG projections.

Consistency of the LEC and MEC labelling patterns

The present data showed that the pattern of LEC to DG projection was the most consistent and reliable. In contrast, labelling in the MEC, and especially in its caudal parts, was not detected to a similar extent in all cases. The lack of MEC labelling in certain cases was likely caused by different locations of the centre of injections. As described in the introduction section, the LEC targets the outermost portions of the molecular layer of the DG (OML), while the MEC projects closer to the middle portions of this layer (MML). It is plausible to think that the tracer spread did not always equally affect the OML and MML laminas. The small injection volumes and/or tracer concentrations used in this study (which were chosen to restrict the tracers' spreads mainly to one of the DG blades) could have caused unequal uptake of the tracers by the MPP and LPP fibres.

Several observations speak in favour of the above argument. First, an injection into the enclosed blade in case TC 19 resulted in hilar labelling only, which indicates that the small tracer volumes used in this study likely do not affect the full radial extent of the molecular layer in the DG. Specifically, in TC 19 the tracer spread in the enclosed blade was likely centred on the inner molecular layer, granule cell layer or the hilus itself – areas that receive almost no entorhinal innervation. Second, cases with the strongest MEC layer III labelling, which represent CA1 projecting cells, also had the weakest MEC layer II labelling following the enclosed blade injections. It is known that the lamina receiving layer III innervation in the CA1 (SLM, stratum lacunosum moleculare) is located directly above the OML of the enclosed blade. Hence, it is reasonable to assume that in certain cases (e.g. TC 15) the tracer spread in the enclosed blade affected mostly SLM and OML but did not sufficiently reach the MML. Together, these arguments indicate that the enclosed blade injections in brains TC 15, 17 and the exposed blade injections in brains TC 15-17, 19 likely did not sufficiently affect the MML and hence, virtually no caudal MEC labelling was present in these cases. Third, regardless of the less consistent caudal MEC labelling, both tracers were often detected in the rostral MEC. As suggested by

Tamamaki (1997), Wyss (1981) and discussed by Witter (2007), the projections from the LEC and MEC to the OML and MML of the DG might not be strictly separated, but rather organised in a continuum-like manner. According to this idea, the MEC regions located closest to the LEC (i.e. rostral MEC) project closer to the OML. Hence, a more consistent detection of the rostral MEC labelling in comparison to the caudal MEC in the present study supports the above argument that most of the DG injections affected the OML rather than the MML, which led to a less often observed caudal MEC labelling.

Despite the less consistently observed caudal MEC labelling, it was possible to infer the differences in the patterns of the caudal MEC projections to the enclosed and exposed blades of the DG. Strong caudal MEC labelling was observed after enclosed (TC 16, 24) as well as exposed blade injections (TC 24). Specifically, in brain TC 24 all entorhinal levels (i.e. LEC and MEC) were *dually* labelled throughout the entire rostrocaudal extent of the EC. Moreover, pilot cases that involved only single tracer injections (see Supplementary data, pp. 104-105) strongly suggest that the caudal MEC projects to both the enclosed and exposed blades of the DG. Importantly, brain TC 24 showed that the dorsoventral gradient of projection origins' might indeed be present not only at the level of the caudal LEC and the rostral MEC, but also in the caudal MEC.

Data comparison of the current and previous tracing studies

The results of the present study support previous reports that layer II cells are the origin of the EC to the DG projection (van Groen et al., 2003; Steward and Scoville, 1976). Two facts from this study specifically support this claim. First, EC layer II labelling was reliably found following the enclosed and exposed blade injections. Second, EC layer III labelling, on the other hand, was less consistently observed. Particularly, MEC layer III labelling was only observed after enclosed blade injections. As mentioned before, this labelling likely represents CA1 projecting cells, since the SLM is located directly above the molecular layer of the enclosed blade. Also, other studies report EC layer III cells as the origin of the CA1 projection (Steward and Scoville 1976, van Groen et al., 2003). Furthermore, virtually no labelling was observed in LEC layer III cells following DG injections, which could be explained by the fact that the LEC targets mainly distal portions of the CA1 (Tamamaki and Nojyo, 1995), which were almost unaffected by the mediolateral positions of the injection sites in the enclosed blade of the DG.

Next, despite a previous study by Van Groen et al. (2003), which found that the EC to CA3/CA2 projection in mice originates in layer III, the present data suggest that the CA3 and CA2, similar

to the DG, receive innervation from the cells located in layer II of the LEC and MEC. This conclusion is supported by numerous other reports, showing that the CA3 and CA2 in mice are innervated by the EC layer II and not layer III cells (Witter, 2007; Hitti and Siegelbaum, 2014 Cui et al., 2014; Kohara et al., 2014) similar to innervation patterns described in rats and monkeys (Steward and Scoville 1976; Witter and Amaral 1991).

Most importantly, the objective of the present study was to investigate whether the enclosed blade of the DG receives stronger projection from the spatially modulated MEC, while the LEC is preferentially targeting the exposed blade. Results show that the projection pattern does not follow such a simple segregation and it departs from the previously reported gradients of the EC innervation of the enclosed and exposed blades (Wyss, 1981; Tamamaki, 1997). The two previous studies found that the LEC preferentially targets the enclosed blade, while the MEC either has no preference or projects more to the exposed one. Both studies implemented anterograde tracing of entorhinal efferents and based their conclusions on the measurement of the thickness of the MPP and LPP laminas (Tamamaki, 1997) or the density of the anterogradely transported tracing particles in the molecular layers of the DG blades (Wyss, 1981). Since both studies were conducted in rats, the differences with the present work might reflect species differences between rats and mice. However, Luna et al. (2019) conducted similar anterograde investigations in mice and by measuring the thickness of the MPP and LPP laminas they successfully replicated the results reported by the studies in rats. Thus, it is likely that the discrepancy between the present results and the studies conducted in rats is not due to species differences. Instead, the different conclusions derived from the other studies might be a consequence of the assessed parameters (i.e. thickness of the fibre laminas) rather than a reflection of the true target preferences of the LEC and MEC. In line with this argument, it was previously reported that a single EC cell projecting to the DG could occupy a thin portion of the molecular layer in one of the blades, but in the other spread within a thicker lamina (Tamamaki and Nojyo, 1993). In that study, single EC layer II neurons were filled with a tracer and their axons were traced to the molecular layer of the DG. It was revealed that some MEC cells give rise to axonal branches in the DG forming a narrow formation in the MML of the enclosed blade but occupy both MML and OML in the exposed blade. This evidence indicates that the thickness of the MPP or LPP laminas do not directly reflect the amount of EC cells innervating them, but rather the spread of the axonal bifurcation. Consequently, measuring MEC and LEC lamina thicknesses in the enclosed or exposed blades does not optimally reflect the target preferences of the MEC and LEC.

Potential functional implications of the current findings

Departing from the original hypothesis and from the results shown by others (Wyss, 1981; Tamamaki, 1997; Luna et al., 2021; Van Groen et al., 2003), the present study found that instead of preferentially targeting a specific blade, both the MEC and LEC contain cells that predominantly target one blade or the other and cells that target both DG subregions. Altogether, the DG blades receive their innervation along the entire rostrocaudal axis of the EC (i.e. including both EC subdivisions). Cells in the rostral part of the LEC almost exclusively project to both DG blades, indicated by a heavy overlap of the tracers in this region. Of note, it is unlikely that the colocalisation of the tracers in the rostral LEC occurred due to a partial overlap of the tracers at the injection sites, because the laminas receiving the LEC projection are furthest away from each other within the radial DG organisation. If both tracers were taken up by the axonal terminals in each of these regions, tracers' overlap would also happen in the MML laminas and the colocalisation of the tracers would have been observed also in the MEC. In contrast to this, in the caudal LEC as well as rostral and caudal MEC, a dorsoventral split of the cells projecting to the enclosed or exposed blade was observed. Moreover, with increasingly more caudal levels in the MEC, the cells projecting to either of the DG blades were mostly nonoverlapping.

The fact that the rostral LEC projects to both DG blades in a more or less homogeneous manner could indicate that this region might equally support spatial and non-spatial processing and/or it might have a fundamentally different role. For example, recordings in the rostral parts of the LEC indicate that this region supports both spatial and non-spatial information processing (Huang et al., 2023). A few cortical and subcortical connectivity gradients also suggest that this region might play an especially relevant part in nonvisual information processing, e.g. olfactory, affective, and attentional processes (Insausti et al., 1997; Kerr et al., 2007; Agster and Burwell, 2009; Burwell and Amaral, 1998). Notably, the LEC has been implicated in multimodal and associative processing underlying episodic-like memories (Doan et al., 2019; Wilson et al, 2013; Persson et al., 2022; Chao et al., 2016; Morrissey et al., 2012). Together, it might be that the rostral LEC in comparison to the caudal LEC and MEC plays a more prominent role in multimodal input convergence and this may be further reflected in equal projections of this region to the both DG blades. It might, however, also signify that the rostral LEC supports spatial and non-spatial processing similarly.

In comparison to the rostral LEC, cells in the MEC and caudal LEC do not project homogeneously to the two DG blades, i.e. some cells have a preference for the enclosed blade

while others mainly innervate the exposed one. Therefore, functional double dissociation of the DG blades for spatial and non-spatial memories might come from the fact that caudal entorhinal levels (including caudal LEC, rostral and caudal MEC) might contain two functionally distinct populations of cells that preferentially support spatial or non-spatial information processing. Despite the classical view that the MEC is spatially modulated and the LEC is non-spatially tuned, cumulative evidence suggests that both entorhinal subdivisions are involved in spatial and non-spatial processing (*LEC*: Huang et al., 2023; Deshmukh and Knierim, 2011; Tsao et al., 2013; Van Cauter et al., 2013; Beer et al., 2013; *MEC*: Sauvage et al., 2010; Lipton and Eichenbaum, 2008; Hales et al., 2021; Schlesiger et al., 2015; Diehl et al., 2017; Aronov et al., 2017; Boccara et al., 2019; Butler et al., 2019; Xu et al., 2022). Therefore, it is plausible to assume that the LEC and MEC each might contain different cell populations that could differentially process spatial and non-spatial signals. In particular, the present data indicate that dorsocaudal EC cells would be spatially modulated, while the adjacent ventral portions would be non-spatially tuned. Such functional differences could in turn occur because the two cell populations might, for example, comprise different cells, receive different projections or have different local wiring with inhibitory cell types (for further discussion see Chapter V).

In summary, the current tracing experiment provided the first-time evidence that the innervation of the DG blades by the LEC and MEC is not as homogeneous as previously thought. The two blades receive potentially different (qualitative) EC inputs, since they are partially innervated by different EC cells. Thus, this study provides further evidence to the growing list of differences between the enclosed and exposed blades of the DG.

V.

General Discussion

The overall aim of the present work was to investigate the role of the dentate gyrus (DG) in spatial and non-spatial mnemonic processes. A particular focus was made on two anatomically segregated regions within the area – the enclosed and exposed blades – and their individual contribution to spatial and non-spatial memories. By implementing behavioural, optogenetic, molecular imaging, and anatomical tracing approaches, four main observations were made. First, the blades of the DG do not share a similar role in memory processes. The enclosed blade selectively supports spatial processing. In contrast, the exposed blade is specifically involved in non-spatial processing. Second, the two blades might be embedded in larger-scale hippocampal spatial and non-spatial subnetworks, as their manipulation altered the activity of the downstream spatial and non-spatial hippocampal subregions. Third, the mechanisms supporting spatial and non-spatial memory retrieval in the networks involving the DG blades appear to be fundamentally different. Silencing of the enclosed blade increased the activity of the spatial and non-spatial hippocampal subnetworks. Inhibition of the exposed blade, on the other hand, decreased the activity of the non-spatial hippocampal subnetwork. Fourth, the two DG blades receive different innervation by cells of the lateral (LEC) and medial (MEC) entorhinal cortices. There are two cell populations at the caudal levels of the entorhinal cortex (EC) that preferentially project to one of the DG blades and as discussed later in this chapter,

these populations might support spatial and non-spatial processing differently. Consequently, functionally distinct entorhinal input to the DG might contribute to the functional double dissociation of the enclosed and exposed blades for spatial/non-spatial memories that was established throughout this work.

The enclosed blade of the DG selectively contributes to spatial memories, the exposed blade – to non-spatial memories

To date, when investigating the role of the DG in different cognitive processes, for example episodic memory, this region was viewed as a homogeneous structure. Despite a plethora of studies indicating that the enclosed and exposed blades of the DG are in fact quite different from each other (for overview see Chapter I: The dentate gyrus is a heterogeneous structure), the belief that these subregions support memory processing in a similar manner comes from the observation that the non-spatially tuned LEC and spatial-tuned MEC (i.e. main input areas to the DG) project onto the same DG cells regardless of whether these cells are located in the enclosed or the exposed blade. This observation strongly influenced the current consensus that the DG is involved in converging functionally distinct cortical information, which is then relayed to the rest of the hippocampus. However, previous studies did not systematically investigate whether the innervation of the 'enclosed' DG cells differs from the inputs to the 'exposed' ones. Moreover, the DG projects onto anatomically and functionally segregated (i.e. spatial and non-spatial) downstream hippocampal subregions. Consequently, it seems counterintuitive that the DG would receive and send forward spatial and non-spatial information in a segregated manner, but process the two types of information conjointly within itself. In line with this argument, the present work shows that domain-specific memories depend either on the activity of the enclosed blade or the exposed blade of the DG. By optogenetically perturbing the activity of one of the blades while animals were engaging in spatial or non-spatial memory tasks, it was shown that the enclosed blade is necessary for spatial information processing, while the exposed blade mainly supports the non-spatial processing. This functional-double dissociation of the two DG regions is reported for the first time, since the few previous studies that did dissociate between the enclosed and exposed DG blades investigated their roles in either spatial or non-spatial but not both types of processing, and especially not in mnemonic processing (Ramírez-Amaya et al., 2005; Chawla et al., 2005; Soulé et al., 2008; Snyder et al., 2011; Satvat et al., 2011; Hoang et al., 2018; Chaillan et al., 1997).

While most studies on the DG either do not distinguish between the contribution of the enclosed and exposed blades' or conduct their investigations on the activity of the enclosed blade only, a

body of evidence from different research fields reinforces the reported double-dissociation found in the present work. As introduced in Chapter I, the enclosed blade of the DG seems to be under stronger inhibitory control, as indicated by the proportion of inhibitory cells in this region (Woodson et al., 1989; Seress and Pokorny, 1981). This is also demonstrated by the fact that electrical stimulations of the enclosed blade elicit smaller local population spikes in comparison to stimulating the exposed blade, despite stronger postsynaptic potentials in the former blade (Scharfman, 2002). It is also well-established that alcohol affects the inhibitory neuronal activity by acting on GABA receptors (Mody et al., 2007) and exerts strong influences on DG physiology (Anderson et al., 2012; Dhanabalan et al., 2018; Nalberczak-Skóra et al., 2023). Because of this it is not surprising that the enclosed blade of the DG seems to be stronger affected by alcohol than the exposed blade (Cadete-Leite et al., 1997). Therefore, because the enclosed blade is more spatially modulated, one might expect that alcohol affects spatial memory processing stronger than non-spatial processing. Several studies provide evidence for this and report harmful effects on spatial memories due to alcohol consumption (García-Moreno et al., 2012; Cippitelli et al., 2010; Matthews et al., 1999; Markwiese et al., 1998; Rajendran and Spear, 2004). Non-spatial memories, on the other hand, are less affected (García-Moreno et al., 2012; Cippitelli et al., 2010).

With regards to the exposed blade, evidence indicates that this subregion has a higher number of type II metabotropic glutamate receptors (Shigemoto et al., 1997), which are required for intact non-spatial memory performance, but leave spatial memories unaffected (Pitsikas and Markou, 2014). The exposed blade also shows increased reactivity for metabotropic glutamate receptor 5 (Shigemoto et al., 1997), a key player for a certain form of long-term potentiation, the suppression of which decreases rats' performance in a non-spatial olfactory discrimination task (Wang et al., 2016). Moreover, studies in humans and rodents also show that non-spatial cognitive deficits precede spatial ones during ageing (Reagh et al., 2018; Yassa et al., 2011; Johnson et al., 2017). This parallels the observations that the exposed blade is more vulnerable to ageing-related modifications (Sugaya et al., 1996; Simonyi et al., 2000).

Altogether, different studies – from anatomical to functional investigations of the DG in cognition and otherwise – have been pointing towards functionally distinct roles of the DG blades in terms of spatial and non-spatial processing. In the present work this prediction was tested and it was concluded that the two types of processing are indeed supported by the enclosed and exposed blades of the DG to different extents.

The enclosed blade of the DG might be a part of the spatial hippocampal subnetwork and the exposed blade – of the non-spatial one

The enclosed and exposed blades of the DG not only have specific roles in spatial and non-spatial memory processing, but they also affect the activity of the downstream hippocampal spatial and non-spatial subnetworks. This was established by a molecular imaging of the activity of the spatial (distal CA3-proximal CA1) and the non-spatial (proximal CA3-distal CA1) hippocampal subnetworks following optogenetic inhibition of the cell firing in one blade or the other during spatial or non-spatial memory retrieval. The results revealed that the non-spatial hippocampal subnetwork was selectively affected when the exposed blade was inactivated during non-spatial memory retrieval. Specifically, the activity of the proximal CA3, as measured with *Arc*, decreased. In contrast, in animals with a spatial memory deficit (i.e. after silencing cell firing in the enclosed blade), the activity of the spatial and non-spatial hippocampal subnetworks were affected. In particular, the activity of the distal and proximal CA3 increased. Altogether, these results indicate that the exposed blade is functionally linked to the activity of the proximal CA3 and thus, is likely a part of the non-spatial hippocampal subnetwork. For the enclosed blade, the situation is more complex, as inhibition of the cell firing in this area led to different activity in the CA3 subregions, which are parts of the spatial and non-spatial subnetworks. Most likely this is because the enclosed blade of the DG projects to the proximal and distal parts of CA3 (Claiborne et al., 1986), even though its functional role suggests stronger functional ties with the distal CA3. Alternatively, it is also plausible that the enclosed blade exerts more control over the activity of the distal CA3, which in turn affects the activity of the proximal CA3. The distal CA3 is known to send recurrent collaterals to the proximal CA3, but not receive much of the proximal CA3 innervation in return (Witter, 2007). Hence, the effect of enclosed blade inhibition on the proximal CA3 may be a byproduct of distal-to-proximal CA3 connectivity. In summary, these data show that the enclosed blade of the DG might be a part of the spatial hippocampal subnetwork, albeit not exclusively.

Spatial and non-spatial memory retrieval likely recruits different mechanisms in the DG-CA3 circuit

In general, the mechanisms by which the enclosed and exposed blades of the DG contribute to spatial and non-spatial memory retrieval appear to be fundamentally different. This was illustrated by the observation that inactivation of the enclosed blade increased the recruitment

of the proximal and distal CA3, while the activity of the proximal CA3 was suppressed by silencing the exposed blade. It seems plausible to conclude that suppression of the granule cells activity in this blade leads to a reduction of the excitatory drive on the pyramidal cells of the CA3, which in turn results in decreased recruitment of the CA3. This supports the observations that signal transmission from the DG to the CA3, and specifically from the exposed blade to the proximal CA3, is excitatory (Scharfman et al., 2002; Gloor et al., 1963; Andersen et al., 1969). In contrast, the fact that inactivating the enclosed blade increased the activity of the proximal and distal CA3 suggests that this blade interacts with CA3 subregions in a different manner. A possible mechanism for this interregional communication comes from the fact that mossy fibres (DG axons) contact not only pyramidal cells in the CA3 but also interneurons (Acsády et al., 1998; Neubrandt et al., 2017), which exert inhibitory control over the CA3 pyramidal cells (Mori et al., 2004, Henze et al., 2002; Acsády et al., 1998). This is further illustrated by findings that, in addition to the excitation of the CA3 by the DG, stimulations of the DG lead to inhibitory postsynaptic potentials in the CA3 pyramidal cells (Yamamoto 1972; Brown and Johnston, 1983; Barrionuevo et al., 1986). Interestingly, in the latter studies, stimulations of the DG occurred exclusively in the enclosed blade. Hence, it is yet to be explored whether the exposed blade of the DG can activate the inhibitory CA3 cells like its counterpart region. This prompts speculation that the feedforward inhibition in the DG-CA3 circuit might originate only (or at least to a stronger extent) in the enclosed blade of the DG. If this is indeed the case, it could explain the present finding that only enclosed blade inhibition led to increased CA3 activity. In support of this hypothesis, the distal CA3, which predominantly receives inputs from the enclosed blade, has a higher number of inhibitory cells compared to its proximal counterpart (Sun et al., 2018). It is therefore tempting to propose that spatial memory retrieval in the enclosed blade-distal CA3 network is specifically supported by inhibitory mechanisms, which are not engaged in the exposed blade-proximal CA3 circuit during non-spatial memory retrieval.

The relevance of feedforward inhibition in memory processing has been demonstrated in previous works (Ruediger and Vittori et al., 2011; Guo et al., 2018; Twarkowski et al., 2022). These studies show that the recruitment of feedforward inhibition in the DG-CA3 system promotes memory stability and precision. Interestingly, this mechanism is highly plastic. The number of contacts between the DG mossy fibres and CA3 interneurons was shown to increase with learning, especially in tasks with a strong spatial component (Ruediger and Vittori et al., 2011). In line with the present results, the aforementioned study clearly demonstrated that blocking the feedforward inhibition leads to increased CA3 activation and accompanying

retrieval impairments. The present work, however, is the first to suggest that different mechanisms are employed when the hippocampus (or more specifically the DG-CA3 network) is retrieving spatial or non-spatial memories.

Given that spatial and non-spatial memory retrieval might be supported by different circuit mechanisms, a question arises as to how the retrieval of 'full' memories (typical episodic memory with both spatial and non-spatial dimensions present) occurs? Usually, when investigating neural correlates underlying episodic memory processing, studies rarely use mnemonic tasks, in which more than one dimension is present or relevant to successfully 'solve' the task. Also, studies that do focus on 'full' mnemonic representations often implement lesioning approaches and only characterise the behavioural consequences following such manipulations (e.g. Langston and Wood, 2010; Ergorul and Eichenbaum, 2004; Gilbert and Kesner, 2002; Gilbert and Kesner, 2003; Dees and Kesner, 2013; Day et al., 2003; Goodrich-Hunsaker et al., 2009). Alternatively, studies with 'rich' tasks focus on conjunctive coding properties of single cells (Komorowski et al., 2009; Wood et al., 1999; Manns and Eichenbaum, 2009; Ásgeirsdóttir et al., 2020; Burke et al., 2011; Deshmukh and Knierim, 2013). Thus, is it not surprising that virtually no studies describing the neural circuits supporting typical episodic memory processing at the networks' level exist (but see Beer and Vavra et al., 2018). One possibility is that - when spatial and non-spatial information are relevant - both DG blades are actively retrieving mnemonic information and both proximal and distal CA3 are activated due to their respective connections with the exposed and enclosed blades. Additionally, the activity of the distal CA3 might be kept in balance by a feedforward inhibitory circuitry. This mechanism may be of particular importance, since the distal CA3 receives more of the entorhinal and autoassociative innervation in comparison to its proximal counterpart (Witter, 2007). Hence, without the additional inhibition, the distal CA3 might be 'overexcited', which is detrimental for successful memory retrieval (Ruediger and Vittori et al., 2011; Reagh et al., 2018; Yassa et al., 2011). Also, feedforward inhibition might activate certain molecular mechanisms that are critical for spatial memory processing but not for non-spatial processing. By recruiting potentially different mechanisms for spatial and non-spatial processing, the overall hippocampal network might be able to perform both and flexibly switch between the retrieval of 'single-dimension' memories or more 'rich' mnemonic representations. This further suggests that the subnetworks relevant for spatial and non-spatial processing are not in a direct competition with each other, but rather complementary. This was also illustrated in Beer and Vavra et al. (2018). The authors demonstrated that in a task with two distinct dimensions ('what-were' and 'what-when') animals with successful retrieval of both mnemonic representations

had increased recruitment of both spatial and non-spatial hippocampal subnetworks. Their study also revealed that the activity of one of the subnetworks likely does not depend on the recruitment of the other, as animals with successful spatial or non-spatial memories showed increased recruitment of the relevant subnetwork only. Altogether, these speculations suggest that the two blades of the DG might be complementary systems and not in a direct competition with each other. It can be argued that complementary organisation of the mnemonic systems supporting 'single-dimension' memory retrieval is beneficial, because a failure or loss of one of the circuits would not necessarily cause global mnemonic deficits.

Functional segregation of the DG blades may be partially explained by different inputs arising from the LEC and MEC

At last, the present work suggests that functional differences of the enclosed and exposed blades of the DG might stem from different innervation of these regions by the MEC and LEC. Originally it was hypothesised that the MEC might preferentially target the enclosed blade of the DG, while the LEC may predominantly wire with the exposed one based on the functional profiles of the MEC and LEC (Fernández-Ruiz et al., 2021; Fyhn et al., 2008; Tennant et al., 2018; Hargreaves et al., 2005; Deshmukh et al., 2012; Tsao et al., 2013). Prior research reported several findings contradicting this hypothesis. First, the LEC and MEC project to the same DG granule cells, regardless of the cells' positions (i.e. either in the enclosed or exposed blades). The LEC targets the most distal parts of granule cell dendrites, while the MEC makes synaptic contacts closer to the granule somas (Hjorth-Simonsen and Jeune, 1972, Steward, 1976; Tamamaki, 1997). Second, the studies that did identify differences in the innervation pattern by the MEC and LEC indicate that the LEC preferentially targets the enclosed blade, while the MEC mainly projects to the exposed one (Wyss, 1989; Tamamaki, 1997, Luna et al., 2019). This gradient of innervation directly opposes the functional roles of the DG blades in spatial and non-spatial memories as described in the present work. However, the aforementioned studies assessed the preference of the LEC and MEC for one of the DG blades by measuring the thickness of the LEC or MEC axon laminas in the molecular layer of the DG. In my opinion this approach reflects the distribution of entorhinal axons in the molecular layer of the blades but not the amount of axons present. Thus, interpretations regarding the preference of the LEC or MEC for either of the DG blades might not be appropriate given the type of data collected in those studies. In comparison, the present study used a dual-tracing retrograde tracing approach to show that both DG blades receive projections originating throughout the entire rostrocaudal extent of the EC (i.e. including the LEC and MEC). Interestingly and departing from the original

prediction, the same cells in the rostral levels of the EC (i.e. rostral LEC) projected to both DG blades, but at more caudal EC levels (i.e. caudal LEC and MEC) distinct dorsoventral cell populations had a preference for one the blades. Dorsally located cells (closest to the rhinal fissure) preferentially targeted the enclosed blade, while the adjacent ventral cells predominantly projected to the exposed blade. This segregation persisted until the most caudal MEC parts, where the overlap of the two cell populations was virtually non-existent.

Together, the above-described projection pattern suggests that caudal levels of the EC might contain two functionally distinct cell populations that support spatial or non-spatial processing to different extents. What evidence would support such a hypothesis? The present tracing results suggest that cells projecting to the enclosed blade are the most dorsally located cells (closest to the rhinal fissure) throughout the rostrocaudal EC extent. These levels are also known as dorsolateral EC band and has been importantly shown as relevant for spatial memories (Steffenach et al., 2005). Next, regardless of the preferential spatial tuning of the MEC and non-spatial tuning of the LEC, studies indicate that both subdivisions are in fact sensitive to spatial and non-spatial signals. For example, on the level of the MEC, available evidence indicates that this region also plays a role in non-spatial processing and memories (Sauvage et al., 2010; Lipton and Eichenbaum, 2008; Hales et al., 2021; Schlesiger et al., 2015; Diehl et al., 2017; Aronov et al., 2017; Boccara et al., 2019; Butler et al., 2019; Xu et al., 2022). While these reports do not address the dorsoventral differences in spatial modulation of the MEC, they show that non-spatial processing exists alongside spatial processing in this region. Importantly, several works illustrate that dorsal parts of the MEC are more spatially modulated. Most prominently, grid cells were discovered in dorsocaudal parts of the MEC, while progressively more ventral portions of the same region exhibit less spatial modulation (Fyhn et al., 2004; Hafting et al., 2005). The latter observation is reinforced by reports showing that the scale of the grid cells expands in the dorsoventral direction (Stensola et al., 2012; Brun et al., 2008; Giocomo et al., 2011), matching the increasing dorsoventral gradient in the scale of place cells' representation in the hippocampus (Jung et al., 1994; Kjelstrup et al., 2008). The rate of another important aspect of spatial processing – phase precession – also changes (decreases) in dorsoventral direction in the caudal MEC (Hafting et al., 2008). Furthermore, the dorsocaudal MEC is a main hub not only for grid cells, but also for a number of spatially modulated cells, such as head direction or border cells (Sargolini et al., 2006; Solstad et al., 2008; Savelli et al., 2008). Similar to the grid cells, head direction cells are topographically organised (dorsoventral scaling gradient), with the dorsally located cells having the sharpest directionality tuning (Giocomo et al., 2014). As a reminder, the current tracing data revealed that a number of

dorsocaudal MEC cells also projected to the exposed blade of the DG. Importantly, these cells were different from the majority of cells detected in this region, which projected to the enclosed blade. In line with this observation, Obenhaus et al. (2022) demonstrated that the grid cells in the dorsocaudal MEC exhibit very little overlap with the object-vector cells, a subclass of cells exhibiting much stronger non-spatial modulation in comparison to the grid cells (Høydal et al., 2019).

At the level of the LEC, spatial alongside non-spatial processing is also well-described (e.g. Deshmukh and Knierim, 2011; Tsao et al., 2013; Van Cauter et al., 2013; Beer et al., 2013). Interestingly, a recent study by Huang et al. (2023) suggested the existence of a spatial gradient along the rostrocaudal extent of the LEC. Specifically, electrophysiological recordings revealed that rostral parts of the LEC are more spatially modulated than the caudal parts of the LEC. After investigating the dorsoventral recording sites in that study, it was clear that the most dorsal levels (closest to the rhinal fissure) were avoided. In the rostral LEC, the recordings usually took place at the levels, which according to the present tracing data project to both DG blades and thus, it is not surprising that both types of modulation were detected at these levels in the study by Huang et al. In contrast, in the caudal LEC, the recording sites corresponded more to the levels projecting predominantly to the exposed blade. This observation might explain why these levels appeared less spatially modulated. The present tracing results are further supported by a study by Tsao et al. (2013). Here, neural activity of the caudal LEC was recorded, albeit no differentiations were made with regard to the dorsoventral position of the recorded cells. The authors identified two independent cell classes that responded either to objects or locations, where the objects were previously encountered. The authors reported that the two cell classes were vastly independent, which supports the current data claiming that at the caudal LEC two different populations of cells can be identified, each preferentially targeting one of the DG blades and thus, mainly supporting either spatial or non-spatial processing. However, since it is unclear whether the ‘object’ or ‘object-trace’ responsive cells identified in Tsao et al. (2013) were located at different dorsoventral positions in the caudal LEC, further systematic investigations are required to address this hypothesis.

The proposed functional segregation of the dorsal vs more ventrally located caudal EC cells could have several causes. For example, it may arise from different inputs targeting the two cell populations. While several anatomical studies indicate that the dorsolateral EC band (i.e. the levels of the ‘enclosed blade-projecting’ cells) receives a substantial amount of inputs from areas with spatial tuning, e.g. postrhinal cortex (Doan et al., 2019), presubiculum (van Haeften et al., 1997), it is currently unclear whether the adjacent, slightly more ventrally located caudal

EC cells receive less of such innervation. Another possible cause of the hypothesised functional segregation of the dorsoventral cell populations in the caudal EC could be the differences in local circuitry wiring. Interestingly, EC levels closest to the rhinal fissure coincide with the strongest parvalbumin (PV) expression (Wouterlood et al., 1995; Kobro-Flatmoen and Witter, 2019). Despite the lack of a clear functional link between the PV-positive cells and spatial processing to date (but see: Miao et al., 2017; Korotkova and Fuchs et al., 2010), it seems that regions with a higher number of PV-expressing cells tend to be more spatially modulated. Particularly, the enclosed blade of the DG and distal CA3 have a higher number of PV-cells than the exposed blade of the DG and the proximal CA3 (Sun et al., 2018; Woodson et al., 1989, Seress and Pokorny, 1981). Also, the MEC in comparison to the LEC has a higher number of PV-expressing cells (Kobro-Flatmoen and Witter, 2019). Within the caudal MEC, dorsally located cells receive stronger modulation by the PV-positive interneurons than the ventral MEC levels (Beed et al., 2013; Grosser et al., 2021). In the LEC, PV expression is confined mainly to the levels closest to the rhinal fissure. Thus, it might be that the functional differences of the caudal EC cells preferentially projecting to the enclosed or exposed blades arise from differences in their wiring with the local cells. Together, if the dorsally located caudal MEC and LEC cells are indeed more spatial in their function and more ventrally located cells are more non-spatial, the LEC and MEC innervation pattern observed in the present work would support the functional segregation of the enclosed and exposed blades of the DG.

Beside LEC/MEC innervation of the DG cells *per se*, evidence indicates that the enclosed and exposed blades (at least in rodents) might prioritise connections with one entorhinal subdivision over the other. For example, Gallitano et al. (2016) reported that granule cells within the enclosed blade of the DG have greater dendritic material (i.e. amount of dendritic processes) in the region receiving the fibres from the MEC than the corresponding region in the exposed blade. Moreover, within the enclosed blade, the layer receiving the MEC inputs has more spine volume than the one with the LEC fibres (Hama et al., 1989). Also, in the exposed blade dendritic pruning (elimination of dendritic processes) occurs in the lamina with the MEC fibres, while synaptic proliferation (formation of new synapses) is observed in the region with the LEC fibres (Zehr et al., 2008). Altogether, it seems that the enclosed blade preferentially builds synaptic contacts with the MEC, while in the exposed blade the pattern might be reversed and preferential connections are established with the LEC. This pattern of synaptic connectivity along with the anatomical projection patterns discovered in the present work might be a further source for spatial/non-spatial functional dissociation of the DG blades.

Moreover, subcortical modulation of the DG might also tilt the DG blades into processing spatial or non-spatial signals preferentially. The supramammillary nucleus (SuM) is one of the regions providing substantial innervation of the DG, with the enclosed blade receiving twice as many SuM axons as the exposed blade (Wyss et al., 1979; Vertes, 1992). Functionally, the SuM activity synchronises with the DG during spatial memory retrieval and is not required during non-spatial memory retrieval (Li et al., 2020). Furthermore, the DG is known to be modulated by cholinergic innervation arising from the medial septum, an area with strong functional ties to the spatial domain (Kelsey and Vargas, 1993; Mizumori et al., 1990; Schwegler et al., 1996). While the septal projections do not target the blades directly, but the hilar region, it was shown that acetylcholine together with the perforant path inputs leads to a disinhibition of the granule cells (Ogando et al., 2021). Since the number of inhibitory neurons in the enclosed blade is higher than in the exposed blade, the resulting excitatory activity caused by cholinergic modulation is expected to be stronger in the former blade. Consequently, projections from the spatially tuned medial septum may provide additional excitatory drive onto the granule cells of the enclosed blade. Together, the subcortical modulation of the DG might also contribute to the divergent roles of the DG blades in spatial and non-spatial processing.

Conclusions, limitations and outlook

The collective evidence presented in this thesis strongly supports a functional segregation of the enclosed and exposed blades of the DG in terms of spatial and non-spatial memory retrieval. These processing within the DG-CA3 circuitry potentially involves complex divergent mechanisms. Along with other works, which report differential anatomical projections and wiring, as well as functional gradients in the DG's upstream and downstream areas, the present data reinforce the model of segregated spatial and non-spatial information processing relevant for episodic memories throughout the cortical and hippocampal medial temporal lobe areas. Yet, in order to broaden and generalise the impact of the current findings, several points remain to be addressed.

First, the focus of the present work was the dorsal part of the DG. This was done because of its prominent role in cognitive processing in comparison to more ventral portions, which are reported to be rather involved in emotional processing (Fanselow and Dong, 2010; Moser and Moser, 1998; Strange et al., 2014). For this reason, optogenetic manipulation of the DG blades, molecular imaging of the proximodistal hippocampal subnetworks and anatomical tracing of the entorhinal inputs were performed exclusively in the dorsal pole of the DG. Whether similar spatial/non-spatial functional segregation of the DG blades exists at the ventral DG levels,

requires further investigations. However, there is evidence that the ventral hippocampus, including the DG, also plays a role in spatial and non-spatial processing (Snyder et al., 2009; Beer et al., 2013; Atucha et al., 2017; Weeden et al., 2014; Kirk et al., 2017). Moreover, proximodistal spatial/non-spatial functional segregation of the hippocampal CA1 and CA3 areas was reported not only at the dorsal hippocampal levels but also in more ventral portions (Nakamura et al., 2013). Hence, it is reasonable to think that the functional segregation of the DG blades observed in the dorsal levels might also exist in the ventral DG.

Second, the present data clearly demonstrates that the enclosed and exposed blades of the DG are *necessary* for spatial and non-spatial discriminations of memories. However, it does not allow for conclusions regarding whether the DG blades are *sufficient* on their own for retrieving memories. The current *Arc* imaging data suggest that the DG blades strongly affect the activity of the hippocampal CA3 area during retrieval. Since memory performance after CA3 inactivation was not assessed in the present study, it remains unclear whether the entire DG-CA3 system is required for mnemonic retrieval (i.e. the DG provides optimal conditions for the CA3 to retrieve mnemonic discriminations) or whether the DG does so alone and the different profiles of CA3 activity after inactivation of the DG blades are a mere consequence of the direct anatomical connections in this circuit. Further experiments including CA3 inactivation are necessary to address this point.

Third, differential recruitment of the proximodistal CA1 and CA3 spatial/non-spatial subnetworks, and now also of the enclosed and exposed blades of the DG, were described mainly for memory retrieval (Beer and Vavra et al., 2018; Ku et al., 2023; Nakamura et al., 2013; Flasbeck et al., 2018; Nakazawa et al., 2016). It remains untested whether such functional segregation would also apply during memory encoding or consolidation, for which the hippocampal subregions are known to be critical. To address this point, further investigations are needed.

Finally, while the present data show that, at the caudal levels, different populations of EC cells project to the enclosed or exposed blade of the DG, one can only hypothesise that ‘EC-enclosed DG’ cells preferentially support spatial processing in comparison to the ‘EC-exposed DG’ cells, which are mainly involved in non-spatial processing. A systematic analysis of the functional roles of these cell populations could be achieved with future experiments involving manipulation (e.g. optogenetic, chemogenetic) of these cells’ activities during spatial or non-spatial mnemonic processing. Moreover, recent technological advances (e.g. development of RNAscope, Retro-TRAP) open the possibility of future experiments involving more precise

characterisation (i.e. molecular profiles) of the cortical and hippocampal neural circuits supporting spatial and non-spatial memory processing.

Final comments

Thinking back on the model of multiple streams of episodic memory processing one might ask, how are the spatial and non-spatial aspects of memories processed to successfully form or retrieve a full memory of an event. On the one hand, the evidence described and discussed in the present thesis supports functional and anatomical segregation of spatial and non-spatial information flow throughout the majority of areas in the medial temporal lobe. However, the segregated spatial and non-spatial networks in the medial temporal lobe have been exclusively described in conditions, in which only one of the dimensions (i.e. spatial *or* non-spatial) was relevant. On the other hand, it is believed that conjoint or integrated processing exists at the levels of multiple areas within the medial temporal lobe. Several scenarios might be proposed to reconcile both segregation and integration models. Maybe the separation into spatial and non-spatial subnetworks is too simplistic and spatial/non-spatial processing is organised in a continuum-like manner across the different subfields. According to this view, the integration of different types of information might occur at the levels located between the respective subnetworks (e.g. mediolateral intermediate CA1/CA3, crest of the dentate gyrus etc.). Alternatively, it might be that mnemonic information flow always remains segregated and coincidental activation of the two neural systems ensures the integration of spatial and non-spatial information. In both cases, it seems plausible to assume that information integration might only take place when both dimensions are relevant for a given mnemonic representation. However, it might not occur when only one type of information is relevant for an appropriate behavioural outcome. For example, when searching for a book that I was recently reading, I try to recall the last location (spatial feature) where I was reading the book but not its size or the cover's colour (non-spatial features). In contrast, when describing how this book looks to a friend who is assisting me in my search, I recall the non-spatial features of the book but not the locations where I was reading it. In these two scenarios, it might be beneficial for the brain *not to* integrate irrelevant information and to use only the circuit supporting the retrieval of the relevant dimension to achieve the fastest behavioural outcome. In summary, I believe it will be undoubtedly interesting and important to investigate under which circumstances and conditions our brains process information in a segregated manner and when integration takes place.

Finally, we still lack an understanding of the fundamental principles behind episodic memory processing, especially when it comes to understanding how our brains differentiate between

different mnemonic dimensions. As suggested in this thesis, the mechanisms supporting the retrieval of spatial and non-spatial memories are likely very different. Does this observation reflect some core differences between spatial and non-spatial memories or is it a mere byproduct of the spatial and non-spatial circuits' organisation? I believe that answering these questions would be a big leap towards preserving and improving humans' ability to properly form and recall episodic memories.

References

Acsady, L., Kamondi, A., Sık, A., Freund, T., Buzsáki, G., 1998. GABAergic cells are the major postsynaptic targets of mossy fibers in the rat hippocampus. *Journal of neuroscience*, *18*(9), pp.3386-3403.

Agster, K.L.,Burwell, R.D., 2009. Cortical efferents of the perirhinal, postrhinal, and entorhinal cortices of the rat. *Hippocampus*, *19*(12), pp.1159-1186.

Allen, T.A., Fortin, N.J., 2013. The evolution of episodic memory. *Proceedings of the National Academy of Sciences* 110, no. supplement_2 (2013): 10379-10386.

Altman, J., Bayer, S.A., 1990. Mosaic organization of the hippocampal neuroepithelium and the multiple germinal sources of dentate granule cells. *Journal of comparative neurology*, *301*(3), pp.325-342.

Alves, N.D., Patrício, P., Correia, J.S., Mateus-Pinheiro, A., Machado-Santos, A.R., Loureiro-Campos, E., Morais, M., Bessa, J.M., Sousa, N., Pinto, L., 2018. Chronic stress targets adult neurogenesis preferentially in the suprapyramidal blade of the rat dorsal dentate gyrus. *Brain Structure and Function*, *223*(1), pp.415-428.

Amaral, D.G., Witter, M.P., 1989. The three-dimensional organization of the hippocampal formation: a review of anatomical data. *Neuroscience*, *31*(3), pp.571-591.

Anacker, C., Luna, V.M., Stevens, G.S., Millette, A., Shores, R., Jimenez, J.C., Chen, B., Hen, R., 2018. Hippocampal neurogenesis confers stress resilience by inhibiting the ventral dentate gyrus. *Nature*, *559*(7712), pp.98-102.

Andersen, P., Bliss, T.V., Lomo, T., Olsen, L.I., Skrede, K.K., 1969. Lamellar organization of hippocampal excitatory pathways. *Acta physiologica Scandinavica*, *76*(1), pp.4A-5A.

Andersen, P., Bliss, T.V.P., Skrede, K.K., 1971. Lamellar organization of hippocampal excitatory pathways. *Experimental brain research*, *13*, pp.222-238.

Anderson, M.L., Nokia, M.S., Govindaraju, K.P., Shors, T.J., 2012. Moderate drinking? Alcohol consumption significantly decreases neurogenesis in the adult hippocampus. *Neuroscience*, *224*, pp.202-209.

Aronov, D., Nevers, R., Tank, D.W., 2017. Mapping of a non-spatial dimension by the hippocampal–entorhinal circuit. *Nature*, *543*(7647), pp.719-722.

Ásgeirsdóttir, H.N., Cohen, S.J., Stackman Jr, R.W., 2020. Object and place information processing by CA1 hippocampal neurons of C57BL/6J mice. *Journal of neurophysiology*, *123*(3), pp.1247-1264.

Atucha, E., Karew, A., Kitsukawa, T., Sauvage, M.M., 2017. Recognition memory: Cellular evidence of a massive contribution of the LEC to familiarity and a lack of involvement of the hippocampal subfields CA1 and CA3. *Hippocampus*, *27*(10), pp.1083-1092.

Atucha, E., Ku, S.P., Lippert, M.T., Sauvage, M.M., 2021. Remembering the gist of an event over a lifetime depends on the hippocampus. *bioRxiv*, pp.2021-04.

Bakker, A., Kirwan, C.B., Miller, M., Stark, C.E., 2008. Pattern separation in the human hippocampal CA3 and dentate gyrus. S*cience*, *319*(5870), pp.1640-1642.

Barrionuevo, G., Kelso, S.R., Johnston, D., Brown, T.H., 1986. Conductance mechanism responsible for long-term potentiation in monosynaptic and isolated excitatory synaptic inputs to hippocampus. *Journal of neurophysiology*, *55*(3), pp.540-550.

Bartko, S.J., Winters, B.D., Cowell, R.A., Saksida, L.M., Bussey, T.J., 2007. Perceptual functions of perirhinal cortex in rats: zero-delay object recognition and simultaneous oddity discriminations. *Journal of Neuroscience*, *27*(10), pp.2548-2559.

Beed, P., Gundlfinger, A., Schneiderbauer, S., Song, J., Böhm, C., Burgalossi, A., Brecht, M., Vida, I., Schmitz, D., 2013. Inhibitory gradient along the dorsoventral axis in the medial entorhinal cortex. *Neuron*, *79*(6), pp.1197-1207.

Beer, Z., Chwiesko, C., Kitsukawa, T., Sauvage, M.M., 2013. Spatial and stimulus-type tuning in the LEC, MEC, POR, PrC, CA1, and CA3 during spontaneous item recognition memory. *Hippocampus*, *23*(12), pp.1425-1438.

Beer, Z., Vavra, P., Atucha, E., Rentzing, K., Heinze, H.J., Sauvage, M.M., 2018. The memory for time and space differentially engages the proximal and distal parts of the hippocampal subfields CA1 and CA3. *PLoS biology*, *16*(8), p.e2006100.

Berron, D., Schütze, H., Maass, A., Cardenas-Blanco, A., Kuijf, H.J., Kumaran, D., Düzel, E., 2016. Strong evidence for pattern separation in human dentate gyrus. *Journal of Neuroscience*, *36*(29), pp.7569-7579.

Blankvoort, S., Witter, M.P., Noonan, J., Cotney, J., Kentros, C., 2018. Marked diversity of unique cortical enhancers enables neuron-specific tools by enhancer-driven gene expression. *Current Biology*, *28*(13), pp.2103-2114.

Brown, M.W., Aggleton, J.P., 2001. Recognition memory: what are the roles of the perirhinal cortex and hippocampus?. *Nature Reviews Neuroscience*, *2*(1), pp.51-61.

Boccara, C.N., Nardin, M., Stella, F., O'Neill, J., Csicsvari, J., 2019. The entorhinal cognitive map is attracted to goals. *Science*, *363*(6434), pp.1443-1447.

Bowles, B., Crupi, C., Pigott, S., Parrent, A., Wiebe, S., Janzen, L., Köhler, S., 2010. Double dissociation of selective recollection and familiarity impairments following two different surgical treatments for temporal-lobe epilepsy. *Neuropsychologia*, *48*(9), pp.2640-2647.

Brown, T.H., Johnston, D., 1983. Voltage-clamp analysis of mossy fiber synaptic input to hippocampal neurons. *Journal of Neurophysiology*, *50*(2), pp.487-507.

Bowles, B., Crupi, C., Mirsattari, S.M., Pigott, S.E., Parrent, A.G., Pruessner, J.C., Yonelinas, A.P., Köhler, S., 2007. Impaired familiarity with preserved recollection after anterior temporal-lobe resection that spares the hippocampus. *Proceedings of the National Academy of Sciences*, *104*(41), pp.16382-16387.

Brun, V.H., Otnæss, M.K., Molden, S., Steffenach, H.A., Witter, M.P., Moser, M.B., Moser, E.I., 2002. Place cells and place recognition maintained by direct entorhinal-hippocampal circuitry. *Science*, *296*(5576), pp.2243-2246.

Brun, V.H., Solstad, T., Kjelstrup, K.B., Fyhn, M., Witter, M.P., Moser, E.I., Moser, M.B., 2008. Progressive increase in grid scale from dorsal to ventral medial entorhinal cortex. *Hippocampus*, *18*(12), pp.1200-1212.

Burke, S.N., Maurer, A.P., Nematollahi, S., Uprety, A.R., Wallace, J.L., Barnes, C.A., 2011. The influence of objects on place field expression and size in distal hippocampal CA1. *Hippocampus*, *21*(7), pp.783-801.

Burwell, R.D., Amaral, D.G., 1998. Cortical afferents of the perirhinal, postrhinal, and entorhinal cortices of the rat. *Journal of comparative neurology*, *398*(2), pp.179-205.

Butler, W.N., Hardcastle, K., Giocomo, L.M., 2019. Remembered reward locations restructure entorhinal spatial maps. *Science*, *363*(6434), pp.1447-1452.

Buzsáki, G., 1984. Feed-forward inhibition in the hippocampal formation. *Progress in neurobiology*, *22*(2), pp.131-153.

Cadete-Leite, A., BRANDÃO, F., Andrade, J.P., Ribeiro-da-Silva, A., Paula-Barbosa, M.M., 1997. The GABAergic system of the dentate gyrus after withdrawal from chronic alcohol consumption: effects of intracerebral grafting and putative neuroprotective agents. *Alcohol and alcoholism*, *32*(4), pp.471-484.

Canto, C.B., Wouterlood, F.G., Witter, M.P., 2008. What does the anatomical organization of the entorhinal cortex tell us?. *Neural plasticity*, *2008*.

Chaillan, F.A., Devigne, C., Diabira, D., Khrestchatisky, M., Roman, F.S., Ben-Ari, Y., Soumireu-Mourat, B., 1997. Neonatal γ-Ray Irradiation Impairs Learning and Memory of an Olfactory Associative Task in Adult Rats. *European Journal of Neuroscience*, *9*(5), pp.884-894.

Chandramohan, Y., Droste, S.K., Reul, J.M., 2007. Novelty stress induces phospho-acetylation of histone H3 in rat dentate gyrus granule neurons through coincident signalling via the N-methyl-d-aspartate receptor and the glucocorticoid receptor: relevance for c-fos induction. *Journal of neurochemistry*, *101*(3), pp.815-828.

Chao, O.Y., Huston, J.P., Li, J.S., Wang, A.L., de Souza Silva, M.A., 2016. The medial prefrontal cortex—Lateral entorhinal cortex circuit is essential for episodic-like memory and associative object-recognition. *Hippocampus*, *26*(5), pp.633-645.

Chawla, M.K., Guzowski, J.F., Ramirez-Amaya, V., Lipa, P., Hoffman, K.L., Marriott, L.K., Worley, P.F., McNaughton, B.L., Barnes, C.A., 2005. Sparse, environmentally selective expression of Arc RNA in the upper blade of the rodent fascia dentata by brief spatial experience. *Hippocampus*, *15*(5), pp.579-586.

Cinalli Jr, D.A., Cohen, S.J., Guthrie, K., Stackman Jr, R.W., 2020. Object recognition memory: distinct yet complementary roles of the mouse CA1 and perirhinal cortex. *Frontiers in molecular neuroscience*, *13*, p.527543.

Cippitelli, A., Zook, M., Bell, L., Damadzic, R., Eskay, R.L., Schwandt, M., Heilig, M., 2010. Reversibility of object recognition but not spatial memory impairment following binge-like alcohol exposure in rats. *Neurobiology of learning and memory*, *94*(4), pp.538-546.

Claiborne, B.J., Amaral, D.G., Cowan, W.M., 1990. Quantitative, three-dimensional analysis of granule cell dendrites in the rat dentate gyrus. *Journal of comparative neurology*, *302*(2), pp.206-219.

Claiborne, B.J., Amaral, D.G., Cowan, W.M., 1986. A light and electron microscopic analysis of the mossy fibers of the rat dentate gyrus. *Journal of comparative neurology*, *246*(4), pp.435-458.

Clark, R.E., Zola, S.M., Squire, L.R., 2000. Impaired recognition memory in rats after damage to the hippocampus. *Journal of Neuroscience*, *20*(23), pp.8853-8860.

Clelland, C.D., Choi, M., Romberg, C.C.G.J., Clemenson Jr, G.D., Fragniere, A., Tyers, P., Jessberger, S., Saksida, L.M., Barker, R.A., Gage, F.H., Bussey, T., 2009. A functional role for adult hippocampal neurogenesis in spatial pattern separation. *Science*, *325*(5937), pp.210-213.

Cohen, S.J., Munchow, A.H., Rios, L.M., Zhang, G., Ásgeirsdóttir, H.N., Stackman, R.W., 2013. The rodent hippocampus is essential for nonspatial object memory. *Current Biology*, *23*(17), pp.1685-1690.

Covolan, L., Mello, L.E.A.M., 2000. Temporal profile of neuronal injury following pilocarpine or kainic acid-induced status epilepticus. *Epilepsy research*, *39*(2), pp.133-152.

Cui, Z., Gerfen, C.R., Young 3rd, W.S., 2013. Hypothalamic and other connections with dorsal CA2 area of the mouse hippocampus. *Journal of comparative neurology*, *521*(8), pp.1844-1866.

Day, M., Langston, R., Morris, R.G., 2003. Glutamate-receptor-mediated encoding and retrieval of paired-associate learning. *Nature*, *424*(6945), pp.205-209.

Dees, R.L., Kesner, R.P., 2013. The role of the dorsal dentate gyrus in object and object-context recognition. *Neurobiology of learning and memory*, *106*, pp.112-117.

Deller, T., Martinez, A., Nitsch, R., Frotscher, M., 1996. A novel entorhinal projection to the rat dentate gyrus: direct innervation of proximal dendrites and cell bodies of granule cells and GABAergic neurons. *Journal of Neuroscience*, *16*(10), pp.3322-3333.

Dengler, C.G., Coulter, D.A., 2016. Normal and epilepsy-associated pathologic function of the dentate gyrus. *Progress in brain research*, *226*, pp.155-178.

Deshmukh, S.S., Johnson, J.L., Knierim, J.J., 2012. Perirhinal cortex represents nonspatial, but not spatial, information in rats foraging in the presence of objects: comparison with lateral entorhinal cortex. *Hippocampus*, *22*(10), pp.2045-2058.

Deshmukh, S.S., Knierim, J.J., 2011. Representation of non-spatial and spatial information in the lateral entorhinal cortex. *Frontiers in behavioral neuroscience*, *5*, p.69.

Deshmukh, S.S., Knierim, J.J., 2013. Influence of local objects on hippocampal representations: Landmark vectors and memory. *Hippocampus*, *23*(4), pp.253-267.

Desmond, N.L., Levy, W.B., 1982. A quantitative anatomical study of the granule cell dendritic fields of the rat dentate gyrus using a novel probabilistic method. *Journal of Comparative Neurology*, *212*(2), pp.131-145.

Desmond, N.L., Levy, W.B., 1985. Granule cell dendritic spine density in the rat hippocampus varies with spine shape and location. *Neuroscience letters*, *54*(2-3), pp.219-224.

Dhanabalan, G., Le Maitre, T.W., Bogdanovic, N., Alkass, K., Druid, H., 2018. Hippocampal granule cell loss in human chronic alcohol abusers. *Neurobiology of disease*, *120*, pp.63-75.

Diana, R.A., Yonelinas, A.P., Ranganath, C., 2007. Imaging recollection and familiarity in the medial temporal lobe: a three-component model. *Trends in cognitive sciences*, *11*(9), pp.379-386.

Diehl, G.W., Hon, O.J., Leutgeb, S., Leutgeb, J.K., 2017. Grid and nongrid cells in medial entorhinal cortex represent spatial location and environmental features with complementary coding schemes. *Neuron*, *94*(1), pp.83-92.

Dimsdale-Zucker, H.R., Ritchey, M., Ekstrom, A.D., Yonelinas, A.P., Ranganath, C., 2018. CA1 and CA3 differentially support spontaneous retrieval of episodic contexts within human hippocampal subfields. *Nature communications*, *9*(1), p.294.

Doan, T.P., Lagartos-Donate, M.J., Nilssen, E.S., Ohara, S., Witter, M.P., 2019. Convergent projections from perirhinal and postrhinal cortices suggest a multisensory nature of lateral, but not medial, entorhinal cortex. *Cell reports*, *29*(3), pp.617-627.

Dolorfo, C.L., Amaral, D.G., 1998. Entorhinal cortex of the rat: topographic organization of the cells of origin of the perforant path projection to the dentate gyrus. *Journal of Comparative Neurology*, *398*(1), pp.25-48.

Druga, R., Mareš, P., Kubová, H., 2010. Time course of neuronal damage in the hippocampus following lithium-pilocarpine status epilepticus in 12-day-old rats. *Brain research*, *1355*, pp.174-179.

Eichenbaum, H., Sauvage, M., Fortin, N., Komorowski, R., Lipton, P., 2012. Towards a functional organization of episodic memory in the medial temporal lobe. *Neuroscience & Biobehavioral Reviews*, *36*(7), pp.1597-1608.

Eichenbaum, H., Yonelinas, A.P., Ranganath, C., 2007. The medial temporal lobe and recognition memory. *Annu. Rev. Neurosci.*, *30*, pp.123-152.

Ennaceur, A., Delacour, J., 1988. A new one-trial test for neurobiological studies of memory in rats. 1: Behavioral data. *Behavioural brain research*, *31*(1), pp.47-59.

Ergorul, C., Eichenbaum, H., 2004. The hippocampus and memory for "what," "where," and "when". *Learning & Memory*, *11*(4), pp.397-405.

Ertürk, A., Becker, K., Jährling, N., Mauch, C.P., Hojer, C.D., Egen, J.G., Hellal, F., Bradke, F., Sheng, M., Dodt, H.U., 2012. Three-dimensional imaging of solvent-cleared organs using 3DISCO. *Nature protocols*, *7*(11), pp.1983-1995.

Erwin, S.R., Sun, W., Copeland, M., Lindo, S., Spruston, N., Cembrowski, M.S., 2020. A sparse, spatially biased subtype of mature granule cell dominates recruitment in hippocampal-associated behaviors. *Cell reports*, *31*(4), p.107551.

Fanselow, M.S., Dong, H.W., 2010. Are the dorsal and ventral hippocampus functionally distinct structures?. *Neuron*, *65*(1), pp.7-19.

Fernández-Ruiz, A., Oliva, A., Soula, M., Rocha-Almeida, F., Nagy, G.A., Martin-Vazquez, G., Buzsáki, G., 2021. Gamma rhythm communication between entorhinal cortex and dentate gyrus neuronal assemblies. *Science*, *372*(6537), p.eabf3119.

Fevurly, R.D., Spencer, R.L., 2004. Fos expression is selectively and differentially regulated by endogenous glucocorticoids in the paraventricular nucleus of the hypothalamus and the dentate gyrus. *Journal of neuroendocrinology*, *16*(12), pp.970-979.

Flasbeck, V., Atucha, E., Nakamura, N.H., Yoshida, M., Sauvage, M.M., 2018. Spatial information is preferentially processed by the distal part of CA3: implication for memory retrieval. *Behavioural brain research*, *354*, pp.31-38.

Fontana, R., Agostini, M., Murana, E., Mahmud, M., Scremin, E., Rubega, M., Sparacino, G., Vassanelli, S., Fasolato, C., 2017. Early hippocampal hyperexcitability in PS2APP mice: role of mutant PS2 and APP. *Neurobiology of aging*, *50*, pp.64-76.

Fortin, N.J., Wright, S.P., Eichenbaum, H., 2004. Recollection-like memory retrieval in rats is dependent on the hippocampus. *Nature*, *431*(7005), pp.188-191.

Freund, T.F., Maglóczky, Z., 1993. Early degeneration of calretinin-containing neurons in the rat hippocampus after ischemia. *Neuroscience*, *56*(3), pp.581-596.

Fricke, R., Cowan, W.M., 1977. An autoradiographic study of the development of the entorhinal and commissural afferents to the dentate gyrus of the rat. *Journal of Comparative Neurology*, *173*(2), pp.231-250.

Fyhn, M., Hafting, T., Witter, M.P., Moser, E.I., Moser, M.B., 2008. Grid cells in mice. *Hippocampus*, *18*(12), pp.1230-1238.

Gall, C., Brecha, N., Karten, H.J., Chang, K.J., 1981. Localization of enkephalin-like immunoreactivity to identified axonal and neuronal populations of the rat hippocampus. *Journal of Comparative Neurology*, *198*(2), pp.335-350.

Gallitano, A.L., Satvat, E., Gil, M., Marrone, D.F., 2016. Distinct dendritic morphology across the blades of the rodent dentate gyrus. *Synapse*, *70*(7), pp.277-282.

García-Moreno, L.M., Cimadevilla, J.M., 2012. Acute and chronic ethanol intake: effects on spatial and non-spatial memory in rats. *Alcohol*, *46*(8), pp.757-762.

Gilbert, P.E., Kesner, R.P., 2003. Localization of function within the dorsal hippocampus: the role of the CA3 subregion in paired-associate learning. *Behavioral neuroscience*, *117*(6), p.1385.

Gilbert, P.E., Kesner, R.P., 2002. Role of rodent hippocampus in paired-associate learning involving associations between a stimulus and a spatial location. *Behavioral neuroscience*, *116*(1), p.63.

Gilbert, P.E., Kesner, R.P., 2002. The amygdala but not the hippocampus is involved in pattern separation based on reward value. *Neurobiology of Learning and Memory*, *77*(3), pp.338-353.

Gilbert, P.E., Kesner, R.P., Lee, I., 2001. Dissociating hippocampal subregions: A double dissociation between dentate gyrus and CA1. *Hippocampus*, *11*(6), pp.626-636.

Giocomo, L.M., Hussaini, S.A., Zheng, F., Kandel, E.R., Moser, M.B., Moser, E.I., 2011. Grid cells use HCN1 channels for spatial scaling. *Cell*, *147*(5), pp.1159-1170.

Giocomo, L.M., Stensola, T., Bonnevie, T., Van Cauter, T., Moser, M.B., Moser, E.I., 2014. Topography of head direction cells in medial entorhinal cortex. *Current Biology*, *24*(3), pp.252-262.

Gloor, P., Vera, C.L., Sperti, L., 1963. Electrophysiological studies of hippocampal neurons I. Configuration and laminar analysis of the "resting" potential gradient, of the main-transient response to perforant path, fimbrial and mossy fiber volleys and of "spontaneous" activity. *Electroencephalography and Clinical Neurophysiology*, *15*(3), pp.353-378.

Goodrich-Hunsaker, N.J., Gilbert, P.E., Hopkins, R.O., 2009. The role of the human hippocampus in odor–place associative memory. *Chemical senses*, *34*(6), pp.513-521.

GoodSmith, D., Kim, S.H., Puliyadi, V., Ming, G.L., Song, H., Knierim, J.J., Christian, K.M., 2022. Flexible encoding of objects and space in single cells of the dentate gyrus. *Current Biology*, *32*(5), pp.1088-1101.

Gottlieb, D.I., Cowan, W.M., 1972. On the distribution of axonal terminals containing spheroidal and flattened synaptic vesicles in the hippocampus and dentate gyrus of the rat and cat. *Zeitschrift für Zellforschung und mikroskopische Anatomie*, *129*(3), pp.413-429.

Gould, E., Woolley, C.S., McEwen, B.S., 1991. Naturally occurring cell death in the developing dentate gyrus of the rat. *Journal of comparative neurology*, *304*(3), pp.408-418.

Grosser, S., Barreda, F.J., Beed, P., Schmitz, D., Booker, S.A., Vida, I., 2021. Parvalbumin interneurons are differentially connected to principal cells in inhibitory feedback microcircuits along the dorsoventral axis of the medial entorhinal cortex. *Eneuro*, *8*(1).

Gschwend, O., Abraham, N.M., Lagier, S., Begnaud, F., Rodriguez, I., Carleton, A., 2015. Neuronal pattern separation in the olfactory bulb improves odor discrimination learning. *Nature neuroscience*, *18*(10), pp.1474-1482.

Guo, N., Soden, M.E., Herber, C., Kim, M.T., Besnard, A., Lin, P., Ma, X., Cepko, C.L., Zweifel, L.S., Sahay, A., 2018. Dentate granule cell recruitment of feedforward inhibition governs engram maintenance and remote memory generalization. *Nature medicine*, *24*(4), pp.438-449.

Guzowski, J.F., McNaughton, B.L., Barnes, C.A., Worley, P.F., 1999. Environment-specific expression of the immediate-early gene Arc in hippocampal neuronal ensembles. *Nature neuroscience*, *2*(12), pp.1120-1124.

Guzowski, J.F., Setlow, B., Wagner, E.K., McGaugh, J.L., 2001. Experience-dependent gene expression in the rat hippocampus after spatial learning: a comparison of the immediate-early genesArc, c-fos, and zif268. *Journal of Neuroscience*, *21*(14), pp.5089-5098.

Ha, S., Tripathi, P.P., Daza, R.A., Hevner, R.F., Beier, D.R., 2020. Reelin mediates hippocampal Cajal-Retzius cell positioning and infrapyramidal blade morphogenesis. *Journal of developmental biology*, *8*(3), p.20.

Hafting, T., Fyhn, M., Molden, S., Moser, M.B., Moser, E.I., 2005. Microstructure of a spatial map in the entorhinal cortex. *Nature*, *436*(7052), pp.801-806.

Hafting, T., Fyhn, M., Bonnevie, T., Moser, M.B., Moser, E.I., 2008. Hippocampus-independent phase precession in entorhinal grid cells. *Nature*, *453*(7199), pp.1248-1252.

Hales, J.B., Reitz, N.T., Vincze, J.L., Ocampo, A.C., Leutgeb, S., Clark, R.E., 2021. A role for medial entorhinal cortex in spatial and nonspatial forms of memory in rats. *Behavioural brain research*, *407*, p.113259.

Hama, K., Arii, T., Kosaka, T., 1989. Three-dimensional morphometrical study of dendritic spines of the granule cell in the rat dentate gyrus with HVEM stereo images. *Journal of Electron Microscopy Technique*, *12*(2), pp.80-87.

Han, X., Chow, B.Y., Zhou, H., Klapoetke, N.C., Chuong, A., Rajimehr, R., Yang, A., Baratta, M.V., Winkle, J., Desimone, R., Boyden, E.S., 2011. A high-light sensitivity optical neural silencer: development and application to optogenetic control of non-human primate cortex. *Frontiers in systems neuroscience*, *5*, p.18.

Hara, H., Onodera, H., Kyuya, K., Akaike, N., 1990. The regional difference of neuronal susceptibility in the dentate gyrus to hypoxia. *Neuroscience letters*, *115*(2-3), pp.189-194.

Hargreaves, E.L., Rao, G., Lee, I., Knierim, J.J., 2005. Major dissociation between medial and lateral entorhinal input to dorsal hippocampus. *science*, *308*(5729), pp.1792-1794.

Henriksen, E.J., Colgin, L.L., Barnes, C.A., Witter, M.P., Moser, M.B., Moser, E.I., 2010. Spatial representation along the proximodistal axis of CA1. *Neuron*, *68*(1), pp.127-137.

Henze, D.A., Wittner, L., Buzsáki, G., 2002. Single granule cells reliably discharge targets in the hippocampal CA3 network in vivo. *Nature neuroscience*, *5*(8), pp.790-795.

Hitti, F.L., Siegelbaum, S.A., 2014. The hippocampal CA2 region is essential for social memory. *Nature*, *508*(7494), pp.88-92.

Hjorth-Simonsen, A., Jeune, B., 1972. Origin and termination of the hippocampal perforant path in the rat studied by silver impregnation. *Journal of Comparative Neurology*, *144*(2), pp.215-231.

Hoang, T.H., Aliane, V., Manahan-Vaughan, D., 2018. Novel encoding and updating of positional, or directional, spatial cues are processed by distinct hippocampal subfields: Evidence for parallel information processing and the “what” stream. *Hippocampus*, *28*(5), pp.315-326.

Hoffman, A.N., Anouti, D.P., Lacagnina, M.J., Nikulina, E.M., Hammer Jr, R.P., Conrad, C.D., 2013. Experience-dependent effects of context and restraint stress on corticolimbic c-Fos expression. *Stress*, *16*(5), pp.587-591.

Høydal, Ø.A., Skytøen, E.R., Andersson, S.O., Moser, M.B., Moser, E.I., 2019. Object-vector coding in the medial entorhinal cortex. *Nature*, *568*(7752), pp.400-404.

Hunsaker, M.R., Chen, V., Tran, G.T., Kesner, R.P., 2013. The medial and lateral entorhinal cortex both contribute to contextual and item recognition memory: A test of the binding ofitems and context model. *Hippocampus*, *23*(5), pp.380-391.

Huang, L.Q., Rowan, M.J., Anwyl, R., 1999. Role of protein kinases A and C in the induction of mGluR-dependent long-term depression in the medial perforant path of the rat dentate gyrus in vitro. *Neuroscience letters*, *274*(2), pp.71-74.

Huang X, Schlesiger MI, Barriuso-Ortega I, Leibold C, MacLaren DAA, Bieber N, Monyer H, 2023. Distinct spatial maps and multiple object codes in the lateral entorhinal cortex. *Neuron*

Insausti, Ricardo. "Comparative anatomy of the entorhinal cortex and hippocampus in mammals." *Hippocampus* 3, no. S1 (1993): 19-26.

Insausti, R., Herrero, M.T., Witter, M.P., 1997. Entorhinal cortex of the rat: cytoarchitectonic subdivisions and the origin and distribution of cortical efferents. *Hippocampus*, *7*(2), pp.146-183.

Ishizuka, N., Weber, J., Amaral, D.G., 1990. Organization of intrahippocampal projections originating from CA3 pyramidal cells in the rat. *Journal of comparative neurology*, *295*(4), pp.580-623.

Johnson, S.A., Turner, S.M., Santacroce, L.A., Carty, K.N., Shafiq, L., Bizon, J.L., Maurer, A.P., Burke, S.N., 2017. Rodent age-related impairments in discriminating perceptually similar objects parallel those observed in humans. *Hippocampus*, *27*(7), pp.759-776.

Jung, M.W., McNaughton, B.L., 1993. Spatial selectivity of unit activity in the hippocampal granular layer. *Hippocampus*, *3*(2), pp.165-182.

Jung, M.W., Wiener, S.I., McNaughton, B.L., 1994. Comparison of spatial firing characteristics of units in dorsal and ventral hippocampus of the rat. *Journal of Neuroscience*, *14*(12), pp.7347-7356.

Kelsey, J.E., Vargas, H., 1993. Medial septal lesions disrupt spatial, but not nonspatial, working memory in rats. *Behavioral neuroscience*, *107*(4), p.565.

Kerr, K.M., Agster, K.L., Furtak, S.C., Burwell, R.D., 2007. Functional neuroanatomy of the parahippocampal region: the lateral and medial entorhinal areas. *Hippocampus*, *17*(9), pp.697-708.

Kesner, R.P., 2018. An analysis of dentate gyrus function (an update). *Behavioural Brain Research*, *354*, pp.84-91.

Kesner, R.P., 2013. An analysis of the dentate gyrus function. *Behavioural brain research*, *254*, pp.1-7.

Kesner, R.P., Hunsaker, M.R., Gilbert, P.E., 2005. The role of CA1 in the acquisition of an object-trace-odor paired associate task. *Behavioral neuroscience*, *119*(3), p.781.

Kesner, R.P., Ravindranathan, A., Jackson, P., Giles, R., Chiba, A.A., 2001. A neural circuit analysis of visual recognition memory: role of perirhinal, medial, and lateral entorhinal cortex. *Learning & Memory*, *8*(2), pp.87-95.

Kheirbek, M.A., Drew, L.J., Burghardt, N.S., Costantini, D.O., Tannenholz, L., Ahmari, S.E., Zeng, H., Fenton, A.A., Hen, R., 2013. Differential control of learning and anxiety along the dorsoventral axis of the dentate gyrus. *Neuron*, *77*(5), pp.955-968.

Kim, S.Y., Min, D.S., Choi, J.S., Choi, Y.S., Park, H.J., Sung, K.W., Kim, J., Lee, M.Y., 2004. Differential expression of phospholipase D isozymes in the hippocampus following kainic acid-induced seizures. *Journal of Neuropathology & Experimental Neurology*, *63*(8), pp.812-820.

Kirk, R.A., Redmon, S.N., Kesner, R.P., 2017. The ventral dentate gyrus mediates pattern separation for reward value. *Behavioral Neuroscience*, *131*(1), p.42.

Kjelstrup, K.B., Solstad, T., Brun, V.H., Hafting, T., Leutgeb, S., Witter, M.P., Moser, E.I., Moser, M.B., 2008. Finite scale of spatial representation in the hippocampus. *Science*, *321*(5885), pp.140-143.

Knierim, J.J., Neunuebel, J.P., Deshmukh, S.S., 2014. Functional correlates of the lateral and medial entorhinal cortex: objects, path integration and local–global reference frames. *Philosophical Transactions of the Royal Society B: Biological Sciences*, *369*(1635), p.20130369.

Kobro-Flatmoen, A., Witter, M.P., 2019. Neuronal chemo-architecture of the entorhinal cortex: a comparative review. *European Journal of Neuroscience*, *50*(10), pp.3627-3662.

Kohara, K., Pignatelli, M., Rivest, A.J., Jung, H.Y., Kitamura, T., Suh, J., Frank, D., Kajikawa, K., Mise, N., Obata, Y., Wickersham, I.R., 2014. Cell type–specific genetic and optogenetic tools reveal hippocampal CA2 circuits. *Nature neuroscience*, *17*(2), pp.269-279.

Komorowski, R.W., Manns, J.R., Eichenbaum, H., 2009. Robust conjunctive item–place coding by hippocampal neurons parallels learning what happens where. *Journal of Neuroscience*, *29*(31), pp.9918-9929.

Korotkova, T., Fuchs, E.C., Ponomarenko, A., von Engelhardt, J., Monyer, H., 2010. NMDA receptor ablation on parvalbumin-positive interneurons impairs hippocampal synchrony, spatial representations, and working memory. *Neuron*, *68*(3), pp.557-569.

Kosaka, T., Katsumaru, H., Hama, K., Wu, J.Y., Heizmann, C.W., 1987. GABAergic neurons containing the Ca2+-binding protein parvalbumin in the rat hippocampus and dentate gyrus. *Brain research*, *419*(1-2), pp.119-130.

Kreisman, N.R., Soliman, S., Gozal, D., 2000. Regional differences in hypoxic depolarization and swelling in hippocampal slices. *Journal of neurophysiology*, *83*(2), pp.1031-1038.

Ku, S.P., Atucha, E., Alavi, N., Mulla-Osman, H., Kayumova, R., Yoshida, M., Csicsvari, J., Sauvage, M.M., 2023. Phase-locking of hippocampal CA3 neurons to distal CA1 oscillations selectively predicts memory performance. *Neuron* (2nd round of revision)

Kuruvilla, M.V., Wilson, D.I., Ainge, J.A., 2020. Lateral entorhinal cortex lesions impair both egocentric and allocentric object–place associations. *Brain and neuroscience advances*, *4*, p.2398212820939463.

LaChance, P.A., Todd, T.P., Taube, J.S., 2019. A sense of space in postrhinal cortex. *Science*, *365*(6449), p.eaax4192.

Langston, R.F., Wood, E.R., 2010. Associative recognition and the hippocampus: Differential effects of hippocampal lesions on object-place, object-context and object-place-context memory. *Hippocampus*, *20*(10), pp.1139-1153.

Lawston, J., Borella, A., Robinson, J.K., Whitaker-Azmitia, P.M., 2000. Changes in hippocampal morphology following chronic treatment with the synthetic cannabinoid WIN 55,212-2. *Brain research*, *877*(2), pp.407-410.

Lee, J.W., Jung, M.W., 2017. Separation or binding? Role of the dentate gyrus in hippocampal mnemonic processing. *Neuroscience & Biobehavioral Reviews*, *75*, pp.183-194.

Leutgeb, J.K., Leutgeb, S., Moser, M.B., Moser, E.I., 2007. Pattern separation in the dentate gyrus and CA3 of the hippocampus. *Science*, *315*(5814), pp.961-966.

Li, Y., Bao, H., Luo, Y., Yoan, C., Sullivan, H.A., Quintanilla, L., Wickersham, I., Lazarus, M., Shih, Y.Y.I., Song, J., 2020. Supramammillary nucleus synchronizes with dentate gyrus to regulate spatial memory retrieval through glutamate release. *Elife*, *9*, p.e53129.

Lipton, P.A., Eichenbaum, H., 2008. Complementary roles of hippocampus and medial entorhinal cortex in episodic memory. *Neural plasticity*, *2008*.

Liu, X., Ramirez, S., Tonegawa, S., 2014. Inception of a false memory by optogenetic manipulation of a hippocampal memory engram. *Philosophical Transactions of the Royal Society B: Biological Sciences*, *369*(1633), p.20130142.

Luna, V.M., Anacker, C., Burghardt, N.S., Khandaker, H., Andreu, V., Millette, A., Leary, P., Ravenelle, R., Jimenez, J.C., Mastrodonato, A., Denny, C.A., 2019. Adult-born hippocampal neurons bidirectionally modulate entorhinal inputs into the dentate gyrus. *Science*, *364*(6440), pp.578-583.

Lux, V., Masseck, O.A., Herlitze, S., Sauvage, M.M., 2017. Optogenetic destabilization of the memory trace in CA1: insights into reconsolidation and retrieval processes. *Cerebral Cortex*, *27*(1), pp.841-851.

Lynch, M., Sutula, T., 2000. Recurrent excitatory connectivity in the dentate gyrus of kindled and kainic acid–treated rats. *Journal of neurophysiology*, *83*(2), pp.693-704.

Manns, J.R., Eichenbaum, H., 2005. Time and treason to the trisynaptic teachings: theoretical comment on Kesner et Al.(2005).

Manns, J.R., Eichenbaum, H., 2009. A cognitive map for object memory in the hippocampus. *Learning & memory*, *16*(10), pp.616-624.

Markwiese, B.J., Acheson, S.K., Levin, E.D., Wilson, W.A., Swartzwelder, H.S., 1998. Differential effects of ethanol on memory in adolescent and adult rats. *Alcoholism: Clinical and Experimental Research*, *22*(2), pp.416-421.

Matthews, D.B., Ilgen, M., White, A.M., Best, P.J., 1999. Acute ethanol administration impairs spatial performance while facilitating nonspatial performance in rats. *Neurobiology of learning and memory*, *72*(3), pp.169-179.

McHugh, S.B., Lopes-dos-Santos, V., Gava, G.P., Hartwich, K., Tam, S.K., Bannerman, D.M., Dupret, D., 2022. Adult-born dentate granule cells promote hippocampal population sparsity. *Nature Neuroscience*, *25*(11), pp.1481-1491.

McHugh, T.J., Jones, M.W., Quinn, J.J., Balthasar, N., Coppari, R., Elmquist, J.K., Lowell, B.B., Fanselow, M.S., Wilson, M.A., Tonegawa, S., 2007. Dentate gyrus NMDA receptors mediate rapid pattern separation in the hippocampal network. *Science*, *317*(5834), pp.94-99.

McNaughton, B.L., Barnes, C.A., Meltzer, J., Sutherland, R.J., 1989. Hippocampal granule cells are necessary for normal spatial learning but not for spatially-selective pyramidal cell discharge. *Experimental brain research*, *76*, pp.485-496.

McNaughton, B.L., Morris, R.G., 1987. Hippocampal synaptic enhancement and information storage within a distributed memory system. *Trends in neurosciences*, *10*(10), pp.408-415.

Meyer, M.A., Anstötz, M., Ren, L.Y., Fiske, M.P., Guedea, A.L., Grayson, V.S., Schroth, S.L., Cicvaric, A., Nishimori, K., Maccaferri, G., Radulovic, J., 2020. Stress-related memories disrupt sociability and associated patterning of hippocampal activity: a role of hilar oxytocin receptor-positive interneurons. *Translational psychiatry*, *10*(1), p.428.

Miao, C., Cao, Q., Moser, M.B., Moser, E.I., 2017. Parvalbumin and somatostatin interneurons control different space-coding networks in the medial entorhinal cortex. *Cell*, *171*(3), pp.507-521.

Miranda, M., Kent, B.A., Morici, J.F., Gallo, F., Weisstaub, N.V., Saksida, L.M., Bussey, T.J., Bekinschtein, P., 2017. Molecular mechanisms in perirhinal cortex selectively necessary for discrimination of overlapping memories, but independent of memory persistence. *Eneuro*, *4*(5).

Miranda, M., Morici, J.F., Gallo, F., Piromalli Girado, D., Weisstaub, N.V., Bekinschtein, P., 2021. Molecular mechanisms within the dentate gyrus and the perirhinal cortex interact during discrimination of similar nonspatial memories. *Hippocampus*, *31*(2), pp.140-155.

Mishkin, M., Ungerleider, L.G., Macko, K.A., 1983. Object vision and spatial vision: two cortical pathways. *Trends in neurosciences*, *6*, pp.414-417.

Mizumori, S.J.Y., Perez, G.M., Alvarado, M.C., Barnes, C.A., McNaughton, B.L., 1990. Reversible inactivation of the medial septum differentially affects two forms of learning in rats. *Brain research*, *528*(1), pp.12-20.

Mody, I., Glykys, J., Wei, W., 2007. A new meaning for "Gin & Tonic": tonic inhibition as the target for ethanol action in the brain. *Alcohol*, *41*(3), pp.145-153.

Mori, M., Abegg, M.H., Gähwiler, B.H., Gerber, U., 2004. A frequency-dependent switch from inhibition to excitation in a hippocampal unitary circuit. *Nature*, *431*(7007), pp.453-456.

Morrissey, M.D., Maal-Bared, G., Brady, S., Takehara-Nishiuchi, K., 2012. Functional dissociation within the entorhinal cortex for memory retrieval of an association between temporally discontiguous stimuli. *Journal of Neuroscience*, *32*(16), pp.5356-5361.

Moser, M.B., Moser, E.I., 1998. Functional differentiation in the hippocampus. *Hippocampus*, *8*(6), pp.608-619.

Mumby, D.G., Gaskin, S., Glenn, M.J., Schramek, T.E., Lehmann, H., 2002. Hippocampal damage and exploratory preferences in rats: memory for objects, places, and contexts. *Learning & memory*, *9*(2), pp.49-57.

Nalberczak-Skóra, M., Beroun, A., Skonieczna, E., Cały, A., Ziółkowska, M., Pagano, R., Taheri, P., Kalita, K., Salamian, A., Radwanska, K., 2023. Impaired synaptic transmission in dorsal dentate gyrus increases impulsive alcohol seeking. *Neuropsychopharmacology*, *48*(3), pp.436-447.

Nakamura, N.H., Flasbeck, V., Maingret, N., Kitsukawa, T., Sauvage, M.M., 2013. Proximodistal segregation of nonspatial information in CA3: preferential recruitment of a proximal CA3-distal CA1 network in nonspatial recognition memory. *Journal of Neuroscience*, *33*(28), pp.11506-11514.

Nakazawa, Y., Pevzner, A., Tanaka, K.Z., Wiltgen, B.J., 2016. Memory retrieval along the proximodistal axis of CA1. *Hippocampus*, *26*(9), pp.1140-1148.

Neubrandt, M., Olah, V.J., Brunner, J., Szabadics, J., 2017. Feedforward inhibition is randomly wired from individual granule cells onto CA3 pyramidal cells. *Hippocampus*, *27*(10), pp.1034-1039.

Neunuebel, J.P., Knierim, J.J., 2014. CA3 retrieves coherent representations from degraded input: direct evidence for CA3 pattern completion and dentate gyrus pattern separation. *Neuron*, *81*(2), pp.416-427.

Niibori, Y., Yu, T.S., Epp, J.R., Akers, K.G., Josselyn, S.A., Frankland, P.W., 2012. Suppression of adult neurogenesis impairs population coding of similar contexts in hippocampal CA3 region. *Nature communications*, *3*(1), p.1253.

Nilssen, E.S., Doan, T.P., Nigro, M.J., Ohara, S., Witter, M.P., 2019. Neurons and networks in the entorhinal cortex: A reappraisal of the lateral and medial entorhinal subdivisions mediating parallel cortical pathways. *Hippocampus*, *29*(12), pp.1238-1254.

Niswender, C.M., Conn, P.J., 2010. Metabotropic glutamate receptors: physiology, pharmacology, and disease. *Annual review of pharmacology and toxicology*, *50*, pp.295-322.

Obenhaus, H.A., Zong, W., Jacobsen, R.I., Rose, T., Donato, F., Chen, L., Cheng, H., Bonhoeffer, T., Moser, M.B., Moser, E.I., 2022. Functional network topography of the medial entorhinal cortex. *Proceedings of the National Academy of Sciences*, *119*(7), p.e2121655119.

Ogando, M.B., Pedroncini, O., Federman, N., Romano, S.A., Brum, L.A., Lanuza, G.M., Refojo, D., Marin-Burgin, A., 2021. Cholinergic modulation of dentate gyrus processing through dynamic reconfiguration of inhibitory circuits. *Cell Reports*, *36*(8), p.109572.

Olarte-Sánchez, C.M., Amin, E., Warburton, E.C., Aggleton, J.P., 2015. Perirhinal cortex lesions impair tests of object recognition memory but spare novelty detection. *European Journal of Neuroscience*, *42*(12), pp.3117-3127.

O'Mara, S., 2005. The subiculum: what it does, what it might do, and what neuroanatomy has yet to tell us. *Journal of anatomy*, *207*(3), pp.271-282.

Oulé, M., Atucha, E., Wells, T.M., Macharadze, T., Sauvage, M.M., Kreutz, M.R., Lopez-Rojas, J., 2021. Dendritic Kv4. 2 potassium channels selectively mediate spatial pattern separation in the dentate gyrus. *Iscience*, *24*(8), p.102876.

Pérez-Delgado, M.M., Serrano-Aguilar, P.G., Castañeyra-Perdomo, A., Ferres-Torres, R., 1992. Postnatal development of the dentate gyrus: a karyometric and topographic study. *Cells Tissues Organs*, *144*(2), pp.160-166.

Persson, B.M., Ambrozova, V., Duncan, S., Wood, E.R., O'Connor, A.R., Ainge, J.A., 2022. Lateral entorhinal cortex lesions impair odor-context associative memory in male rats. *Journal of neuroscience research*, *100*(4), pp.1030-1046.

Petrulis, A., Alvarez, P., Eichenbaum, H., 2005. Neural correlates of social odor recognition and the representation of individual distinctive social odors within entorhinal cortex and ventral subiculum. *Neuroscience*, *130*(1), pp.259-274.

Pforte, C., Henrich-Noack, P., Baldauf, K., Reymann, K.G., 2005. Increase in proliferation and gliogenesis but decrease of early neurogenesis in the rat forebrain shortly after transient global ischemia. *Neuroscience*, *136*(4), pp.1133-1146.

Pitsikas, N., Markou, A., 2014. The metabotropic glutamate 2/3 receptor agonist LY379268 counteracted ketamine-and apomorphine-induced performance deficits in the object recognition task, but not object location task, in rats. *Neuropharmacology*, *85*, pp.27-35.

Rajendran, P., Spear, L.P., 2004. The effects of ethanol on spatial and nonspatial memory in adolescent and adult rats studied using an appetitive paradigm. *Annals of the New York Academy of Sciences*, *1021*(1), pp.441-444.

Ramirez, S., Liu, X., Lin, P.A., Suh, J., Pignatelli, M., Redondo, R.L., Ryan, T.J., Tonegawa, S., 2013. Creating a false memory in the hippocampus. *Science*, *341*(6144), pp.387-391.

Ramírez-Amaya, V., Vazdarjanova, A., Mikhael, D., Rosi, S., Worley, P.F., Barnes, C.A., 2005. Spatial exploration-induced Arc mRNA and protein expression: evidence for selective, network-specific reactivation. *Journal of Neuroscience*, *25*(7), pp.1761-1768.

Ramirez-Amaya, V., Angulo-Perkins, A., Chawla, M.K., Barnes, C.A., Rosi, S., 2013. Sustained transcription of the immediate early gene Arc in the dentate gyrus after spatial exploration. *Journal of Neuroscience*, *33*(4), pp.1631-1639.

Raven, F., Meerlo, P., Van der Zee, E.A., Abel, T., Havekes, R., 2019. A brief period of sleep deprivation causes spine loss in the dentate gyrus of mice. *Neurobiology of learning and memory*, *160*, pp.83-90.

Reagh, Z.M., Noche, J.A., Tustison, N.J., Delisle, D., Murray, E.A., Yassa, M.A., 2018. Functional imbalance of anterolateral entorhinal cortex and hippocampal dentate/CA3 underlies age-related object pattern separation deficits. *Neuron*, *97*(5), pp.1187-1198.

Ruediger, S., Vittori, C., Bednarek, E., Genoud, C., Strata, P., Sacchetti, B., Caroni, P., 2011. Learning-related feedforward inhibitory connectivity growth required for memory precision. *Nature*, *473*(7348), pp.514-518.

Rush, A.M., Wu, J., Rowan, M.J., Anwyl, R., 2001. Activation of group II metabotropic glutamate receptors results in long-term potentiation following preconditioning stimulation in the dentate gyrus. *Neuroscience*, *105*(2), pp.335-341.

Rush, A.M., Wu, J., Rowan, M.J., Anwyl, R., 2002. Group I metabotropic glutamate receptor (mGluR)-dependent long-term depression mediated via p38 mitogen-activated protein kinase is inhibited by previous high-frequency stimulation and activation of mGluRs and protein kinase C in the rat dentate gyrus in vitro. *Journal of Neuroscience*, *22*(14), pp.6121-6128.

Ruth, R.E., Collier, T.J., Routtenberg, A., 1982. Topography between the entorhinal cortex and the dentate septotemporal axis in rats: I. Medial and intermediate entorhinal projecting cells. *Journal of Comparative Neurology*, *209*(1), pp.69-78.

Ruth, R.E., Collier, T.J., Routtenberg, A., 1988. Topographical relationship between the entorhinal cortex and the septotemporal axis of the dentate gyrus in rats: II. Cells projecting from lateral entorhinal subdivision. *Journal of Comparative Neurology*, *270*(4), pp.506-516.

Sargolini, F., Fyhn, M., Hafting, T., McNaughton, B.L., Witter, M.P., Moser, M.B., Moser, E.I., 2006. Conjunctive representation of position, direction, and velocity in entorhinal cortex. *Science*, *312*(5774), pp.758-762.

Sasaki, T., Piatti, V.C., Hwaun, E., Ahmadi, S., Lisman, J.E., Leutgeb, S., Leutgeb, J.K., 2018. Dentate network activity is necessary for spatial working memory by supporting CA3 sharp-wave ripple generation and prospective firing of CA3 neurons. *Nature neuroscience*, *21*(2), pp.258-269.

Satvat, E., Schmidt, B., Argraves, M., Marrone, D.F., Markus, E.J., 2011. Changes in task demands alter the pattern of zif268 expression in the dentate gyrus. *Journal of Neuroscience*, *31*(19), pp.7163-7167.

Sauvage, M.M., 2010. ROC in animals: uncovering the neural substrates of recollection and familiarity in episodic recognition memory. *Consciousness and cognition*, *19*(3), pp.816-828.

Sauvage, M.M., Beer, Z., Ekovich, M., Ho, L., Eichenbaum, H., 2010. The caudal medial entorhinal cortex: a selective role in recollection-based recognition memory. *Journal of Neuroscience*, *30*(46), pp.15695-15699.

Sauvage, M., Kitsukawa, T., Atucha, E., 2019. Single-cell memory trace imaging with immediate-early genes. *Journal of neuroscience methods*, *326*, p.108368.

Sauvage, M.M., Nakamura, N.H., Beer, Z., 2013. Mapping memory function in the medial temporal lobe with the immediate-early gene Arc. *Behavioural brain research*, *254*, pp.22-33.

Save, E., Sargolini, F., 2017. Disentangling the role of the MEC and LEC in the processing of spatial and non-spatial information: contribution of lesion studies. *Frontiers in systems neuroscience*, *11*, p.81.

Savelli, F., Yoganarasimha, D., Knierim, J.J., 2008. Influence of boundary removal on the spatial representations of the medial entorhinal cortex. *Hippocampus*, *18*(12), pp.1270-1282.

Scoville, William Beecher, and Brenda Milner. "Loss of recent memory after bilateral hippocampal lesions." *Journal of neurology, neurosurgery, and psychiatry* 20, no. 1 (1957): 11.

Seo, D.O., Zhang, E.T., Piantadosi, S.C., Marcus, D.J., Motard, L.E., Kan, B.K., Gomez, A.M., Nguyen, T.K., Xia, L., Bruchas, M.R., 2021. A locus coeruleus to dentate gyrus noradrenergic circuit modulates aversive contextual processing. *Neuron*, *109*(13), pp.2116-2130.

Scharfman, H.E., Sollas, A.L., Smith, K.L., Jackson, M.B., Goodman, J.H., 2002. Structural and functional asymmetry in the normal and epileptic rat dentate gyrus. *Journal of Comparative Neurology*, *454*(4), pp.424-439.

Schlesiger, M.I., Cannova, C.C., Boublil, B.L., Hales, J.B., Mankin, E.A., Brandon, M.P., Leutgeb, J.K., Leibold, C., Leutgeb, S., 2015. The medial entorhinal cortex is necessary for temporal organization of hippocampal neuronal activity. *Nature neuroscience*, *18*(8), pp.1123-1132.

Schlessinger, A.R., Cowan, W.M., Gottlieb, D.I., 1975. An autoradiographic study of the time of origin and the pattern of granule cell migration in the dentate gyrus of the rat. *Journal of Comparative Neurology*, *159*(2), pp.149-175.

Schmidt, B., Marrone, D.F., Markus, E.J., 2012. Disambiguating the similar: the dentate gyrus and pattern separation. *Behavioural brain research*, *226*(1), pp.56-65.

Schwegler, H., Boldyreva, M., Linke, R., Wu, J., Zilles, K., Crusio, W.E., 1996. Genetic variation in the morphology of the septo-hippocampal cholinergic and GABAergic systems in mice: II. Morpho-behavioral correlations. *Hippocampus*, *6*(5), pp.535-545.

Seress, L., Pokorny, J., 1981. Structure of the granular layer of the rat dentate gyrus. A light microscopic and Golgi study. *Journal of anatomy*, *133*(Pt 2), p.181.

Shigemoto, R., Kinoshita, A., Wada, E., Nomura, S., Ohishi, H., Takada, M., Flor, P.J., Neki, A., Abe, T., Nakanishi, S., Mizuno, N., 1997. Differential presynaptic localization of metabotropic glutamate receptor subtypes in the rat hippocampus. *Journal of Neuroscience*, *17*(19), pp.7503-7522.

Simonyi, A., Miller, L.A., Sun, G.Y., 2000. Region-specific decline in the expression of metabotropic glutamate receptor 7 mRNA in rat brain during aging. *Molecular brain research*, *82*(1-2), pp.101-106.

Snyder, J.S., Ferrante, S.C., Cameron, H.A., 2012. Late maturation of adult-born neurons in the temporal dentate gyrus. *PloS one*, *7*(11), p.e48757.

Snyder, J.S., Radik, R., Wojtowicz, J.M., Cameron, H.A., 2009. Anatomical gradients of adult neurogenesis and activity: young neurons in the ventral dentate gyrus are activated by water maze training. *Hippocampus*, *19*(4), pp.360-370.

Snyder, J.S., Ramchand, P., Rabbett, S., Radik, R., Wojtowicz, J.M., Cameron, H.A., 2011. Septo-temporal gradients of neurogenesis and activity in 13-month-old rats. *Neurobiology of aging*, *32*(6), pp.1149-1156.

Solstad, T., Boccara, C.N., Kropff, E., Moser, M.B., Moser, E.I., 2008. Representation of geometric borders in the entorhinal cortex. *Science*, *322*(5909), pp.1865-1868.

Soulé, J., Penke, Z., Kanhema, T., Alme, M.N., Laroche, S., Bramham, C.R., 2009. Object-place recognition learning triggers rapid induction of plasticity-related immediate early genes and synaptic proteins in the rat dentate gyrus. *Neural plasticity*, *2008*.

Squire, L.R., Zola-Morgan, S., 1991. The medial temporal lobe memory system. *Science*, *253*(5026), pp.1380-1386.

Stackman Jr, R.W., Cohen, S.J., Lora, J.C., Rios, L.M., 2016. Temporary inactivation reveals that the CA1 region of the mouse dorsal hippocampus plays an equivalent role in the retrieval of long-term object memory and spatial memory. *Neurobiology of learning and memory*, *133*, pp.118-128.

Steffenach, H.A., Witter, M., Moser, M.B., Moser, E.I., 2005. Spatial memory in the rat requires the dorsolateral band of the entorhinal cortex. *Neuron*, *45*(2), pp.301-313.

Stensola, H., Stensola, T., Solstad, T., Frøland, K., Moser, M.B., Moser, E.I., 2012. The entorhinal grid map is discretized. *Nature*, *492*(7427), pp.72-78.

Steward, O., 1976. Topographic organization of the projections from the entorhinal area to the hippocampal formation of the rat. *Journal of Comparative Neurology*, *167*(3), pp.285-314.

Steward, O., Scoville, S.A., 1976. Cells of origin of entorhinal cortical afferents to the hippocampus and fascia dentata of the rat. *Journal of Comparative Neurology*, *169*(3), pp.347-370.

Strange, B.A., Witter, M.P., Lein, E.S., Moser, E.I., 2014. Functional organization of the hippocampal longitudinal axis. *Nature Reviews Neuroscience*, *15*(10), pp.655-669.

Sugaya, K., Chouinard, M., Greene, R., Robbins, M., Personett, D., Kent, C., Gallagher, M., McKinney, M., 1996. Molecular indices of neuronal and glial plasticity in the hippocampal formation in a rodent model of age-induced spatial learning impairment. *Journal of Neuroscience*, *16*(10), pp.3427-3443.

Sun, Q., Sotayo, A., Cazzulino, A.S., Snyder, A.M., Denny, C.A., Siegelbaum, S.A., 2017. Proximodistal heterogeneity of hippocampal CA3 pyramidal neuron intrinsic properties, connectivity, and reactivation during memory recall. *Neuron*, *95*(3), pp.656-672.

Swanson, L.W., Wyss, J.M., Cowan, W.M., 1978. An autoradiographic study of the organization of intrahippocampal association pathways in the rat. *Journal of comparative neurology*, *181*(4), pp.681-715.

Tamamaki, N., 1999. Development of afferent fiber lamination in the infrapyramidal blade of the rat dentate gyrus. *Journal of Comparative Neurology*, *411*(2), pp.257-266.

Tamamaki, N., 1997. Organization of the entorhinal projection to the rat dentate gyrus revealed by Dil anterograde labeling. *Experimental brain research*, *116*, pp.250-258.

Tamamaki, N., Nojyo, Y., 1993. Projection of the entorhinal layer II neurons in the rat as revealed by intracellular pressure-injection of neurobiotin. *Hippocampus*, *3*(4), pp.471-480.

Tamamaki, N., Nojyo, Y., 1995. Preservation of topography in the connections between the subiculum, field CA1, and the entorhinal cortex in rats. *Journal of Comparative Neurology*, *353*(3), pp.379-390.

Tennant, S.A., Fischer, L., Garden, D.L., Gerlei, K.Z., Martinez-Gonzalez, C., McClure, C., Wood, E.R., Nolan, M.F., 2018. Stellate cells in the medial entorhinal cortex are required for spatial learning. *Cell reports*, *22*(5), pp.1313-1324.

Tsao, A., Moser, M.B., Moser, E.I., 2013. Traces of experience in the lateral entorhinal cortex. *Current biology*, *23*(5), pp.399-405.

Tuncdemir, S.N., Grosmark, A.D., Turi, G.F., Shank, A., Bowler, J.C., Ordek, G., Losonczy, A., Hen, R., Lacefield, C.O., 2022. Parallel processing of sensory cue and spatial information in the Dentate Gyrus. *Cell reports*, *38*(3), p.110257.

Twarkowski, H., Steininger, V., Kim, M.J., Sahay, A., 2022. A dentate gyrus-CA3 inhibitory circuit promotes evolution of hippocampal-cortical ensembles during memory consolidation. *Elife*, *11*, p.e70586.

Van Cauter, T., Camon, J., Alvernhe, A., Elduayen, C., Sargolini, F., Save, E., 2013. Distinct roles of medial and lateral entorhinal cortex in spatial cognition. *Cerebral Cortex*, *23*(2), pp.451-459.

Van Groen, T., Miettinen, P., Kadish, I., 2003. The entorhinal cortex of the mouse: organization of the projection to the hippocampal formation. *Hippocampus*, *13*(1), pp.133-149.

Van Haeften, T., Wouterlood, F.G., Jorritsma-Byham, B., Witter, M.P., 1997. GABAergic presubicular projections to the medial entorhinal cortex of the rat. *Journal of Neuroscience*, *17*(2), pp.862-874.

Van Hagen, B.T.J., Van Goethem, N.P., Lagatta, D.C., Prickaerts, J., 2015. The object pattern separation (OPS) task: a behavioral paradigm derived from the object recognition task. *Behavioural brain research*, *285*, pp.44-52.

Vazdarjanova, A., McNaughton, B.L., Barnes, C.A., Worley, P.F., Guzowski, J.F., 2002. Experience-dependent coincident expression of the effector immediate-early genes arc and Homer 1a in hippocampal and neocortical neuronal networks. *Journal of Neuroscience*, *22*(23), pp.10067-10071.

Vazdarjanova, A., Ramirez-Amaya, V., Insel, N., Plummer, T.K., Rosi, S., Chowdhury, S., Mikhael, D., Worley, P.F., Guzowski, J.F., Barnes, C.A., 2006. Spatial exploration induces ARC, a plasticity-related immediate-early gene, only in calcium/calmodulin-dependent protein kinase II-positive principal excitatory and inhibitory neurons of the rat forebrain. *Journal of Comparative Neurology*, *498*(3), pp.317-329.

Vertes, R.P., 1992. PHA-L analysis of projections from the supramammillary nucleus in the rat. *Journal of Comparative Neurology*, *326*(4), pp.595-622.

Wang, L., Park, L., Wu, W., King, D., Medina, A.V., Raven, F., Martinez, J.D., Ensing, A., Yang, Z., Jiang, S., Aton, S., 2022. Reactivation of memory-encoding dentate gyrus neurons during memory consolidation is associated with subregion-specific, learning-and sleep-mediated biosynthetic changes. *bioRxiv*, pp.2022-11.

Wang, W., Trieu, B.H., Palmer, L.C., Jia, Y., Pham, D.T., Jung, K.M., Karsten, C.A., Merrill, C.B., Mackie, K., Gall, C.M., Piomelli, D., 2016. A primary cortical input to hippocampus expresses a pathway-specific and endocannabinoid-dependent form of long-term potentiation. *Eneuro*, *3*(4).

Weeden, C.S., Hu, N.J., Ho, L.U., Kesner, R.P., 2014. The role of the ventral dentate gyrus in olfactory pattern separation. *Hippocampus*, *24*(5), pp.553-559.

Weeden, C.S., Roberts, J.M., Kamm, A.M., Kesner, R.P., 2015. The role of the ventral dentate gyrus in anxiety-based behaviors. *Neurobiology of Learning and Memory*, *118*, pp.143-149.

West, M.J., 1999. Stereological methods for estimating the total number of neurons and synapses: issues of precision and bias. *Trends in neurosciences*, *22*(2), pp.51-61.

Williams, P.A., Larimer, P., Gao, Y., Strowbridge, B.W., 2007. Semilunar granule cells: glutamatergic neurons in the rat dentate gyrus with axon collaterals in the inner molecular layer. *Journal of Neuroscience*, *27*(50), pp.13756-13761.

Wilson, D.I., Watanabe, S., Milner, H., Ainge, J.A., 2013. Lateral entorhinal cortex is necessary for associative but not nonassociative recognition memory. *Hippocampus*, *23*(12), pp.1280-1290.

Witter, M.P., 2007. The perforant path: projections from the entorhinal cortex to the dentate gyrus. *Progress in brain research*, *163*, pp.43-61.

Witter, M.P., Amaral, D.G., 1991. Entorhinal cortex of the monkey: V. Projections to the dentate gyrus, hippocampus, and subicular complex. *Journal of Comparative Neurology*, *307*(3), pp.437-459.

Witter, M.P., Doan, T.P., Jacobsen, B., Nilssen, E.S., Ohara, S., 2017. Architecture of the entorhinal cortex a review of entorhinal anatomy in rodents with some comparative notes. *Frontiers in systems neuroscience*, *11*, p.46.

Wixted, J.T., Squire, L.R., 2010. The role of the human hippocampus in familiarity-based and recollection-based recognition memory. *Behavioural brain research*, *215*(2), pp.197-208.

Wood, E.R., Dudchenko, P.A., Eichenbaum, H., 1999. The global record of memory in hippocampal neuronal activity. *Nature*, *397*(6720), pp.613-616.

Woodson, W., Nitecka, L., Ben-Ari, Y., 1989. Organization of the GABAergic system in the rat hippocampal formation: a quantitative immunocytochemical study. *Journal of Comparative Neurology*, *280*(2), pp.254-271.

Wouterlood, F.G., Härtig, W., Brückner, G., Witter, M.P., 1995. Parvalbumin-immunoreactive neurons in the entorhinal cortex of the rat: localization, morphology, connectivity and ultrastructure. *Journal of neurocytology*, *24*(2), pp.135-153.

Michael Wyss, J., 1981. An autoradiographic study of the efferent connections of the entorhinal cortex in the rat. *Journal of Comparative Neurology*, *199*(4), pp.495-512.

Wyss, J.M., Swanson, L.W., Cowan, W.M., 1979. Evidence for an input to the molecular layer and the stratum granulosum of the dentate gyrus from the supramammillary region of the hypothalamus. *Anatomy and embryology*, *156*(2), pp.165-176.

Xu, Z., Mo, F., Yang, G., Fan, P., Wang, Y., Lu, B., Xie, J., Dai, Y., Song, Y., He, E., Xu, S., 2022. Grid cell remapping under three-dimensional object and social landmarks detected by implantable microelectrode arrays for the medial entorhinal cortex. *Microsystems & Nanoengineering*, *8*(1), p.104.

Yamamoto, C., 1972. Intracellular study of seizure-like afterdischarges elicited in thin hippocampal sections in vitro. *Experimental neurology*, *35*(1), pp.154-164.

Yamazaki, R., Wang, D., De Laet, A., Maciel, R., Agnorelli, C., Cabrera, S., Arthaud, S., Libourel, P.A., Fort, P., Lee, H., Luppi, P.H., 2021. Granule cells in the infrapyramidal blade of the dentate gyrus are activated during paradoxical (REM) sleep hypersomnia but not during wakefulness: a study using TRAP mice. *Sleep*, *44*(12), p.zsab173.

Yassa, M.A., Stark, C.E., 2011. Pattern separation in the hippocampus. *Trends in neurosciences*, *34*(10), pp.515-525.

Yassa, M.A., Lacy, J.W., Stark, S.M., Albert, M.S., Gallagher, M., Stark, C.E., 2011. Pattern separation deficits associated with increased hippocampal CA3 and dentate gyrus activity in nondemented older adults. *Hippocampus*, *21*(9), pp.968-979.

Yassa, M.A., Stark, S.M., Bakker, A., Albert, M.S., Gallagher, M., Stark, C.E., 2010. High-resolution structural and functional MRI of hippocampal CA3 and dentate gyrus in patients with amnestic mild cognitive impairment. *Neuroimage*, *51*(3), pp.1242-1252.

Zehr, J.L., Nichols, L.R., Schulz, K.M., Sisk, C.L., 2008. Adolescent development of neuron structure in dentate gyrus granule cells of male Syrian hamsters. *Developmental neurobiology*, *68*(14), pp.1517-1526.

Zou, Y.M., Lu, D., Liu, L.P., Zhang, H.H., Zhou, Y.Y., 2016. Olfactory dysfunction in Alzheimer's disease. *Neuropsychiatric disease and treatment*, pp.869-875.

Appendix

Supplementary data

Behavioural patterns in the imaging groups match those observed in the behavioural assessment experiments

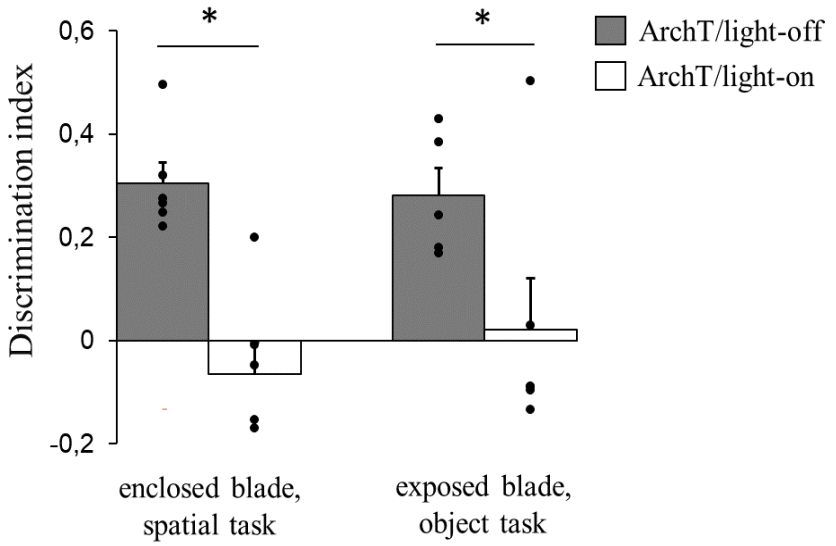

Figure S 1: Behavioural performance of mice used for *Arc* imaging. Similar memory impairments as described in Chapter II were observed. Enclosed blade inhibition impaired spatial memory retrieval, exposed blade inhibition – non-spatial. *: $p < 0.050$.

Similar behavioural patterns were observed in animals used for *Arc* imaging and groups used exclusively for the behavioural assessment in Chapter II. Control animals, but not the inhibition groups, showed discrimination indices significantly above zero in the spatial and non-spatial tasks (one-sample t-tests, comparisons against zero: enclosed blade/spatial task/light-off: $t_{(5)}=7.48$, $p<0.001$; exposed blade/object task/light-off: $t_{(4)}=5.26$, $p=0.006$; enclosed blade/spatial task/light-on: $t_{(5)}=-1.06$, $p=0.338$; exposed blade/object task/light-on: $t_{(5)}=0.21$, $p=0.840$). The enclosed blade inhibition group showed a significant decrease in spatial memory performance when compared to the control animals (two-sample t-test: spatial task/ enclosed blade (no-light vs light): $t_{(10)}=5.01$, $p<0.001$). The exposed blade inhibition group showed a significant decrease in non-spatial memory performance when compared to the control animals (two-sample t-test: object task/ exposed blade (no-light vs light): $t_{(9)}=2.17$, $p=0.029$) (**Figure S1**).

Analyses with non-normalised (raw) *Arc* imaging data

To exclude the possibility that the observed *Arc* expression patterns in Chapter III emerged due to the normalisation procedure, the same analyses with non-normalised (raw) data were performed. Similar patterns of *Arc* activity were found between the inhibition and control groups across hippocampal subregions.

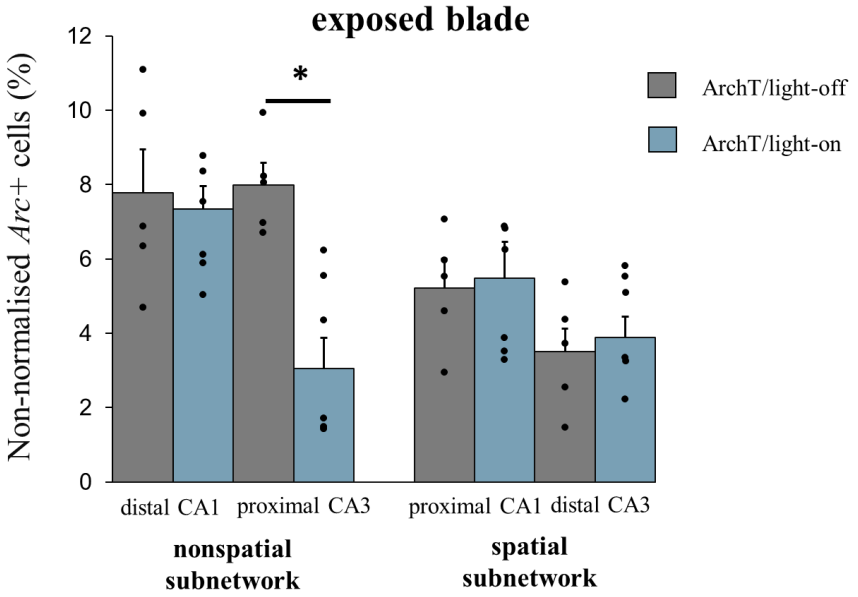

Figure S 2: *Arc* RNA expression, raw data in the exposed blade groups. Percentage of *Arc*-positive cells in distal CA1, proximal CA1, distal CA3, and proximal CA3 compared between the inhibition (light-on) and control (light-off) groups. Exposed blade inhibition decreased the recruitment of the proximal CA3. *: $p<0.050$.

As was the case with the normalised data, significant effects of 'subregion' and 'subregion × inhibition' were found on the hippocampal recruitment levels in mice with exposed blade injections (main effect 'subregion': $F_{(3,27)}= 8.81$, $p<0.001$; interaction effect: $F_{(3,27)}=5.51$, $p=0.004$; no significant main effect of 'inhibition': p-values >0.050). Post-hoc pairwise comparisons showed a significant difference in the recruitment levels of the proximal CA3 between the inhibition and control groups (two-sample t-tests, two-tailed: proximal CA3 (no-light vs light): $t_{(9)}=4.06$, $p=0.012$) (**Figure S2**). When comparing recruitment levels of the distal CA1 vs the proximal CA3, a significant difference was observed in the inhibition group but not the control animals (two-sample paired t-test: light-off, distal CA1 vs proximal CA3: $t_{(4)}=-0.14$, $p=0.894$; light-on, distal CA1 vs proximal CA3: $t_{(4)}=2.66$, $p=0.046$). A comparison of activity levels between the spatial and non-spatial CA3 and CA1 subregions showed that in control animals the proximal CA3 was recruited significantly more than the distal CA3 (two-sample

paired t-test: exposed blade light-off, distal CA3 vs proximal CA3: $t_{(4)}$=-8.96, p=0.004), but this was not the case in the inhibition group ($t_{(4)}$=0.89, p=0.832). For CA1 subregions, a trend effect was observed in the control animals (light-off, distal CA1 vs. proximal CA1: $t_{(4)}$=2.97, p=0.084) and a significant difference was detected in the inhibition group (light-on, distal CA1 vs proximal CA1: $t_{(5)}$=6.99, p=0.004).

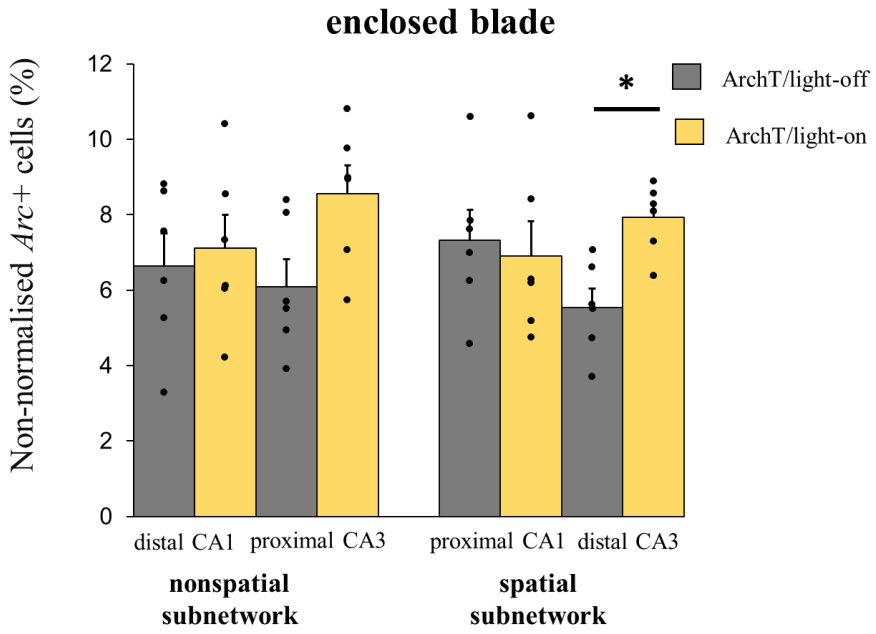

Figure S 3: *Arc* RNA expression, raw data in the enclosed blade groups. Percentage of *Arc*-positive cells in distal CA1, proximal CA1, distal CA3, and proximal CA3 compared between the inhibition (light-on) and control (light-off) groups. Enclosed blade inhibition increased the recruitment of the distal CA3. *: p<0.050.

For enclosed blade groups, a significant interaction effect of 'subregion × inhibition' was observed when comparing the subregions of spatial and non-spatial subnetworks between the control and enclosed blade inhibition group (interaction effect: $F_{(3,30)}$= 3.66, p = 0.023; no significant main effects of 'inhibition' or 'subregion' were detected, p-values >0.050). Post-hoc pairwise comparisons showed a significant difference in recruitment levels of the distal CA3 between the enclosed blade inhibition and control group (two-sample t-tests, two-tailed: distal CA3 (light-off vs light-on): $t_{(10)}$=-3.81, p=0.012) (**Figure S3**). Further post-hoc comparisons between the recruitment of the CA1 and CA3 subregions did not reveal any significant differences (all p-values >0.050).

Altogether, this shows that comparable patterns of *Arc* RNA expression were observed when analysing non-normalised data, indicating that the interpretation of the task-induced activity is not influenced by the normalisation procedure.

Pilot retrograde tracing data

In a pilot experiment, single tracer retrograde injections (n=11) aimed at the enclosed or exposed blades of the DG were performed to establish the best coordinates to target either of the DG blades. The injected volumes varied between 60 and 5 nl. Four selected cases with injection volumes of 30 and 5 nl are shown in **Figure S4**. As a reminder, in the dual tracing experiment described in Chapter IV, exposed blade injections often did not lead to any caudal MEC labelling. The selected data in **Figure S4** illustrate that the caudal MEC was labelled following both the enclosed and exposed blade injections. This shows than the brain TC 24 (dual retrograde experiment; Chapter IV), based on which the pattern of caudal MEC labelling differences were inferred for the enclosed and exposed blades of the DG, was not the only case with labelled caudal MEC following exposed blade injections.

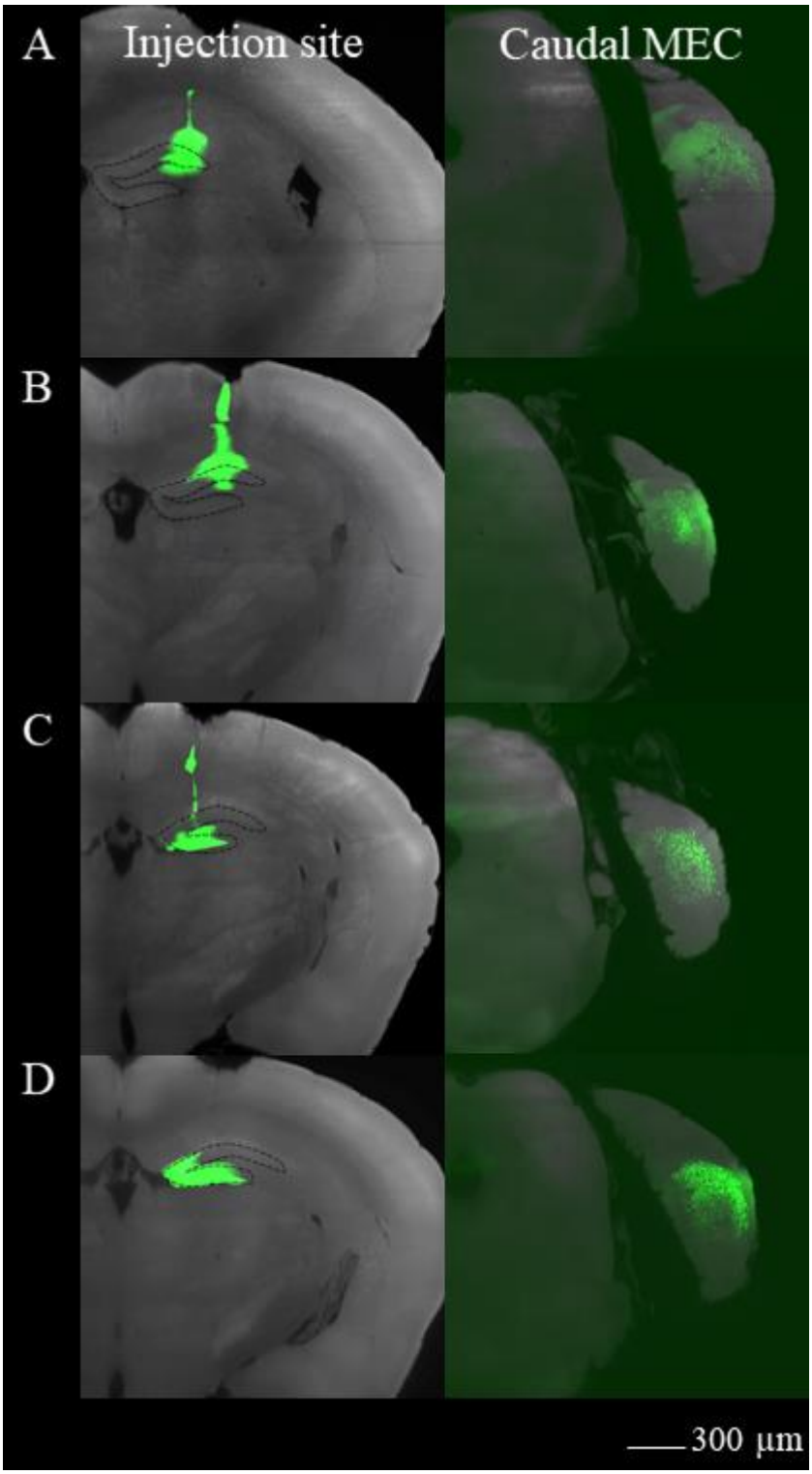

Figure S 4: Pilot data with single tracer injections. A-D: four different brains are shown with injection sites and the most caudal MEC labelling. A: enclosed, 30 nl, 1% w/v CTB-555. B: enclosed, 5 nl, 1% w/v CTB-555 C: exposed, 30 nl, 1% w/v CTB-555. D: exposed, 5 nl, 1% w/v CTB-555. Note a present labelling in the caudal MEC in all four cases. Black dashed lines indicate the outlines of the molecular layer of the DG at the injection sites. To snapshoot the images, digital zoom-in was applied to original datasets captured with a 4× objective lens. Scale bar 300 µm.

List of abbreviations

ANOVA	analysis of variance
Arc	activity-regulated cytoskeletal-associated gene
BSA	bovine serum albumin
CA1-CA3	cornu ammonis 1-3
C/A	commissural/associational
CTB	cholera toxin subunit b
Cy5	cyanine 5
DAPI	4′,6-diamidino-2-phenylindole
DEPC	diethylpyrocarbonate
DNA	deoxyribonucleic acid
DG	dentate gyrus
DIG	digoxigenin
EC	entorhinal cortex
HRP	horseradish peroxidase
IEG	immediate early gene
IgG	Immunoglobulin G
LEC	lateral entorhinal cortex
MEC	medial entorhinal cortex
MF	mossy fibres
ML	molecular layer
MML	middle molecular layer
MTL	medial temporal lobe
OML	outer molecular layer
PER	perirhinal cortex

POR	postrhinal cortex
PaS	parasubiculum
PBS	phosphate-buffered saline
PFA	buffered paraformaldehyde
PV	parvalbumin
rf	rhinal fissure
RNA	ribonucleic acid
SLM	stratum lacunosum moleculare
SuM	supramammillary nucleus
TBST	tris-buffered saline with Tween 20
tRNA	transfer RNA
Zif268	zinc finger protein 268 gene